

Spatiotemporal Patterns and Drivers of Surface Water Quality and Landscape Change in a Semi-Arid, Southern African Savanna

John Tyler Fox

Dissertation submitted to the faculty of the Virginia Polytechnic Institute and State
University in partial fulfillment of the requirements for the degree of

Doctor of Philosophy
In
Fisheries and Wildlife

Kathleen A. Alexander
Adil N. Godrej
Emmanuel A. Frimpong
Stephen P. Prisley

May 16, 2016
Blacksburg, VA

Keywords: (*Escherichia coli*, fecal indicator bacteria, water quality modeling, microbial fate, pollution, remote sensing, savanna disturbance ecology, land cover change, climate change, fire frequency, water-borne pathogens, wildlife, erosion, dryland rivers, water quality, Africa, ecosystem services)

Copyright © 2016
J. Tyler Fox

Spatiotemporal Patterns and Drivers of Surface Water Quality and Landscape Change in a Semi-Arid, Southern African Savanna

John Tyler Fox

Abstract

The savannas of southern Africa are a highly variable and globally-important biome supporting rapidly-expanding human populations, along with one of the greatest concentrations of wildlife on the continent. Savannas occupy a fifth of the earth's land surface, yet despite their ecological and economic significance, understanding of the complex couplings and feedbacks that drive spatiotemporal patterns of change are lacking. In Chapter 1 of my dissertation, I discuss some of the different theoretical frameworks used to understand complex and dynamic changes in savanna structure and composition. In Chapter 2, I evaluate spatial drivers of water quality declines in the Chobe River using spatiotemporal and geostatistical modeling of time series data collected along a transect spanning a mosaic of protected, urban, and developing urban land use. Chapter 3 explores the complex couplings and feedbacks that drive spatiotemporal patterns of land cover (LC) change across the Chobe District, with a particular focus on climate, fire, herbivory, and anthropogenic disturbance. In Chapter 4, I evaluated the utility of Distance sampling methods to: 1) derive seasonal fecal loading estimates in national park and unprotected land; 2) provide a simple, standardized method to estimate riparian fecal loading for use in distributed hydrological water quality models; 3) answer questions about complex drivers and patterns of water quality variability in a semi-arid southern African river system. Together, these findings have important implications to land use planning and water conservation in southern Africa's dryland river ecosystems.

Acknowledgements

Financial support for my dissertation research was provided by the National Science Foundation, award #1114953, in addition to Forest Conservation Botswana, National Institutes of Health, and the Center for Conservation of African Resources, Animals, Communities, and Land Use (CARACAL). I am also extremely grateful for the support of the Virginia Tech College of Natural Resources and Environment and the Department of Fish and Wildlife Conservation.

I am grateful to my committee, Kathleen Alexander, Adil Godrej, Emmanuel Frimpong, and Stephen Prisley for their support, guidance, friendship, and encouragement. I am also deeply indebted to my lab mates, friends, colleagues, and mentors at Virginia Tech and in Botswana for all their assistance and thoughtful conversations without which this project would not have been possible:

Claire Sanderson, Mark Vandewalle, Marcella Kelly, Kuruthumu Mwamende, Megan Holcomb, Peter Laver, Robert Sutcliffe, Cisko, Lipa Nkwalele, Rissa Pesapane, Erica Putman, Carol Ann Nichols, Shaun Clemence and Family, Tempe Adams, Dana Morin, Anne Hilborn, Lindsey Rich, Greg Anderson, Alex Silvis, Cathy Jachowski, Chris Sattter, Dan Schilling, Bernardo Mesa, Christine Proctor, Brian Murphy, Bill Hopkins, Jim Parkhurst, and Vic DiCenzo, to name just a few..

A very special thanks as well to Ginny and Reid Adams, Karen Steelman, and Ronald Butler at the University of Maine at Farmington, and to Kim Dickerson at the US Fish and Wildlife Ecological Services branch in Cheyenne, Wyoming. Joe Neuhof, my canyon-loving brother, Chris Martel, Dale and Stephanie Wiken, Ben and Michelle Wynn-Wheeler, and Monique Barrett –I love and miss you all, your friendship continues to inspire me. Also, Spas and Svetla Uzunovi, dear friends and outstanding husband and wife ecologists, my friends and colleagues from Strandja Nature Park, and the Dodovi Family, who keep reminding me that I need to get a “real” job!

I would like to thank my mother and father with all of my heart, as well as my brother, and my grandmother, Elizabeth E. Eanes, without whom I would surely have never made it this far and whose presence, dignity, and wisdom continue to guide me along this most wonderful journey.

Finally, and most of all, I would like to thank my wife and soul mate, Svetla Dimitrova, for her love and support throughout this entire process of us pursuing our dual doctorates at Virginia Tech and Michigan State; also my daughter and son who gave me strength and kept me centered when things were at their toughest. I love you guys.

Attribution

Below is a brief description of the contributions made by colleagues who assisted with the preparation of manuscripts for the following chapters, and whose contributions rose to the level of co-author for manuscript publication.

Chapter 2: Spatiotemporal variation and the role of wildlife in seasonal water quality declines in the Chobe River, Botswana.

Kathy Alexander (Department of Fish and Wildlife Conservation, Virginia Tech; CARACAL) provided financial and logistic assistance, and edits to the manuscript.

Chapter 3: A multi-temporal remote sensing analysis of land cover change dynamics, recent fire history, and elephant browsing in the semi-arid savanna of northern Botswana.

Kathy Alexander (Department of Fish and Wildlife Conservation, Virginia Tech; CARACAL) provided financial and logistic assistance, and edits to the manuscript.

Chapter 4: Quantifying wildlife-source contributions to terrestrial and aquatic fecal loadings using a Distance sampling approach

Kathy Alexander (Department of Fish and Wildlife Conservation, Virginia Tech; CARACAL) provided financial and logistic assistance, and edits to the manuscript.
Marcella Kelly (Department of Fish and Wildlife Conservation, Virginia Tech) provided technical assistance and edits to the manuscript.

Table of Contents

Abstract	ii
Acknowledgements	iii
Attribution	iv
Table of Contents	v
List of Tables	viii
List of Figures	x
List of Appendices	xvi
Chapter 1: Introduction	1
Spatiotemporal patterns of surface water quality.....	1
Land cover change in semi-arid southern African savanna	2
A Distance sampling approach for estimating seasonal wildlife fecal densities	5
Literature Cited	7
Chapter 2: Spatiotemporal variation and the role of wildlife in seasonal water quality declines in the Chobe River, Botswana.	10
Abstract	10
Introduction	10
Materials and Methods.....	12
Study Area	12
Chobe River floodplain.....	13
Chobe River transect.....	14
Water Sample Collection and Analysis	14
<i>E. coli</i> and total suspended solids	15
Wildlife biomass and fecal count data	15
Simultaneous autoregressive (SAR) spatial models	16
Geostatistical Analysis.....	18
Seasonal and trend decomposition using local regression.....	18
Results.....	19
Spatiotemporal water quality patterns	19
STL time series decomposition.....	20
Kriged water quality maps	20
Landuse and floodplain influence.....	20
Wildlife influence	21
Discussion	21
Conclusion	24
Acknowledgements.....	25
Literature cited	26
Tables.....	33
Figures.....	35
Appendices.....	45
Chapter 3: A multi-temporal remote sensing analysis of land cover change dynamics, recent fire history, and elephant browsing in the semi-arid savanna of northern Botswana.	50
Abstract	50
Introduction.....	51
Methods.....	53

Study area.....	53
Surface water resources	54
Protected woodlands	54
Climatological data	55
Satellite Image Data Sources	55
Image pre-processing.....	56
Principal components analysis.....	56
Land cover classification	57
Classification accuracy assessment.....	58
LC change detection	59
MODIS Active Fire Data	60
Elephant biomass and land cover.....	61
Results.....	61
Chobe District LC change.....	61
Protected areas change	64
Chobe Enclave and Village change	64
Riparian cover change.....	65
Rainfall.....	65
Fire frequency	66
Elephant Biomass and Land Cover.....	67
Discussion	67
Protected Areas	69
Chobe Enclave and villages	69
Riparian buffer	70
Conclusion	72
Literature cited	74
Tables	79
Figures.....	82
Appendices.....	101
Chapter 4: Quantifying wildlife-source contributions to terrestrial and aquatic fecal loadings using a Distance sampling approach	107
Abstract	107
Introduction.....	108
Methods.....	110
Study site.....	110
Fecal transect design and sampling protocol	111
Density analysis using Distance.....	112
Ground cover survey.....	113
Statistical analysis	114
Results.....	114
Wildlife fecal loading	114
Discussion	115
Conclusion	118
Literature cited	120
Tables	123
Figures.....	125

Appendices.....	130
CHAPTER 5: Synthesis.....	131
Literature Cited.....	136

List of Tables

Table 2-1 Arithmetic mean, maximum, and standard deviation of seasonal <i>E. coli</i> and TSS concentrations by land use class, calculated from water quality samples collected bimonthly from July 2011- March 2014.	33
Table 2-2 Model 1 – SAR mixed model results testing the effects of explanatory variables from 2012-2013 on seasonal log-mean <i>E. coli</i> (CFU/100mL)	33
Table 2-3. Model 2 – SAR mixed model results testing the effects of explanatory variables from 2011-2014 on seasonal log-mean <i>E. coli</i> (CFU/100mL).....	34
Table 2-4. Model 3 - SAR mixed model results testing the influence of terrestrial within and between-season fecal loading on log-mean <i>E. coli</i> (CFU/100mL).....	34
Table 3-1. Contingency table results of LC classification accuracy assessment compared to reference data.	79
Table 3-2. Summary of accuracy assessment statistics by LC class. Individual class accuracies include measures of: sensitivity (producer accuracy), specificity (true negatives), positive predictive value (user accuracy), and negative predictive values. Positive and negative predictive values reflect probabilities that a true positive or true negative is correct given the prevalence of classes within the population.	79
Table 3-3. Estimated total area (km ²) and percent land cover for the Chobe District.	80
Table 3-4. Estimated net land cover area (km ²) and percent change for the Chobe District.....	80
Table 3-5. Estimated total gross (class) changes in area (km ²) and percent land for the Chobe District.	80
Table 3-6. Summary of frequency and intensity of fires in the Chobe District, protected areas, settlements, and riparian buffers. Fire intensity is expressed as Fire Radiative Power (FRP) in megawatts (MW) of energy released to the atmosphere. Mean confidence for each location are included along with an area weighted Annual Fire Index (AFI), calculated by dividing average annual fire frequency by the total land area (fires*yr ⁻¹ /km ²) of each feature, and represents a straightforward method of comparing fire intensity in analysis units of varying size.	81
Table 4-1. Distance sampling estimates of wildlife fecal densities (dung piles/ha) by month for unprotected (UP) and protected (CNP) land use, along with the percent coefficient variation (%CV), associated degrees of freedom (df) and 95% confidence intervals (%CV). Fecal density estimates listed as “Other” include all species for which <50 dung piles were recorded or %CV was 50% or higher. Dashes (-) indicate that dung piles were recorded, but that detections were too few to model within acceptable	

confidence limits. Species with zero density estimates indicate that no dung piles were recorded within that particular land use..... 123

Table 4-2. Summary of t-test results comparing seasonal fecal loadings and land use.. 124

Table 4-3. Summary of OLS regression results comparing seasonal mean fecal loadings and percent ground cover..... 124

Table 4-4. Summary of Partial Least Squares regression results comparing seasonal mean fecal loadings and percent ground cover. 124

List of Figures

Figure 2-1. MODIS Terra (left) and Advanced Land Imager, EO-1 satellite imagery acquired on same day, May 8, 2010 (modified image using public domain data available from the USGS EROS Center). The vast Chobe-Zambezi floodplain system is visible at two different scales showing the dominant geological and hydrological influence of the Mambova fault. 35

Figure 2-2. Landsat-based map of the Chobe River study area. Dominant land uses are shown within the three representative land use types, which include: Park (solid green line), Town (red), and Mixed-use (light blue). The Chobe National Park border is also shown (dashed black line), along with water quality transect points (black triangles) and the Kasane water purification facility (blue cross). Chobe River flow direction is indicated by the blue arrow. 36

Figure 2-3. Seasonal relationships among water quality variables are summarized for the different land use classes. Red cells indicate that the mean value for each variable and land use is greater than the global mean for the study area, while blue symbolizes values below the global mean. 37

Figure 2-4. Box plots with outliers retained showing seasonal patterns of *E. coli* (CFU/100mL) and TSS (mg/L), in the Chobe River by land use class. Variability in the concentration data was high across all land use classes during both seasons, but was greatest within the Park and generally lower in Town and Mixed land use. Median wet season *E. coli* and TSS were similar to dry season median concentrations in Park and Town landuse. In Mixed land use, median wet season concentrations were more than twice those observed during the dry season. 38

Figure 2-5. Box plots with outliers retained showing seasonal patterns of water temperature (°C), dissolved oxygen (mg/L), and specific conductivity (mS/cm) in the Chobe River by land use class. Median values were similar across all three land use classes during the dry season, but differed substantially during the wet season. Median wet season DO was highest in the Park (despite having higher water temperature) compared to downstream levels, which may reflect greater primary productivity from vegetation in the Chobe River floodplain and its associated wetland systems. Median seasonal conductivity and interquartile range were highest in Park land use, with monthly median values ranging from a low of 0.04 mS/cm (May) at peak flood height, to a high of 0.42 mS/cm (October) when water levels were lowest. The range of observed seasonal values for water temperature, DO, and conductivity for the Chobe River were comparable to those recorded by Mackay et al. (2011) for the Okavango River Delta in 2006-2007 (Mackay et al. 2011). 39

Figure 2-6. Monthly time series of bi-monthly water sampling data showing temporal and spatial variation of mean *E. coli* (CFU/100mL) and TSS (mg/L) concentrations with standard errors by month and land use class in relation to daily precipitation (mm), and Chobe River height (m). 40

Figure 2-7. Arithmetic means of bi-monthly water sampling data by transect point showing seasonal and spatial variability of *E. coli* (CFU/100mL) and TSS (mg/L) concentrations with standard errors in relation to dry season mean fecal counts of elephant and other wildlife species. Transect points were assigned to three general land use types and proceed in an upstream direction from Mixed-use (1-17, Blue), Town (19-29, Red), Park (31-55, Green). Transect points where in-channel floodplain was present are indicated by the brown bracket. 41

Figure 2-8. Mean *E. coli* (CFU/100ml) and TSS (mg/L) time series data by individual month and transect with standard errors. Monthly averages for the study area (all transect) are indicated by the red horizontal lines. 42

Figure 2-9. Seasonal and trend decomposition using loess (STL) for *E. coli*. and TSS water quality data collected bi-monthly from July 7, 2011 – March 19, 2014. Raw data are displayed in the top panel as averaged values for all transect points with a two week sampling frequency, followed by seasonal, trend, and residual components. Scale differs for each of the components so relative magnitude is indicated by the gray bars on the right side of the panels. The bar in the top panel represents a single unit of variation, with larger bars indicating a smaller amount of variation attributable to a particular component..... 43

Figure 2-10. Raster surfaces of seasonal mean *E. coli* (CFU/100mL) and TSS (mg/L) estimated using ordinary kriging, overlaid with 2012 dry season aerial survey data showing log wildlife biomass (kg/km²). The Chobe National Park (dashed black line), Kasane water plant (light blue cross), transect points (triangles) and general land use classes: Park (green solid line), Town (red), and Mixed (light blue) are also shown. Close spatial overlap between areas of high and low *E. coli* and TSS concentrations can be seen during both wet and dry seasons..... 44

Figure 3-1. Landsat-based map of the Chobe District study area showing protected area boundaries (black border), including the Chobe National Park, forest reserves (FR), forest reserve extensions (FRE), along with the Chobe Enclave (white border), and major settlements..... 82

Figure 3-2. Landsat image mosaics clipped to the study area extent and displayed using a false color 7,4,2 band combination. Healthy vegetation appears as bright green and can saturate during periods of heavy growth, Grasslands appear green, pink areas represent barren soil, oranges and browns represent sparsely vegetated areas, sands and mineral soils appear in a multitude of different colors, and water appears blue to black. 83

Figure 3-3. Land cover classification maps of Chobe District for 1990 (a), 2003 (b), and 2013 (c). 84

Figure 3-4. (a.) Summary of overall disagreement between the 2013 LC classification and reference data. (b.) Summary of agreement, omission disagreement, and commission disagreement by category for the 2013 LC classification..... 85

Figure 3-5. Changes in classified land cover area (km²) for each time step. Error bars for each LC class were calculated using 2013 LC classification and ground truth data by dividing the number of misclassified cells by contingency table row totals. We then multiplied the resulting proportional error for each LC class by the nominal LC class areas, and summed along each column to derive an adjusted LC area representing upper and lower classification uncertainty bounds for the three time steps. Errors were lower than the estimated change associated with each LC class, except for wet/irrigated vegetation in all three time steps, and woodlands change between 2003 and 2013. 86

Figure 3-6. (a) Summary of the overall change during the two time steps in terms of quantity and allocation. (b) Category level summary of quantity and allocation indices for the period 1990-2003 and 2003-2013. The rate of overall change was nearly equal over the two time steps, and that quantity difference accounted for less than a quarter of all change during each time interval, and that exchange exceeded both quantity and shift in both time steps. 87

Figure 3-7. Category-level intensity analysis of gains and losses given observed changes in each time interval. Vertical axes show intensity of annual change during the time interval as a percent of the category. Horizontal (red) lines shows uniform intensity of annual change for the study area. Bars extending above the uniform line indicate change is relatively active for that category, while bars ending below the line indicate change is relatively dormant. 88

Figure 3-8. Transition-level changes among LC classes representing the intensity of Shrubland and Woodland gains (a) and losses (b) to other land cover classes in 1990-2003 and 2003-2013. 89

Figure 3-9. Land cover area (km²) for the three time steps in the Chobe District's protected areas, including Chobe National Park (CNP) and six forest reserves (FR) and reserve extensions (RE). 90

Figure 3-10. Land cover area (km²) for the three time steps in the Chobe District's settlement buffers and the Chobe Enclave. 91

Figure 3-11. Land cover area (km²) for the three time steps within the 1 km² riparian buffer for the entire length of the Chobe River within the Chobe District, and portions of the river within the Chobe Enclave, Chobe National Park (CNP), and Chobe and Kasane Forest Reserves. 92

Figure 3-12. Single spectrum analysis (SSA) of mean monthly precipitation at the Kasane meteorological station between 1922 and 2014 showing the major oscillatory (blue) and long term trend components (red) of the rainfall time series data. The dashed black line indicates a period of missing data. A long-term trend of declining month precipitation is evident in the time series, as are shorter oscillations between wetter and drier periods on the order of approximately 5 -10 years, corresponding closely to the timing of major ENSO events. Mean monthly rainfall was higher in the period leading up to the first time

step of the analysis, followed by a return to drought conditions after 1991 despite above average rainfall in 2008. 93

Figure 3-13. Total number of active fires recorded by the MODIS satellite in the Chobe District by month from 2011-2013. Fire is a dry season phenomenon in the system, with a total of 9288 fires were recorded across the Chobe District form 2001-2013..... 94

Figure 3-14. Comparison of total annual rainfall (mm) and active fires in the Chobe District, along with mean and maximum Fire Radiative Power (FRP) in megawatts. A total of 9288 fires were recorded across the Chobe District from 2001-2013, and fire frequency and intensity are dynamic over time. High fire years were typically preceded by a year with comparatively few fires, and fire frequency and intensity were greater in years with higher rainfall, which may seem contradictory, but suggests that increased wet season plant biomass in years with high rainfall results in greater dry season fuel loads conducive fire spread 95

Figure 3-15. The total number and mean intensity (FRP, megawatts) of active fires in 2003 and 2013 in relation to classified land cover. Fires were concentrated predominately in wet/irrigated vegetation and woodland in 2003. In 2013, woodland and shrubland burned most frequently, while grassland also fueled a greater proportion of fires. Mean fire radiative power in grassland was lower than in woodland and shrubland in both 2003 and 2013. Expansion of shrubland in the region, may lead to a greater number of more intense fires across the District. 96

Figure 3-16. Gettis-Ord G_i^* analysis of fire hot spots using MODIS active fire data from 2001-2013 overlaying 2013 land cover classification map. Significant clusters of high fire frequency were observed along the Chobe River in the Enclave, in the Kasane FRE, and in unprotected land bordering the Kazuma, Maikaelelo, and Sibuyu FRs, extending into neighboring agricultural fields. Fires associated with agricultural areas, however, tended to occur in late April and early May, while land to the west primarily burned from mid-September to late October. Spatiotemporal patterns of significant fire hot spots in the southeastern part of the District indicate they were not driven by fires spreading into Botswana from neighboring Zimbabwe. However, the significant cluster of fire hot spots near the Chobe River in the north of the Enclave suggests many of these fires are started from burning reeds and floodplain vegetation on both the Botswana and Namibian banks of the Chobe River. 97

Figure 3-17. Associations between locations of high elephant density (>20 Large Stock Units/km²) and 2003 and 2013 land cover. Elephant biomass estimates were derived from aerial wildlife survey data collected by the Botswana Department of Wildlife and National Parks (DWNP) during the 2003 and 2012 dry seasons. Areas of high elephant biomass in both were predominately associated with woodland and shrubland cover in both years. 98

Figure 3-18. Associations between locations of high elephant density (>20 Large Stock Units/km²) and 2003-2013 changes from Woodland cover to other land cover classes.

Elephant biomass estimates were derived from aerial wildlife survey data collected by the Botswana Department of Wildlife and National Parks (DWNP) during the 2003 and 2012 dry seasons. Despite locations of high elephant density in woodland and shrubland cover, the majority of woodland in these locations experienced no detectible change from 2003-2013..... 99

Figure 3-19. Map of locations of high elephant biomass (>20 Large Stock Units/km²) in relation to woodland cover class transitions from 2003-2013. Despite locations of high elephant density in woodland and shrubland cover, the majority of woodland in these locations experienced no detectible change from 2003-2013, while 236 km² saw a transition to shrubland. The same pattern was observed for 2013 LC and 2012 elephant biomass, with 916 km² of woodland cover experiencing no change, and 144 km² changed to shrubland from 2003-2013.of high elephant density (> 20 LSU) and 2003-2013 woodland cover change..... 100

Figure 4-1. Map of the study site showing fecal transect locations and dominant land use along the Chobe River. The blue arrow indicates flow direction. 125

Figure 4-2. Bar graph showing relative monthly contributions to fecal counts for species for which <50 dung piles recorded or %CV of fecal density estimate were >50%. Numbers correspond to calendar months with wet season on top and dry season below. 126

Figure 4-3. Wildlife fecal density estimates (dung piles/ha) for unprotected (UP) and protected (CNP) land are shown, together with associated 95% confidence intervals. Species for which too few dung piles were recorded or fecal density estimate %CV was >50% were lumped and modelled as a single source designated as “other”. Dry season fecal density estimates were significantly higher than those in wet season in both the CNP and in UP land. Dry season fecal loading was also significantly higher in protected compared to UP land in both seasons, No impala or buffalo sign was recorded in the riparian zone outside of the protected area, and no domestic cattle were observed inside the boundaries of the Chobe National Park. 127

Figure 4-4. Fecal density estimates (#dung piles/ha.) for transects in unprotected and protected land. Numbers correspond to calendar months with wet season on top and dry season below. Wildlife tended to cluster in similar locations in both wet and dry seasons, albeit at much higher densities during the dry season. Wildlife fecal loadings were consistently lowest at transect points in and near the town of Kasane and highest between transects 35-39 in the CNP. Elephant and impala were by far the largest contributors to terrestrial fecal loads in the Chobe National Park, with impala fecal densities exceeding those of elephant throughout the dry season. Sign from both impala and buffalo were almost never observed in the riparian zone outside of the Chobe National Park, despite there being large areas of suitable habitat. In contrast, elephants appear to be heavily utilizing unprotected land late in the dry season..... 128

Figure 4-5. Scatterplots showing the relationship between (a) mean dry season fecal loading (#dung piles/ha) and mean dry season *E. coli* concentration (CFU/100ml), and (b) mean dry season fecal loading and mean wet season *E. coli* concentration in the first three months of the wet season. (December-February) 129

List of Appendices

Appendix A. Geographical coordinates for water quality sampling transect points.	45
Appendix B. Moran’s I test results for spatial autocorrelation in seasonal <i>E. coli</i> and TSS data.....	46
Appendix C. Cross-validation statistics for semivariogram models that best-predicted seasonal <i>E. coli</i> and TSS water concentrations.....	46
Appendix D. Seasonal and trend decomposition using loess (STL) of <i>E. coli</i> . and TSS water quality data collected over the period July 7, 2011 – March 19, 2014 in Park land use. Raw data are displayed in the top panel as averaged values for all transect points with a two week sampling frequency, followed by seasonal, trend, and residual components. Scale differs for each of the decomposed components so relative magnitude is indicated by the gray bars on the right side of the panels. The bar in the top panel can be considered as a single unit of variation, with larger bars indicating a smaller amount of variation attributable to a particular component.	47
Appendix E. Seasonal and trend decomposition using loess (STL) of <i>E. coli</i> . and TSS water quality data collected over the period July 7, 2011 – March 19, 2014 in Town land use. Raw data are displayed in the top panel as averaged values for all transect points with a two week sampling frequency, followed by seasonal, trend, and residual components. Scale differs for each of the decomposed components so relative magnitude is indicated by the gray bars on the right side of the panels. The bar in the top panel can be considered as a single unit of variation, with larger bars indicating a smaller amount of variation attributable to a particular component.	48
Appendix F. Seasonal and trend decomposition using loess (STL) of <i>E. coli</i> . and TSS water quality data collected over the period July 7, 2011 – March 19, 2014 in Mixed land use. Raw data are displayed in the top panel as averaged values for all transect points with a two week sampling frequency, followed by seasonal, trend, and residual components. Scale differs for each of the decomposed components so relative magnitude is indicated by the gray bars on the right side of the panels. The bar in the top panel can be considered as a single unit of variation, with larger bars indicating a smaller amount of variation attributable to a particular component.	49
Appendix G. Landsat data acquisition list by USGS scene designations indicating the Landsat sensor, the path/row, and year of acquisition.	101
Appendix H. Landsat TM spectral band and spatial resolution characteristics.....	101
Appendix I. Landsat ETM+ spectral band and spatial resolution characteristics.....	101
Appendix J. Landsat-8 (LCDM) spectral band and spatial resolution characteristics...	102

Appendix K. Complete accounting of estimated gross (class) changes in area (km²) and percent land cover in the Chobe District. Initial state class values are listed in columns and rows contain final state values. Land cover values in columns indicate how pixels in each Initial State image was classified in the Final State image. For example, the table shows from 1990-2003, a total of 3150 km² initially classified as woodland in 1990 had changed into shrubland in the 2003 final state image. The Class Changes row indicates the total area for each class in the initial state image that changed into a different class. Total area for each initial state class are shown in the Class Total row, while the Class Total column indicates area of each class in the final state image. 103

Appendix L. Estimated area (km²) and percent (%) land cover for the three periods (1990, 2003, 2013) within the Chobe District's protected areas, the Enclave and buffer areas surrounding the district's settlements and the Chobe River riparian corridor. 105

Appendix M. Estimated net change in land cover area (km²) and percent (%) change in land cover area for each class during the periods (1990-2003, 2003-2013, and 1990-2013) within the Chobe District's protected areas, the Enclave and 10 km (314 km²) buffer areas surrounding the district's settlements, and 1 km riparian buffer along the Chobe River. 106

Appendix N. Histograms of perpendicular distances and fitted detection functions for wet season (a) January, (b) February, and dry season (c) April, (d) July, (e) August, and (f) September. 130

Chapter 1: Introduction

The semi-arid savannas of southern Africa are part of a vast terrestrial biome encompassing around 40% of the continent and 20% of the world's total land area (Scholes and Walker 1993). At the global scale, savannas support one-fifth of the world's human population, placing them at high risk for land degradation due to intensive or exploitative land use activities, together with the effects of climate change (Hoffmann et al. 2002, Sankaran et al. 2005). Many savanna systems, including the Chobe District of northern Botswana which are the focus of this dissertation, represent coupled human-environmental systems in which people are integrated and interact with other ecological components in complex ways that vary considerably across space, time, and organizational units (Liu et al. 2007). These systems frequently exhibit nonlinear dynamics with thresholds, reciprocal feedback loops, and time lags, but also differing degrees of resilience to retain similar structures and functioning following disturbances (Walker and Meyers 2004, Folke 2006, Liu et al. 2007). Spatiotemporal variation contributing to heterogeneity is a common focus of the following three chapters that constitute my dissertation. In each of the following three chapters, I address distinct yet interrelated characteristics of change over time and space across the 21,000 km² Chobe District, in an effort to provide insights into diverse complex forces arising from interactions between humans, wildlife, and their environment.

Spatiotemporal patterns of surface water quality

Perennial dryland rivers in southern Africa and their wetlands often provide a major proportion of water for drinking and irrigation, as well as food resources, traditional medicines, roof thatching, and materials for building and crafts (Schuyt 2005). Surface water resources are limited and of critical importance to dryland regions, and access to clean water is fundamental to both human and wildlife health. Land areas abutting surface water are of high value and often a focus of human development. However, prioritization of waterfront access for human development can restrict and compress wildlife populations particularly in Africa into increasingly smaller areas where routes to surface water remain open. While high wildlife species densities can be a boon for ecotourism operations, they may cause substantial environmental impacts, including loss or modification of woody vegetation structure and cover, soil erosion, and increased rates of fecal deposition (Naiman and Rogers 1997a). Rainfall and

seasonal flooding in impacted areas may amplify surface water inputs of fecal bacterial contamination from water and sanitation system overflows, and runoff of bacteria and sediment from the surrounding landscape (Levy et al. 2009, Alexander et al. 2013).

In Chapter 2 “Spatiotemporal Variation and the Role of Wildlife in Seasonal Water Quality Declines in the Chobe River, Botswana”, I used spatiotemporal and geostatistical modeling to evaluate seasonal patterns and drivers of waterborne concentrations of the Gram-negative bacterium, *Escherichia coli* (*E. coli*) and Total Suspended Solids (TSS) concentrations across a mosaic of varying land use intensity, including protected (Chobe National Park), developing urban, and urban land use. This study was motivated by an analysis of medical data acquired from local health clinics describing diarrheal disease outbreaks in Chobe District from 2006 – 2009 by Alexander and Blackburn (2013), which identified distinct temporal patterns to recurrent disease outbreaks. Diarrheal disease is the leading cause of child malnutrition and the second leading cause of mortality for children under five years of age, with nearly half of all diarrheal deaths occurring in sub-Saharan Africa (WHO, 2002). Impacts of childhood diarrheal disease in Africa may be more severe due, in part, to immune system depression associated with concurrent presence of other infectious diseases including HIV/AIDS (Nair 2004). *E. coli* has been identified as a primary cause of human diarrheal disease morbidity and mortality worldwide (O'Reilly et al. 2012, Croxen et al. 2013). The long-term effects of persistent and repeated bouts of diarrheal disease can be severe, with infections resulting in significant cognitive and physical development problems (Lorntz et al. 2006, Petri et al. 2008). Although limitations exist to the use of *E. coli* as a model organism for predicting the presence of other waterborne pathogens (Seidler et al. 1981, Desmarais et al. 2002) a number of studies have demonstrated the efficacy of its use to examine fecal contamination of water sources and transmission of microorganisms between humans and wildlife (Edberg et al. 2000, Chapman et al. 2006, Skurnik et al. 2006, Rwego et al. 2008, Literak et al. 2010).

Land cover change in semi-arid southern African savanna

Savannas are characterized by the presence of extremely productive and rapidly-growing C4 photosynthetic grasses interspersed with a woody plant field layer typically thinned and maintained in a more or less discontinuous, open-canopy state by feedbacks among climate,

nutrient availability, fire, and herbivory (Scholes and Archer 1997, Archibald et al. 2005, Sankaran et al. 2005, Beckage et al. 2009, Staver and Levin 2012). Proposed mechanisms for maintaining the dynamic coexistence of trees and grassland in savanna fall broadly into two classes that include those which emphasize the role of competition or niche partitioning (Walter and Bottman 1967, Walker et al. 1981, Casper and Jackson 1997) and those which focus on demographic bottlenecks to tree recruitment mediated by disturbance, such as fire, herbivory, and human activities (Higgins et al. 2000, Sankaran et al. 2005, Beckage et al. 2009). Other research has focused on the proposed role that elevated atmospheric CO₂ may play in woody plant expansion success, favoring the regrowth following injury from fire or browsing (Bond and Midgley 2000, 2012), and inducing plant water-saving with a statistically stronger greening response observed in dryland systems (Lu et al. 2016).

Ecological theories describing the specific mechanisms and feedbacks maintaining tree-grass coexistence in savannas have been variously interpreted in the context of equilibrium, non-equilibrium, and disequilibrium dynamics (Higgins et al. 2000, Sankaran et al. 2004). From a theoretical perspective, equilibrium dynamics in savannas have been used to broadly describe long-term coexistence of trees and grasses where competitive balance remains unchanged by disturbances such as drought, fire, and grazing (Scholes and Archer 1997, Sankaran et al. 2004). The term non-equilibrium typically refers to savanna systems in which climate, interannual rainfall variability and drought in particular, are the dominant disturbances regulating tree seedling germination and establishment, fostering coexistence and maintaining dynamic tree-grass ratios away from an equilibrium state (Higgins et al. 2000, Van Wijk and Rodriguez-Iturbe 2002, Sankaran et al. 2004). Lastly, disequilibrium theories assume that disturbances are essential and, together with competitive tree-grass interactions, maintain savanna away from an equilibrium state, without which long-term coexistence would not be possible (Scholes and Archer 1997, Jeltsch et al. 2000, Sankaran et al. 2004, D'Odorico et al. 2006).

While most researchers agree that competition, population demographics, climate, and historical disturbance regimes all are present and interact in dynamic and complex ways to influence structure and function of savanna systems, considerable debate exists about whether these assumptions and mechanisms hold true under all conditions or are mutually exclusive under

certain conditions (Sankaran et al. 2004). Vegetation patterns in savanna ecosystems are clearly shaped by climate variability and disturbances, while positive feedbacks from vegetation and nonlinearities present in the coupled plant-climate system influence the magnitude of plant community responses to external forcing (Zeng and Neelin 2000). A continental-scale analysis of tree cover in African savannas by Bucini and Hanan (2007) suggests the magnitude of a disturbance largely depends upon mean annual precipitation (MAP) regimes across rainfall zones. In semi-arid savannas (MAP 400-650mm) such as those in northern Botswana, MAP exerts a stronger control over maximum tree cover along with disturbances that act as strong modifiers. In mesic savannas (MAP >1600mm), precipitation no longer strongly limits tree cover, and disturbance impacts become more important in maintaining the system, while in arid savannas (MAP <400mm) the opposite is true (Bucini and Hanan 2007). While precipitation controls maximum realizable woody cover in arid savannas, disturbance dynamics control savanna structure in areas that receive MAP in excess of 650 ± 134 mm (Sankaran et al. 2005). In these unstable “disturbance-driven savannas”, fire and herbivory are essential maintain both trees and grasses in the system by preventing woodlands from attaining a closed canopy state (Bond et al. 2003).

In Chapter 3, I classified and mapped savanna land cover (LC) in the Chobe District and characterized patterns of LC change between 1990, 2003, and 2013 using 30-meter resolution imagery from Landsat Thematic Mapper (TM), Enhanced Thematic Mapper Plus (ETM+), and Operational Land Imager (OLI) satellites. Savannas occupy a fifth of the earth’s land surface (Sankaran et al. 2005), yet despite their ecological and economic significance, understanding of the complex couplings and feedbacks that drive spatiotemporal patterns of LC change is lacking. Improved knowledge of the influence of climate, fire, and herbivory on patterns of LC change is needed to develop and implement sound management and conservation policies which increase local and regional ecosystem resilience to future climate change. In addition to identifying spatial and temporal changes on a regional scale, I quantified LC changes occurring within the boundaries of protected areas, including the Chobe National Park and six forest reserves, and in buffer areas surrounding major towns and villages and the riparian corridor of the Chobe River. I also evaluated the intensity of land cover change in the Chobe District and the nature of couplings and feedbacks between ecological, environmental, and anthropogenic components that

influence long-term LC change patterns, with a particular focus on the effects of fire and browsing by elephants on woodland change dynamics.

A Distance sampling approach for estimating seasonal wildlife fecal densities

In Chapter 4, I present a straightforward and low-cost, standardized methodology for estimating wildlife-source fecal loading on the landscape using Distance-sampling of dung piles along line transects in riparian habitat. Spatially-distributed river basin-scale models like the Soil and Water Assessment Tool (SWAT) are increasingly utilized by a diverse body of stakeholders to quantify and predict the impacts of land management decisions on bacterial water quality in large and complex river systems. However, predicting fecal indicator bacteria (FIB) concentrations in surface waters remains the most uncertain watershed model parameter (Suter II et al. 1987, Benham et al. 2006, Parajuli et al. 2009). Wildlife-source fecal bacteria contributions, in particular, have remained difficult to estimate because of the considerable spatiotemporal variability in animal density, habitat resource utilization, and diet in large river basins (Benham et al. 2006). Wildlife-source fecal loadings are rarely quantified, therefore land use and cover data are frequently used to indirectly estimate wildlife numbers and distributions based on likelihood of animal occurrence in a particular habitat (Chapra 2008). For the purpose of hydrological modeling, wildlife population data are frequently distributed equally across all potential habitat for each species (Benham et al. 2006), ignoring potentially important aspects of landscape connectivity and spatiotemporal variability of wildlife habitat use and distribution often observed in heterogeneous landscapes (Turner 1989). This approach may also result in high predictive uncertainty when modeling bacteria concentrations in watersheds where distinct variations in seasonal conditions, habitat, land use, or landscape features influence wildlife to aggregate disproportionately at high densities in certain locations along a watercourse. Building upon research on water quality dynamics in the Chobe River detailed in Chapter 2, I present a standardized Distance-based sampling method for quantifying wildlife-source contributions to fecal bacterial loading of surface waters. This Distance-based method is especially useful for developing knowledge of how wildlife fecal loadings vary across a landscape or particular land use, either seasonally or during major phenological changes in vegetation. I also evaluated the utility of Distance sampling methods to: 1) derive seasonal fecal loading estimates in national park and non-protected land; 2) provide a simple, standardized method to estimate riparian fecal

loading for use in distributed hydrological water quality models; 3) answer questions about complex drivers and patterns of water quality variability in a semi-arid southern African river system.

Literature Cited

- Alexander, K., and J. Blackburn. 2013. Overcoming barriers in evaluating outbreaks of diarrheal disease in resource poor settings: assessment of recurrent outbreaks in Chobe District, Botswana. *BMC Public Health* **13**:1-15.
- Alexander, K. A., M. Carzolio, D. Goodin, and E. Vance. 2013. Climate change is likely to worsen the public health threat of diarrheal disease in Botswana. *International Journal of Environmental Research and Public Health* **10**:1202-1230.
- Archibald, S., W. Bond, W. Stock, and D. Fairbanks. 2005. Shaping the landscape: fire-grazer interactions in an African savanna. *Ecological Applications* **15**:96-109.
- Beckage, B., W. J. Platt, and L. J. Gross. 2009. Vegetation, fire, and feedbacks: a disturbance-mediated model of savannas. *The American Naturalist* **174**:805-818.
- Benham, B. L., C. Baffaut, R. W. Zeckoski, K. R. Mankin, Y. A. Pachepsky, A. M. Sadeghi, K. M. Brannan, M. L. Soupir, and M. J. Habersack. 2006. Modeling bacteria fate and transport in watersheds to support TMDLs. *Transactions of the ASABE* **49**:987-1002.
- Bond, W., G. Midgley, F. Woodward, M. Hoffman, and R. Cowling. 2003. What controls South African vegetation—climate or fire? *South African Journal of Botany* **69**:79-91.
- Bond, W. J., and G. F. Midgley. 2000. A proposed CO₂-controlled mechanism of woody plant invasion in grasslands and savannas. *Global Change Biology* **6**:865-869.
- Bond, W. J., and G. F. Midgley. 2012. Carbon dioxide and the uneasy interactions of trees and savannah grasses. *Philosophical Transactions of the Royal Society of London B: Biological Sciences* **367**:601-612.
- Bucini, G., and N. P. Hanan. 2007. A continental-scale analysis of tree cover in African savannas. *Global Ecology and Biogeography* **16**:593-605.
- Casper, B. B., and R. B. Jackson. 1997. Plant competition underground. *Annual Review of Ecology and Systematics*:545-570.
- Chapra, S. C. 2008. *Surface water-quality modeling*. Waveland press.
- D’Odorico, P., F. Laio, and L. Ridolfi. 2006. A probabilistic analysis of fire-induced tree-grass coexistence in savannas. *The American Naturalist* **167**:E79-E87.
- Folke, C. 2006. Resilience: The emergence of a perspective for social–ecological systems analyses. *Global Environmental Change* **16**:253-267.
- Higgins, S. I., W. J. Bond, and W. S. Trollope. 2000. Fire, resprouting and variability: a recipe for grass–tree coexistence in savanna. *Journal of Ecology* **88**:213-229.

- Hoffmann, W. A., W. Schroeder, and R. B. Jackson. 2002. Positive feedbacks of fire, climate, and vegetation and the conversion of tropical savanna. *Geophysical Research Letters* **29**.
- Jeltsch, F., G. E. Weber, and V. Grimm. 2000. Ecological buffering mechanisms in savannas: a unifying theory of long-term tree-grass coexistence. *Plant Ecology* **150**:161-171.
- Levy, K., A. E. Hubbard, K. L. Nelson, and J. N. Eisenberg. 2009. Drivers of water quality variability in northern coastal Ecuador. *Environmental Science & Technology* **43**:1788-1797.
- Liu, J., T. Dietz, S. R. Carpenter, M. Alberti, C. Folke, E. Moran, A. N. Pell, P. Deadman, T. Kratz, and J. Lubchenco. 2007. Complexity of coupled human and natural systems. *Science* **317**:1513-1516.
- Lu, X., L. Wang, and M. F. McCabe. 2016. Elevated CO₂ as a driver of global dryland greening. *Scientific reports* **6**.
- Naiman, R. J., and K. H. Rogers. 1997. Large animals and system-level characteristics in river corridors. *Bioscience*:521-529.
- Parajuli, P. B., K. R. Mankin, and P. L. Barnes. 2009. Source specific fecal bacteria modeling using soil and water assessment tool model. *Bioresource Technology* **100**:953-963.
- Sankaran, M., N. P. Hanan, R. J. Scholes, J. Ratnam, D. J. Augustine, B. S. Cade, J. Gignoux, S. I. Higgins, X. Le Roux, and F. Ludwig. 2005. Determinants of woody cover in African savannas. *Nature* **438**:846-849.
- Sankaran, M., J. Ratnam, and N. P. Hanan. 2004. Tree–grass coexistence in savannas revisited—insights from an examination of assumptions and mechanisms invoked in existing models. *Ecology Letters* **7**:480-490.
- Scholes, R., and S. Archer. 1997. Tree-grass interactions in savannas. *Annual Review of Ecology and Systematics*:517-544.
- Scholes, R., and B. Walker. 1993. *Nylsvley: the study of an African savanna*. Cambridge University Press Cambridge, UK.
- Schuyt, K. D. 2005. Economic consequences of wetland degradation for local populations in Africa. *Ecological Economics* **53**:177-190.
- Staver, A. C., and S. A. Levin. 2012. Integrating theoretical climate and fire effects on savanna and forest systems. *The American Naturalist* **180**:211-224.
- Suter II, G. W., L. W. Barnhouse, and R. V. O'Neill. 1987. Treatment of risk in environmental impact assessment. *Environmental Management* **11**:295-303.
- Turner, M. G. 1989. Landscape ecology: the effect of pattern on process. *Annual Review of Ecology and Systematics*:171-197.

- Van Wijk, M. T., and I. Rodriguez-Iturbe. 2002. Tree-grass competition in space and time: Insights from a simple cellular automata model based on ecohydrological dynamics. *Water Resources Research* **38**.
- Walker, B., and J. A. Meyers. 2004. Thresholds in ecological and socialecological systems: a developing database. *Ecology and Society* **9**:3.
- Walker, B. H., D. Ludwig, C. S. Holling, and R. M. Peterman. 1981. Stability of semi-arid savanna grazing systems. *The Journal of Ecology*:473-498.
- Walter, W. G., and R. P. Bottman. 1967. Microbiological and chemical studies of an open and closed watershed. *Journal of Environment and Health* **30**:157-163.
- Zeng, N., and J. D. Neelin. 2000. The role of vegetation-climate interaction and interannual variability in shaping the African savanna. *Journal of Climate* **13**:2665-2670.

Chapter 2: Spatiotemporal variation and the role of wildlife in seasonal water quality declines in the Chobe River, Botswana.

Abstract

Sustainable management of dryland river systems is often complicated by extreme variability of precipitation in time and space, especially across large catchment areas. Understanding regional water quality changes in southern African dryland rivers and wetland systems is especially important because of their high subsistence value and provision of ecosystem services essential to both public and animal health. We quantified seasonal variation of *Escherichia coli* (*E. coli*) and Total Suspended Solids (TSS) in the Chobe River using spatiotemporal and geostatistical modeling of water quality time series data collected along a transect spanning a mosaic of protected, urban, and developing urban land use. We found significant relationships in the dry season between *E. coli* concentrations and protected land use ($p=0.0009$), floodplain habitat ($p=0.016$), and fecal counts from elephant ($p=0.017$) and other wildlife ($p=0.001$). Dry season fecal loading by both elephant ($p=0.029$) and other wildlife ($p=0.006$) was also an important predictor of early wet season *E. coli* concentrations. Locations of high *E. coli* concentrations likewise showed close spatial agreement with estimates of wildlife biomass derived from aerial survey data. In contrast to the dry season, wet season bacterial water quality patterns were associated only with TSS ($p<0.0001$), suggesting storm water and sediment runoff significantly influence *E. coli* loads. Our data suggest that wildlife populations, and elephants in particular, can significantly modify river water quality patterns. Loss of habitat and limitation of wildlife access to perennial rivers and floodplains in water-restricted regions may increase the impact of species on surface water resources. Our findings have important implications to land use planning in southern Africa's dryland river ecosystems.

Introduction

In water-stressed regions like southern Africa freshwater resources are under increasing extractive pressures that complicate sustainable management of these systems. Semi-arid and arid regions together constitute nearly 50% of global land area while supporting approximately 20% of the global population (Middleton and Thomas 1997, Tooth and McCarthy 2007). Rivers

in dryland regions exhibit a diversity of forms and behaviors, but typically have greater flow variability than their tropical and temperate counterparts (Walker et al. 1995, Tooth 2013). Precipitation in dryland river basins is exceeded by evapotranspiration, and rainfall is extremely variable in time and space, especially across moderate to large catchments (>100 km²) where both intensity and runoff tend to be high (Tooth 2000). Seasonal flood pulses in these dryland systems can have significant impacts on the timing of agriculture and other human landscape uses, as well as on the movement and ecology of native wildlife (Junk et al. 1989, Omphile and Powell 2002).

Limited infrastructure and uneven temporal and spatial distribution of clean water resources in southern Africa, a predominantly dryland region, means only 61% of the region's population has reliable access to safe drinking water (SADC 2006). Frequent disruptions to existing water treatment and delivery systems can have significant impacts on health and prosperity of human populations (Alexander and Blackburn 2013). Diarrheal disease is the leading cause of child malnutrition worldwide and the second leading cause of mortality for children under five years of age, with nearly half of all diarrheal deaths occurring in sub-Saharan Africa (WHO 2002). The long-term effects of persistent and repeated bouts of diarrheal disease caused by waterborne pathogens such as *Escherichia coli* (*E. coli*) can be severe, with infections resulting in significant cognitive and physical development problems that can have significant life time effects (Steiner et al. 1998, Lorntz et al. 2006, Petri et al. 2008, Mondal et al. 2009, Alexander et al. 2012, O'Reilly et al. 2012, Croxen et al. 2013).

Perennial dryland rivers in southern Africa and their associated wetlands often provide a major proportion of water for drinking and irrigation, as well as food resources, traditional medicines, roof thatching, and other materials for building and crafts (Schuyt 2005). Access to clean water is a critical ecosystem service is fundamental to human health, and while surface water resources are limited and of critical importance to dryland regions, land areas abutting surface water are of high value and often a focus of human development. Prioritization of waterfront access for human development can restrict and compress wildlife populations particularly in Africa into increasingly smaller areas where routes to surface water remain open. While concentrated wildlife can be a boon for ecotourism operations, substantial environmental impacts may ensue, including loss or modification of woody vegetation structure and cover, soil erosion, and

increased rates of fecal deposition (Naiman and Rogers 1997f). Heavy rainfall and seasonal flooding in impacted areas may amplify surface water inputs of fecal bacterial contamination from water and sanitation system overflows, and runoff of fecal material and sediment from the surrounding landscape (Levy et al. 2009, Alexander et al. 2013). Elevated bacterial concentrations in river courses may arise through exogenous sources including fecal loading by humans, livestock, and wildlife concentrated around limited surface water resources, or through microbial survival and growth in-situ (Hardina and Fujioka 1991, Byappanahalli and Fujioka 1998, Fujioka et al. 1998, Desmarais et al. 2002, Levy et al. 2009).

Evaluation of water quality and sustainability of southern Africa's perennial rivers is particularly important given future regional climate change scenarios, which predict a 10-30% decrease in runoff to occur in southern Africa by 2050 (Milly et al. 2005). Even a 10% drop in long-term average annual rainfall amounts in dryland countries such as Botswana in southern Africa is predicted to result in a minimum 42% reduction of perennial drainage entering the country's rivers (De Wit and Stankiewicz 2006). With 94% of Botswana's water resources shared among neighboring countries (Mutembwa and Initiative 1998), sustainable conservation of perennial surface water sources will have considerable consequences for the region's economies, ecosystems, and associated communities. In this study, we use the dryland Chobe River system in Northern Botswana to evaluate the interaction between season, land use, and wildlife and the influence this can have on the spatial and temporal dynamics of water quality in a dryland system.

Materials and Methods

Study Area

The Chobe River in northeast Botswana is part of the vast and interconnected Okavango-Kwando-Zambezi catchment system (~693,000 km²), which has its headwaters in the highlands of Angola (Gaughan and Waylen 2012). This semi-arid, subtropical region on the northern edge of the Kalahari Desert is characterized by highly variable seasonal rainfall, with nearly all the annual precipitation (avg. 604 mm) occurring during the summer wet season (December – April), with a general absence of precipitation during the dry season (May – November). The Chobe River is one of three permanent surface water sources in Botswana and the only

permanent surface water source in the entire Chobe District (21,000 km²). The Chobe District includes communal and private lands used for grazing livestock and agriculture, protected land including forest reserves and wildlife management areas, as well as villages and urban townships. A dominant feature of the study area is the Chobe National Park (CNP), Botswana's second largest (11,700 km²), which provides critical habitat for the largest elephant (*Loxodonta africana*) population in Africa, as well as a host of other wildlife species. Over the past forty years, elephant populations have grown at a mean annual rate of between 5.5% and 7% and currently are among the largest on the continent (Calef 1988, Vandewalle 2003). The town of Kasane is the seat of local government and the largest urban area in Chobe District with an estimated population of 9,008 (BSCO 2011). Kazungula is a growing residential and commercial area (est. population 4,133) with the only border crossing from Botswana to Zambia by ferry and Zimbabwe by road. At the time of the study all settlements in the Chobe District relied almost entirely upon drinking water supplies abstracted from the Chobe River by a single municipal water intake and treatment facility located in Kasane.

Chobe River floodplain

In contrast to the deep layer of well-drained, nutrient-poor Kalahari quartz sand that covers the greater proportion of the study area, soils of the Chobe River's floodplain and alluvial terrace are fine textured and relatively nutrient-rich, with a generally high clay content that increases with depth (Skarpe et al. 2014a). Basalts of the Stormberg lava origin become exposed on the northern rim of the Chobe Plateau above Kasane. The Chobe River channel widens considerably as the river flows east through the CNP, before narrowing and deepening as it crosses the Mambova falls before joining the Zambezi River. The relatively active Mambova fault line defines the eastern edge of the Chobe River floodplain and is a dominant geological feature controlling the location and hydrological character of the present-day Chobe River channel (Pricope 2013). During the annual flood, rising water builds up behind the fault line and spreads outwards across the river floodplain, reaching as far upstream as Lake Liambezi in high flood years (Fig. 1).

Chobe River transect

We established a transect consisting of 55 points spaced 500m apart along a 27.5 km reach of the Chobe River (Fig. 2), starting at the confluence of the Chobe and Zambezi Rivers (transect 1: 17°47'41.4854"S, 25°15'38.9874"E) and ending approximately 12 km inside the CNP (transect 55: 17°49'56.928"S, 25°2'52.7274"E). Land use along the Chobe River transect from west (upstream) to east (downstream) consisted of: Park (transect points 55-31), Town (29-19), and Mixed (17-1). Human settlements are absent within Park land use, although annual visitation is around 110,000, the majority of which occurs during the dry season (Magole and Gojamang 2005). The Chobe River and floodplain are heavily utilized by water-dependent wildlife during the dry season when alternative food and water sources are limited (Omphile and Powell 2002). Kasane and Kazungula are located within Town and Mixed land use, respectively. Town land use consisted primarily of residential and commercial areas, along with various tourist facilities. Mixed land use contained more open areas frequented by wildlife, along with several small commercial farms, which grow fruits and vegetables for local sale. Extensive farming within the region is severely constrained by crop raiding and destruction by wildlife, and livestock production systems are focused on subsistence livelihoods. Cattle densities in the study area are have been low since the spread of tsetse fly (*Glossina spp.*) forced the gradual abandonment of cattle posts after the 1940s, and endemic diseases like Foot-and-mouth disease (*Apthae epizooticae*) prevent the sale of animals to the Botswana Meat Commission (BSCO 2011).

Water Sample Collection and Analysis

Collection of grab samples was conducted bi-monthly from July 7, 2011 to March 19, 2014 (n=1630) at 1km intervals across each of the three land use classes (Appendix A). Samples were taken approximately ten meters from the south (Botswana) riverbank from just below the water surface. Abiotic water quality indices were measured from April 25, 2012 – January 31, 2013 (n=512) using a YSI Pro2030 (YSI Inc., Yellow Springs, Ohio, USA), concurrent with water sample collection, and included dissolved oxygen (DO, mg/L), specific conductivity (Cond, mS/cm), and water temperature (°C). Collection of abiotic water quality data for the entire study period was limited due to damage to the instrument.

***E. coli* and total suspended solids**

In river concentrations of *E. coli* were estimated using United States Environmental Protection Agency (USEPA) methods 1103.1 (USEPA 2000) and 1604 (Oshiro 2002), which represent the accepted industry standard for analysis of *E. coli* in aquatic systems. Although limitations exist to the use of *E. coli* for predicting the presence of other waterborne pathogens (Seidler et al. 1981, Desmarais et al. 2002), numerous studies have demonstrated its efficacy as an indicator organism when evaluating levels of fecal contamination in surface water sources and the potential for transmission of microorganisms between humans and wildlife (Edberg et al. 2000, Chapman et al. 2006, Skurnik et al. 2006, Rwego et al. 2008, Literak et al. 2010). The results of both field and laboratory studies also indicate that enteric bacteria are commonly associated with suspended solids in aquatic environments, and this association may influence microbial transport dynamics (Wilkinson et al. 1995, Jamieson et al. 2005a).

Briefly, water grab samples were collected at transect points and vacuum-filtrated through sterile gridded nitrocellulose membrane filters (0.45 µm pore size; Thermo Fisher Scientific, Waltham, Massachusetts, USA). Following filtration of each sample, the sides of the funnel were rinsed twice with 20–30 mL of sterile reagent-grade de-ionized (DI) water. Filters were then aseptically transferred to the surface of a RAPID[®]E.coli2 (BIORAD, Hercules, California, USA) agar plates, and incubated at 37 °C for 24 hours prior to colony enumeration. Total suspended solids (TSS, mg/L) were evaluated using the USEPA method 160.2(USEPA 1983). Briefly, water samples were filtered (Millipore AP-40; Thermo Fisher) and dried at 103-105 °C for one hour before being weighed. This drying cycle was repeated until a constant weight was obtained.

Wildlife biomass and fecal count data

Wildlife biomass estimates were derived from aerial wildlife survey data collected during the 2012 dry season by the Botswana Department of Wildlife and National Parks (DWNP), and are represented as Large Stock Units (LSU) per km² (Boshoff et al. 2002, DWNP 2014). Aerial census data were collected using a stratified systematic transect sampling design and data from the surveys were analyzed using Jolly's (1969) method for sampling blocks of unequal size to obtain wildlife biomass estimates (Jolly 1969). Fecal count data were collected from points along line transects following survey methods described by Jobbins and Alexander (2015) (Jobbins and Alexander 2015). Briefly, we established 55 fecal transects, each 50m in length and spaced

500m apart, perpendicular to the Chobe River starting at the confluence of the Chobe and Zambezi Rivers. Dry season fecal count data (n = 1565) were collected in July, August, and September, 2012. Fecal deposits were spotted at one meter intervals perpendicular to transects as far as the eye could see, and the species and approximate age associated with each fecal sample were identified by an experienced Basarwa tracker.

Simultaneous autoregressive (SAR) spatial models

Statistical analysis of water quality spatial and environmental factors was conducted in the open source, integrated programming environment R (R Core Team, 2013). Simultaneous autoregressive (SAR) spatial models were run using the spdep (Bivand et al. 2005) and ncf (Bjornstad 2008) statistical packages following methodology described by Kissling and Carl (2008, (Kissling and Carl 2008)). The SAR spatial modeling approach takes into consideration autocorrelation structure present in the data. An assumption of the SAR model is that the response at each location is a function of both the explanatory variable at that location, as well as the values of the response at neighboring locations (Lichstein et al. 2002, Kissling and Carl 2008). Equations for the SAR model include the standard terms for predictors ($X\beta$) and errors (ϵ) used in ordinary least squares (OLS) regression, as well as a row standardized spatial weights matrix (W) which describes the relationships between neighboring observations. The matrix W is not required to be symmetrical and allows for inclusion of anisotropy (i.e. directionality). SAR models can take three different forms depending on whether the spatial autoregressive process occurs only in the error term (SARerr), only in the response variable (SARlag), or in both the response and predictor variables (SARmix) (Anselin 2002, Haining 2003, F Dormann et al. 2007). The SARerr equation takes the form

$$Y = X\beta + \lambda Wu + \epsilon$$

where λ is the spatial autoregression coefficient and u is the spatially-dependent error term. In the SARlag equation

$$Y = \rho WY + X\beta + \epsilon$$

ρ is the autoregression parameter which, combined with W , describes spatial autocorrelation in the response variable Y . The SARmix model

$$Y = \rho WY + X\beta + WX\gamma + \varepsilon$$

includes the term $(WX\gamma)$, which describes the regression coefficient (γ) of the spatially lagged predictor variables (WX) . For a more details on the formulation of SAR equations and the estimation of the covariance matrices see Anselin (2002, (Anselin 2002)), Haining (2003, (Haining 2003)), and Fortin and Dale (2005, (Fortin and Dale 2005)).

We classified floodplain as being present from transect point 55 in the Park to point 25 in Town, immediately upstream of where the Chobe River crosses the Mambova fault (Fig. 1). Floodplain was considered absent from the eastern edge of the fault line to the Chobe River's confluence with the Zambezi River (transect points 23-1). Separate wet and dry season models were fit for water quality, land use, floodplain, and fecal count covariates. Due to the shorter collection period for abiotic data, separate models were analyzed for 2012-2013 (Model 1) and 2011-2014 (Model 2). The influence of dry season fecal loading on wet and dry season *E. coli* concentrations was also evaluated. Elephant-specific fecal count data (n=551) were analyzed separately from other wildlife species (n=1014) in order to assess their potential influence on seasonal *E. coli* concentrations. In addition to assessing within-season associations, we also evaluated the influence of dry season fecal loading on mean *E. coli* concentrations during the first three months of the wet season (December-January). Data from even-numbered transects were combined with values from the nearest odd-numbered downstream transect point for analysis in order to scale up fecal count data collected every 500m to our water sampling transects (every 1km). The models were initially fit using ordinary least squares (OLS) regression and Lagrange multiplier (LM) diagnostics were calculated from model residuals in order to identify the nature of spatial dependence (i.e. error, lag, mixed). LM test statistics allow for distinction and selection between the performance and appropriateness of competing spatial models (Anselin 2003). A natural log and Box-Cox transformations were applied to seasonal water quality and fecal count variables, respectively, to better approximate a normal distribution prior to fitting regression models.

Geostatistical Analysis

Spatial autocorrelation (SAC) patterns in wet and dry season *E. coli* and TSS data were examined using the Moran's Index tool in ESRI ArcGIS (Ver. 10.2, Redlands, California). Ordinary kriging was used to interpolate and map spatial patterns of *E. coli* and TSS concentrations in ArcMap Geostatistical Analyst Extension. Ordinary kriging is essentially a generalized linear regression technique that utilizes underlying spatial correlation structure present in the data to derive optimal weights in order to estimate values at un-sampled points. As a best linear unbiased estimator, ordinary kriging also aims to minimize the variance of model errors. In order to satisfy model assumptions that data are approximately normally distributed, we applied a log transformation to *E. coli* and TSS data prior to model fitting, and verified univariate normality using normal qqplots. Eleven theoretical semivariogram models (Circular, Spherical, Tetraspherical, Pentaspherical, Exponential, Gaussian, Rational Quadratic, Hole effect, K-Bessel, J-Bessel, Stable) were fitted through interactive plotting to explore spatial continuity in wet and dry season *E. coli* and TSS data. The influence of anisotropy was also investigated, and model prediction performance was evaluated by cross-validation. Model suitability was assessed based upon the criteria that root-mean-square error (RMSE) and average standard error were minimized, the standardized mean error was close to zero, and the root-mean square standardized error was close to one. A smaller ratio between root-mean-square prediction errors from cross-validation also provides an indication that prediction standard errors are within reasonable limits (ESRI 2001).

Seasonal and trend decomposition using local regression

Temporal patterns of *E. coli* and TSS were analyzed by seasonal and trend decomposition using local regression (STL). STL is an iterative, nonparametric graphical method for describing a time series by its additive seasonal, trend (i.e. a long-term increase or decrease in the data), and remainder (residual) components of variation using locally-weighted regression (LOESS) smoothing (Cleveland et al. 1990). STL proceeds through a series of two nested recursive loops whereby a weight is defined for each observation. Large residuals (e.g. outliers) are assigned smaller weights and small residuals, larger weights, which has the effect of minimizing or

smoothing the influence of outliers, resulting in a robust procedure for visualizing the nonlinear patterns and periodic components of variability within a time series (Cleveland et al. 1990).

Results

Spatiotemporal water quality patterns

Seasonal water quality statistics for the three land use classes are shown in Table 1 and seasonal relationships among water quality variables are summarized for the different land uses classes in Figure 3. Box plots show overall seasonal patterns of *E. coli* and TSS (Fig. 4), and abiotic water quality variables (Fig. 5) with outliers retained. Dry season mean *E. coli* in Park land use (42 CFU/100mL) was 37% higher than in Town and 43% higher than in Mixed land use. Maximum *E. coli* in the Park (519 CFU/100mL) was more than twice that observed in Town and Mixed land use.

A strong seasonal pattern is evident in both *E. coli* and TSS time series, with mean *E. coli* concentrations increasing in late November coinciding with the onset of heavy wet season rainfall, and then declining at the beginning of the dry season in Mixed and Town land use (Fig. 6). In contrast, TSS concentrations were highest in the late dry season and lowest in May when flood waters peaked. Spatial plots of average seasonal *E. coli* and TSS concentrations (Fig. 7) show points 31-39 were influential in driving high dry season levels observed in Park land use. Wet season mean *E. coli* concentrations in the Park were more than twice as high compared to points in Town. Values also varied widely even over relatively short distances. For example, mean dry season *E. coli* at transect point 33 in the Park was more than six times the value recorded at point 29 in Town, just two kilometers downstream.

Monthly mean values for both *E. coli* and TSS concentrations are shown by transect point in Fig 8. *E. coli* and TSS concentrations were highest in January and February, before experiencing a decline in March. Interestingly, *E. coli* concentrations measured at transect points 23-27 in Town, which were generally lower than in Park and Mixed land use classes during all other months, spiked in April coinciding with peak flood height. In the Park, elevated *E. coli* concentrations occurred between July and October, when comparatively low levels were

recorded in Mixed and Town land use. Mean TSS concentrations were also highest in the Park between the months of July and December.

STL time series decomposition

The results of time series decompositions of *E. coli* and TSS data show the strong influence of seasonal factors on Chobe River water quality dynamics (Fig. 9). The lack of an upward or downward trend indicates that concentrations of *E. coli* and TSS did not exhibit any detectable directional change over the course of the study period. Substantial variation attributed to the residual component of the time series data suggests factors separate from those operating on seasonal time scales impact water quality in the system. Finer-scale seasonal variations in *E. coli* and TSS among the different land use classes were also investigated (Appendices D-F). Seasonal contributions to the variability of *E. coli* concentrations was highest in the Park and lowest in Town, while the effect of seasonality on TSS variability generally decreased in a downstream direction from Park to Mixed land use classes.

Kriged water quality maps

E. coli and TSS exhibited a significant clustered spatial autocorrelation pattern in both wet and dry seasons (Appendix B). Semivariogram analysis of log mean *E. coli* and TSS concentrations showed a Gaussian semivariogram model with anisotropy performed best for predicting dry season log *E. coli* and TSS according to model cross-validation (Appendix C). Wet season *E. coli* semivariance was best described by a J-Bessel model with anisotropy, while cross-validation showed a J-Bessel model without anisotropy performed best in predicting wet season TSS concentrations. RMSE for the model predictions was higher in the wet season compared to dry season models. Water quality maps (Fig. 10) of kriged *E. coli* and TSS values across the study showed close spatial overlap across seasons, particularly in Park land use.

Landuse and floodplain influence

Significant spatial error and lag processes ($p < 0.0001$) were observed in all OLS models for both wet and dry seasons, therefore, a SARmix model was used to account for SAC present in the response and predictor variables. Residuals from all seasonal models were not significant at a 0.05 α -level using the Breusch-Godfrey LM test for serial correlation, indicating that the SARmix models were effective in accounting for SAC. In Model 1 (Table 2) only TSS was

found to be statistically significant and positively associated with log-mean *E. coli* ($p < 0.0001$) concentrations during the wet season. Coefficients for the dry season model were significant for dissolved oxygen ($p < 0.0001$), Park land use ($p = 0.0009$), and presence of floodplain ($p = 0.044$). Park land use and floodplain presence were both positively correlated with dry season *E. coli*, while lower DO levels were associated with higher *E. coli* concentrations. In Model 2 (Table 3), TSS was the only wet season variable significantly associated with *E. coli* ($p < 0.0001$), while in the dry season the coefficients for Park land use ($p = 0.0009$) and floodplain presence ($p = 0.016$) were again significant.

Wildlife influence

Analysis of the relationships between terrestrial fecal loading and bacterial concentrations (Table 4) showed a significant positive influence of dry season elephant-specific fecal count (FC) ($p = 0.017$) and other wildlife species FC ($p = 0.001$) on dry season *E. coli* concentrations. Mean dry season elephant FC ($p = 0.029$) and other wildlife FC ($p = 0.006$) were also significant predictors of *E. coli* concentrations during the first three months of the wet season (December-February). Areas of high log wildlife biomass (LSU/km²) estimated from 2012 dry season showed close spatial overlap between aerial wildlife survey data with locations of high mean *E. coli* and TSS concentrations in the kriged water quality maps, particularly during the wet season (Fig. 10). Graphical comparisons of FC in relation to mean seasonal *E. coli* and TSS by transect (Fig. 6) showed transect locations with high dry season terrestrial fecal deposition were associated with higher mean concentrations of bacteria and suspended solids during both wet and dry seasons. This relationship was most apparent at points adjacent to floodplain habitat.

Discussion

In this dryland river system, we observed important water quality declines during the wet season across all land use classes in association with seasonal rainfall and flood pulse dynamics. Patterns of TSS were predictive of *E. coli* concentrations during the wet season. *E. coli* concentrations at the start of the wet season were also significantly associated with dry season fecal loading by elephant and other wildlife, suggesting storm water and sediment runoff are major factors influencing wet season bacterial loads. We observed the greatest water quality declines and variability in Park land use over both wet and dry seasons. Dry season water quality declines in the Park were especially notable given the considerably lower average concentrations

of *E. coli* and TSS recorded in the other land use classes over the same period. Water quality in Mixed land use was less variable than in the Park and only demonstrated declines in the wet season, while Town land use had generally better water quality over both seasons (Figs. 5 and 6).

Water quality dynamics in Mixed and Town land use were typical of those observed in other flood-pulse systems in which declines frequently coincide with the rising limb of flood pulse events (Nagels et al. 2002). However, Park land use exhibited a different pattern in the dry season with peak *E. coli* levels occurring during flood recession. Interestingly, Alexander et al (Alexander and Blackburn 2013) also document the occurrence of annual dry season outbreaks during the flood recession period in children less than five years of age (2006–2009 and 2011–2012). These results suggest that a one health approach, which importantly incorporates consideration of the environment, is necessary to understanding the complex dynamics that link humans and wildlife, and are potentially influential in determining health outcomes.

Overall water quality trends followed dry season distribution of wildlife in this system where higher densities occurred in the Park and lower densities occurred in urbanized areas (Town and Mixed). Dry season concentrations of *E. coli* were significantly higher at locations where extensive floodplain habitat occurred having close spatial agreement with estimates of wildlife biomass derived from aerial survey data. While surface water quality declines are typically associated primarily with human habitation and landscape change such as agriculture, livestock husbandry, industry, and urban development (Muscutt et al. 1993, Brabec et al. 2002), our results suggest that these expectations may not always hold true in areas where wildlife populations concentrate at very high densities along perennial dryland systems.

Arid and semi-arid regions account for a large proportion of the Earth's total land surface but perennial rivers occupy only a small fraction of these landscapes (Levick et al. 2008). As the only permanent surface water source in the 21,000 km² district, the Chobe River has major influence on the ecology, movement, and life history of the region's wildlife (Omphile and Powell 2002, Makhabu 2005, Jackson et al. 2008). While Chobe National Park has an area of 11,700 km², the Chobe River spans ca. 60 km or only one half of one percent of the CNP's total land area. Wildlife access to the Chobe River outside of the CNP's boundaries is becoming increasingly restricted due to rapid expansion of urban land use within the towns of Kasane and Kazungula (BSCO 2011). The lack of reliable alternative surface water sources in the CNP

during the dry season constrains water-dependent wildlife species to forage within relatively short distances from the river (Redfern et al. 2003). Development of artificial waterholes a management strategy within the CNP, however, has generally been limited as these man-made features can potentially transform patterns of wildlife distributions and landscape use, even when natural surface water sources are available (Smit et al. 2007). While many species of browsers and grazers utilize the Chobe River and floodplain during the dry season, our data show that elephants contributed disproportionately to fecal loading within the riparian corridor (Fig. 6). Estimated average dry season elephant density within the Chobe National Park based on aerial survey data was seven LSU/km², but this increased to 13 LSU/km² within a five kilometer buffer distance from the Chobe River. The high concentration of large animals along the Chobe riverfront, while a boon for the region's growing wildlife safari industry, may significantly impact both vegetation and soil communities, in addition to water quality.

Although we see important associations between riparian wildlife densities and water quality, particularly in protected land use, water quality declines were also observed in urban areas (Town) where limited wildlife presence was identified (Fig. 6), which suggests a human influence on water quality dynamics in these locations. Transects where we noted this effect coincided with high-density residential areas where an estimated 76% of the population rely on traditional pit latrines for sanitation (Alexander and Godrej 2015). This highlights the importance of other management tools that are directed at remediating important direct human impacts on surface water (e.g., off site sanitation, waste water treatment, sewage spill mitigation) in this system.

While seasonal influences on surface water quality have been described in other African river systems (Wright 1986, Blum et al. 1987, Akpan and Offem 1993, Jonnalagadda and Mhere 2001), this study is among first to identify large, free-ranging wildlife populations as having a significant influence on spatiotemporal patterns of water quality. Elephant and other large animals play an important role in maintaining the long-term integrity of river corridors in southern Africa, adding nutrients and increasing patch heterogeneity of the riparian landscape (Naiman and Rogers 1997a). However, high wildlife concentrations in riparian corridors during the dry season due to resource restrictions may extend this environmental influence beyond the terrestrial environment to impact water quality dynamics. Although recent research has led to an

improved understanding of how large animals can function as ecosystem engineers impacting the availability of resources to other species (Jones et al. 1996, Naiman and Rogers 1997a), there has been little recognition of this potential influence on aquatic systems. Management of floodplains and riparian habitat seldom involves consideration of potential terrestrial wildlife effects on river system integrity, although consideration of livestock densities is common practice (Hooda et al. 2000). Our results underline the importance of maintaining large, contiguous areas for animals to access surface water in order to minimize the potential impacts of overcrowding on riparian habitat and water quality in vulnerable dryland systems.

Conclusion

Seasonal patterns of rainfall and hydrology often control the distribution of water-dependent wildlife in dryland regions where surface water resources are limited. While it is accepted that livestock, agriculture, and other types of anthropogenic land use can play an important role in water quality declines, wildlife in high densities may also alter the land-aquatic interface in significant ways, potentially influencing water quality dynamics through fecal loading and increased soil erosion. Restriction of water access and compression of wildlife into smaller natural areas could potentially intensify the severity of water quality declines, in addition to increasing existing levels of human-wildlife conflict over available space. Land concessions for competing needs that reduce protected land areas and divert to human development projects may impact water quality dynamics, feeding back to affect the security and welfare of humans and wildlife alike. Future land use and development planning in the Chobe District and other dryland regions of southern Africa should consider potential impacts of landscape alteration on wildlife movements and access to perennial sources of surface water. Efforts to designate and maintain suitable wildlife corridors should be prioritized, both in rural and urban areas. Availability of and access to surface water and floodplain habitat should also be specifically considered in the design and management of protected areas in dryland regions where large, free-ranging wildlife populations occur. This work highlights the importance of an integrated management approach for surface water resources in dryland regions where the impacts of humans, domestic animals, and wildlife are evaluated within the constraints and circumstances of the ecosystem in which they occur.

Acknowledgements

We would like to thank the Government of Botswana's Ministry of Health, Ministry of Environment Wildlife and Tourism, and the Department of Wildlife and National Parks. We further acknowledge Dr. M. Vandewalle, R. Sutcliffe, Cisco, Dr. C. Sanderson, Dr. S. Jobbins, E. Putman, and B. McDonald of Flame of Africa for their generous assistance with field research.

Literature cited

- Akpan, E., and J. Offem. 1993. Seasonal variation in water quality of the Cross River, Nigeria. *Revue d'hydrobiologie tropicale* **26**:95-103.
- Alexander, K., and J. Blackburn. 2013. Overcoming barriers in evaluating outbreaks of diarrheal disease in resource poor settings: assessment of recurrent outbreaks in Chobe District, Botswana. *BMC Public Health* **13**:1-15.
- Alexander, K., and A. Godrej. 2015. Graywater disposal – when the pit latrine is used as a soak away. *Int. J. Environ. Res. Public Health*:Submitted.
- Alexander, K. A., M. Carzolio, D. Goodin, and E. Vance. 2013. Climate change is likely to worsen the public health threat of diarrheal disease in Botswana. *International Journal of Environmental Research and Public Health* **10**:1202-1230.
- Alexander, K. A., J. Herbein, and A. Zajac. 2012. The occurrence of cryptosporidium and giardia infections among patients reporting diarrheal disease in Chobe District, Botswana. *Advances in Infectious Diseases* **2**:143.
- Anselin, L. 2002. Under the hood issues in the specification and interpretation of spatial regression models. *Agricultural economics* **27**:247-267.
- Anselin, L. 2003. An introduction to spatial regression analysis in R. University of Illinois, Urbana-Champaign.
- Bivand, R., A. Bernat, M. Carvalho, Y. Chun, C. Dormann, S. Dray, R. Halbersma, N. Lewin-Koh, J. Ma, and G. Millo. 2005. The spdep package. *Comprehensive R Archive Network*, Version 0.5-83.
- Bjornstad, O. 2008. The ncf Package: spatial nonparametric covariance functions. Version 1.1-1. April 14, 2008.
- Blum, D., S. Huttly, J. Okoro, C. Akujobi, B. R. Kirkwood, and R. G. Feachem. 1987. The bacteriological quality of traditional water sources in north-eastern Imo State, Nigeria. *Epidemiology and Infection* **99**:429-437.
- Boshoff, A., G. Kerley, and R. Cowling. 2002. Estimated spatial requirements of the medium-to large-sized mammals, according to broad habitat units, in the Cape Floristic Region, South Africa. *African Journal of Range and Forage Science* **19**:29-44.

- Brabec, E., S. Schulte, and P. L. Richards. 2002. Impervious surfaces and water quality: a review of current literature and its implications for watershed planning. *Journal of planning literature* **16**:499-514.
- BSCO. 2011 Population and Housing Census 2011 Analytical Report. Page 506 in B. C. S. Office, editor.
- Byappanahalli, M., and R. Fujioka. 1998. Evidence that tropical soil environment can support the growth of *Escherichia coli*. *Water Science and Technology* **38**:171-174.
- Calef, G. W. 1988. Maximum rate of increase in the African elephant. *African Journal of Ecology* **26**:323-327.
- Chapman, C. A., M. L. Speirs, T. R. Gillespie, T. Holland, and K. M. Austad. 2006. Life on the edge: gastrointestinal parasites from the forest edge and interior primate groups. *American Journal of Primatology* **68**:397-409.
- Cleveland, R. B., W. S. Cleveland, J. E. McRae, and I. Terpenning. 1990. STL: A seasonal-trend decomposition procedure based on loess. *Journal of Official Statistics* **6**:3-73.
- Croxen, M. A., R. J. Law, R. Scholz, K. M. Keeney, M. Wlodarska, and B. B. Finlay. 2013. Recent advances in understanding enteric pathogenic *Escherichia coli*. *Clinical Microbiology Reviews* **26**:822-880.
- De Wit, M., and J. Stankiewicz. 2006. Changes in surface water supply across Africa with predicted climate change. *Science* **311**:1917-1921.
- Desmarais, T. R., H. M. Solo-Gabriele, and C. J. Palmer. 2002. Influence of soil on fecal indicator organisms in a tidally influenced subtropical environment. *Applied and Environmental Microbiology* **68**:1165-1172.
- DWNP. 2014. Aerial census of wildlife and some domestic animals in Botswana. Department of Wildlife and National Parks. Monitoring Unit, Research Division. Gaborone.
- Edberg, S., E. Rice, R. Karlin, and M. Allen. 2000. *Escherichia coli*: the best biological drinking water indicator for public health protection. *Journal of Applied Microbiology* **88**:106S-116S.
- F Dormann, C., J. M McPherson, M. B Araújo, R. Bivand, J. Bolliger, G. Carl, R. G Davies, A. Hirzel, W. Jetz, and W. Daniel Kissling. 2007. Methods to account for spatial autocorrelation in the analysis of species distributional data: a review. *Ecography* **30**:609-628.

- Fortin, M.-J., and M. R. T. Dale. 2005. *Spatial analysis: a guide for ecologists*. Cambridge University Press.
- Fujioka, R., C. Sian-Denton, M. Borja, J. Castro, and K. Morpew. 1998. Soil: the environmental source of *Escherichia coli* and enterococci in Guam's streams. *Journal of Applied Microbiology* **85**:83S-89S.
- Gaughan, A., and P. Waylen. 2012. Spatial and temporal precipitation variability in the Okavango–Kwando–Zambezi catchment, southern Africa. *Journal of Arid Environments* **82**:19-30.
- Haining, R. P. 2003. *Spatial data analysis*. Cambridge University Press Cambridge.
- Hardina, C., and R. Fujioka. 1991. Soil: The environmental source of *Escherichia coli* and enterococci in Hawaii's streams. *Environmental Toxicology and Water Quality* **6**:185-195.
- Hooda, P., A. Edwards, H. Anderson, and A. Miller. 2000. A review of water quality concerns in livestock farming areas. *Science of the Total Environment* **250**:143-167.
- Jackson, T. P., S. Mosojane, S. M. Ferreira, and R. J. van Aarde. 2008. Solutions for elephant *Loxodonta africana* crop raiding in northern Botswana: moving away from symptomatic approaches. *Oryx* **42**.
- Jamieson, R., D. M. Joy, H. Lee, R. Kostaschuk, and R. Gordon. 2005. Transport and deposition of sediment-associated *Escherichia coli* in natural streams. *Water Research* **39**:2665-2675.
- Jobbins, S. E., and K. A. Alexander. 2015. WHENCE THEY CAME-ANTIBIOTIC-RESISTANT *ESCHERICHIA COLI* IN AFRICAN WILDLIFE. *Journal of Wildlife Diseases*.
- Jolly, G. 1969. Sampling methods for aerial censuses of wildlife populations. *East African agricultural and forestry journal* **34**:46-49.
- Jones, C. G., J. H. Lawton, and M. Shachak. 1996. Organisms as ecosystem engineers. Pages 130-147 *Ecosystem management*. Springer.
- Jonnalagadda, S., and G. Mhere. 2001. Water quality of the Odzi River in the eastern highlands of Zimbabwe. *Water Research* **35**:2371-2376.
- Junk, W. J., P. B. Bayley, and R. E. Sparks. 1989. The flood pulse concept in river-floodplain systems. *Canadian special publication of fisheries and aquatic sciences* **106**:110-127.

- Kissling, W. D., and G. Carl. 2008. Spatial autocorrelation and the selection of simultaneous autoregressive models. *Global Ecology and Biogeography* **17**:59-71.
- Levick, L. R., D. C. Goodrich, M. Hernandez, J. Fonseca, D. J. Semmens, J. C. Stromberg, M. Tluczek, R. A. Leidy, M. Scianni, and D. P. Guertin. 2008. The ecological and hydrological significance of ephemeral and intermittent streams in the arid and semi-arid American southwest. US Environmental Protection Agency, Office of Research and Development.
- Levy, K., A. E. Hubbard, K. L. Nelson, and J. N. Eisenberg. 2009. Drivers of water quality variability in northern coastal Ecuador. *Environmental Science & Technology* **43**:1788-1797.
- Lichstein, J. W., T. R. Simons, S. A. Shriner, and K. E. Franzreb. 2002. Spatial autocorrelation and autoregressive models in ecology. *Ecological Monographs* **72**:445-463.
- Literak, I., M. Dolejska, T. Radimersky, J. Klimes, M. Friedman, F. M. Aarestrup, H. Hasman, and A. Cizek. 2010. Antimicrobial-resistant faecal *Escherichia coli* in wild mammals in central Europe: multiresistant *Escherichia coli* producing extended-spectrum beta-lactamases in wild boars. *Journal of Applied Microbiology* **108**:1702-1711.
- Lorntz, B., A. M. Soares, S. R. Moore, R. Pinkerton, B. Gansneder, V. E. Bovbjerg, H. Guyatt, A. M. Lima, and R. L. Guerrant. 2006. Early childhood diarrhea predicts impaired school performance. *The Pediatric infectious disease journal* **25**:513-520.
- Magole, L. I., and O. Gojamang. 2005. The dynamics of tourist visitation to national parks and game reserves in Botswana. *Botswana Notes and Records*:80-96.
- Makhabu, S. W. 2005. Resource partitioning within a browsing guild in a key habitat, the Chobe Riverfront, Botswana. *Journal of Tropical Ecology* **21**:641.
- Middleton, N., and D. Thomas. 1997. *World atlas of desertification*. Arnold, Hodder Headline, PLC.
- Milly, P. C., K. A. Dunne, and A. V. Vecchia. 2005. Global pattern of trends in streamflow and water availability in a changing climate. *Nature* **438**:347-350.
- Mondal, D., R. Haque, R. B. Sack, B. D. Kirkpatrick, and W. A. Petri. 2009. Attribution of malnutrition to cause-specific diarrheal illness: evidence from a prospective study of preschool children in Mirpur, Dhaka, Bangladesh. *The American journal of tropical medicine and hygiene* **80**:824-826.

- Muscutt, A., G. Harris, S. Bailey, and D. Davies. 1993. Buffer zones to improve water quality: a review of their potential use in UK agriculture. *Agriculture, Ecosystems & Environment* **45**:59-77.
- Mutembwa, A., and G. S. F. Initiative. 1998. Water and the potential for resource conflicts in southern Africa. Global Security Fellows Initiative.
- Nagels, J., R. Davies-Colley, A. Donnison, and R. Muirhead. 2002. Faecal contamination over flood events in a pastoral agricultural stream in New Zealand. *Water Science & Technology* **45**:45-52.
- Naiman, R. J., and K. H. Rogers. 1997a. Large animals and system-level characteristics in river corridors. *Bioscience* **47**:521-529.
- Naiman, R. J., and K. H. Rogers. 1997b. Large animals and system-level characteristics in river corridors. *Bioscience*:521-529.
- O'Reilly, C. E., P. Jaron, B. Ochieng, A. Nyaguara, J. E. Tate, M. B. Parsons, C. A. Bopp, K. A. Williams, J. Vinjé, and E. Blanton. 2012. Risk factors for death among children less than 5 years old hospitalized with diarrhea in rural western Kenya, 2005–2007: a cohort study. *PLoS medicine* **9**:e1001256.
- Omphile, U. J., and J. Powell. 2002. Large ungulate habitat preference in Chobe National Park, Botswana. *Journal of range management*:341-349.
- Oshiro, R. 2002. Method 1604: Total Coliforms and *Escherichia coli* in water by membrane filtration using a simultaneous detection technique (MI Medium). Washington, DC: US Environmental Protection Agency.
- Petri, W. A., M. Miller, H. J. Binder, M. M. Levine, R. Dillingham, and R. L. Guerrant. 2008. Enteric infections, diarrhea, and their impact on function and development. *The Journal of clinical investigation* **118**:1277-1290.
- Pricope, N. G. 2013. Variable-source flood pulsing in a semi-arid transboundary watershed: the Chobe River, Botswana and Namibia. *Environmental Monitoring and Assessment* **185**:1883-1906.
- Redfern, J. V., R. Grant, H. Biggs, and W. M. Getz. 2003. Surface-water constraints on herbivore foraging in the Kruger National Park, South Africa. *Ecology* **84**:2092-2107.

- Rwego, I. B., G. ISABIRYE-BASUTA, T. R. Gillespie, and T. L. Goldberg. 2008. Gastrointestinal bacterial transmission among humans, mountain gorillas, and livestock in Bwindi Impenetrable National Park, Uganda. *Conservation Biology* **22**:1600-1607.
- SADC. 2006. Regional Water Policy. Southern African Marketing Company, Gabarone.
- Schuyt, K. D. 2005. Economic consequences of wetland degradation for local populations in Africa. *Ecological Economics* **53**:177-190.
- Seidler, R. J., T. Evans, J. Kaufman, C. Warwick, and M. W. LeChevallier. 1981. Limitations of standard coliform enumeration techniques. *Journal of the American Water Works Association* **73**:538-342.
- Skarpe, C., J. du Toit, and S. R. Moe. 2014. Elephants and savanna woodland ecosystems: a study from Chobe National Park, Botswana. John Wiley & Sons.
- Skurnik, D., R. Ruimy, A. Andremont, C. Amorin, P. Rouquet, B. Picard, and E. Denamur. 2006. Effect of human vicinity on antimicrobial resistance and integrons in animal faecal *Escherichia coli*. *Journal of Antimicrobial Chemotherapy* **57**:1215-1219.
- Smit, I. P., C. C. Grant, and B. J. Devereux. 2007. Do artificial waterholes influence the way herbivores use the landscape? Herbivore distribution patterns around rivers and artificial surface water sources in a large African savanna park. *Biological Conservation* **136**:85-99.
- Steiner, T., A. Lima, J. Nataro, and R. Guerrant. 1998. Enteroaggregative *Escherichia coli* produce intestinal inflammation and growth impairment and cause interleukin-8 release from intestinal epithelial cells. *Journal of Infectious Diseases* **177**:88-96.
- Tooth, S. 2000. Process, form and change in dryland rivers: a review of recent research. *Earth-Science Reviews* **51**:67-107.
- Tooth, S. 2013. Dryland fluvial environments: assessing distinctiveness and diversity from a global perspective. *Treatise on Geomorphology*. San Diego: Academic Press.
- Tooth, S., and T. S. McCarthy. 2007. Wetlands in drylands: geomorphological and sedimentological characteristics, with emphasis on examples from southern Africa. *Progress in Physical Geography* **31**:3-41.
- USEPA. 1983. *Methods for Chemical Analysis of Water and Wastes*, EPA-600/4-79-020. Methods 160.2. Washington, DC.

- USEPA. 2000. Improved Enumeration Methods for the Recreational Water Quality Indicators: Enterococci and Escherichia coli EPA-821/R97/004. Section 10.3 Modified E coli method. Page 53. Washington, DC.
- Vandewalle, M. 2003. Historic and recent trends in the size and distribution of northern Botswana's elephant population. Pages 7-16 *in* Effects of fire, elephants and other herbivores on the Chobe riverfront ecosystem. Proceedings of a Conference organised by the Botswana-Norway institutional Cooperation and Capacity Building Project (BONIC). Gaborone: Government Printer.
- Walker, K. F., F. Sheldon, and J. T. Puckridge. 1995. A perspective on dryland river ecosystems. *Regulated Rivers: Research & Management* **11**:85-104.
- WHO. 2002. "Health and Environment in Sustainable Development." World Health Organization, Geneva.
- Wilkinson, J., A. Jenkins, M. Wyer, and D. Kay. 1995. Modelling faecal coliform dynamics in streams and rivers. *Water Research* **29**:847-855.
- Wright, R. 1986. The seasonality of bacterial quality of water in a tropical developing country (Sierra Leone). *Journal of Hygiene* **96**:75-82.

Tables

Table 2-1 Arithmetic mean, maximum, and standard deviation of seasonal E. coli and TSS concentrations by land use class, calculated from water quality samples collected bimonthly from July 2011- March 2014.

Location	E.coli (CFU/100mL)						TSS (mg/L)					
	Wet			Dry			Wet			Dry		
	Mean	Max	sd	Mean	Max	sd	Mean	Max	sd	Mean	Max	sd
Mixed	56	257	38	27	197	21	7.9	18.2	3.5	4.3	14.0	2.3
Town	36	397	39	29	239	40	6.0	23.6	3.8	3.9	10.0	2.2
Park	54	373	63	42	519	44	7.3	45.0	7.3	6.4	43.3	6.7

Table 2-2 Model 1 – SAR mixed model results testing the effects of explanatory variables from 2012-2013 on seasonal log-mean E. coli (CFU/100mL)

Variable	Dry Season				Wet Season			
	Coefficient	Std. error	Z-value	P-value	Coefficient	Std. error	Z-value	P-value
LN_TSS	0.1477	0.0848	1.7422	0.081	0.7507	0.1512	4.9655	<0.0001
LN_Cond	-0.0411	0.0815	-0.5042	0.614	0.0501	0.1425	0.3515	0.725
LN_DO	-2.0939	0.3386	-6.1833	<0.0001	0.0330	0.1057	0.3121	0.755
LN_Temp	-0.6993	0.4740	3.1704	0.056	-1.0189	1.3822	-0.7372	0.461
Land use (reference is Mixed)								
Park	1.5029	0.3359	0.4456	0.002	-0.1213	0.7975	-0.1521	0.879
Town	0.1497	0.3401	0.3585	0.656	-0.5214	0.6105	-0.8540	0.393
Floodplain (reference is Absent)								
FldPln Present	0.6576	0.3270	2.0108	0.044	-0.3173	0.5970	-0.5316	0.595

Table 2-3. Model 2 – SAR mixed model results testing the effects of explanatory variables from 2011-2014 on seasonal log-mean *E. coli* (CFU/100mL)

Variable	Dry Season				Wet Season			
	Coefficient	Std. error	z-value	P-value	Coefficient	Std. error	z-value	P-value
LN_TSS	0.0316	0.0361	0.8758	0.381	0.3306	0.0502	6.5885	<0.0001
Land use (reference is Mixed)								
Park	1.0802	0.3270	3.3034	0.0009	0.6327	0.4028	1.5708	0.116
Town	-0.0992	0.2495	-0.3976	0.691	-0.0694	0.3096	-0.2243	0.823
Floodplain (reference is Absent)								
FldPln Present	0.5470	0.2265	2.5151	0.016	0.2477	0.2215	1.1179	0.264

Table 2-4. Model 3 - SAR mixed model results testing the influence of terrestrial within and between-season fecal loading on log-mean *E. coli* (CFU/100mL).

Variable	Dry Season				Wet Season			
	Coefficient	Std. error	z-value	P-value	Coefficient	Std. error	z-value	P-value
Ele_FC ⁺	0.1324	0.0552	2.4001	0.017	-	-	-	-
Wild_FC [*]	0.2201	0.0669	3.2883	0.001	-	-	-	-
Dry_ele_FC ⁺	-	-	-	-	0.1297	0.0593	2.1863	0.029
Dry_wild_FC [*]	-	-	-	-	0.2233	0.0816	2.7364	0.006

Dry season fecal counts for elephant⁺ and for all other wildlife species excluding elephants^{*}, were compared to dry season *E. coli* concentrations. We also assessed the influence of dry season fecal count data on *E. coli* concentrations at the start of the wet season (December-February).

Figures

Figure 2-1. MODIS Terra (left) and Advanced Land Imager, EO-1 satellite imagery acquired on same day, May 8, 2010 (modified image using public domain data available from the USGS EROS Center). The vast Chobe-Zambezi floodplain system is visible at two different scales showing the dominant geological and hydrological influence of the Mambova fault.

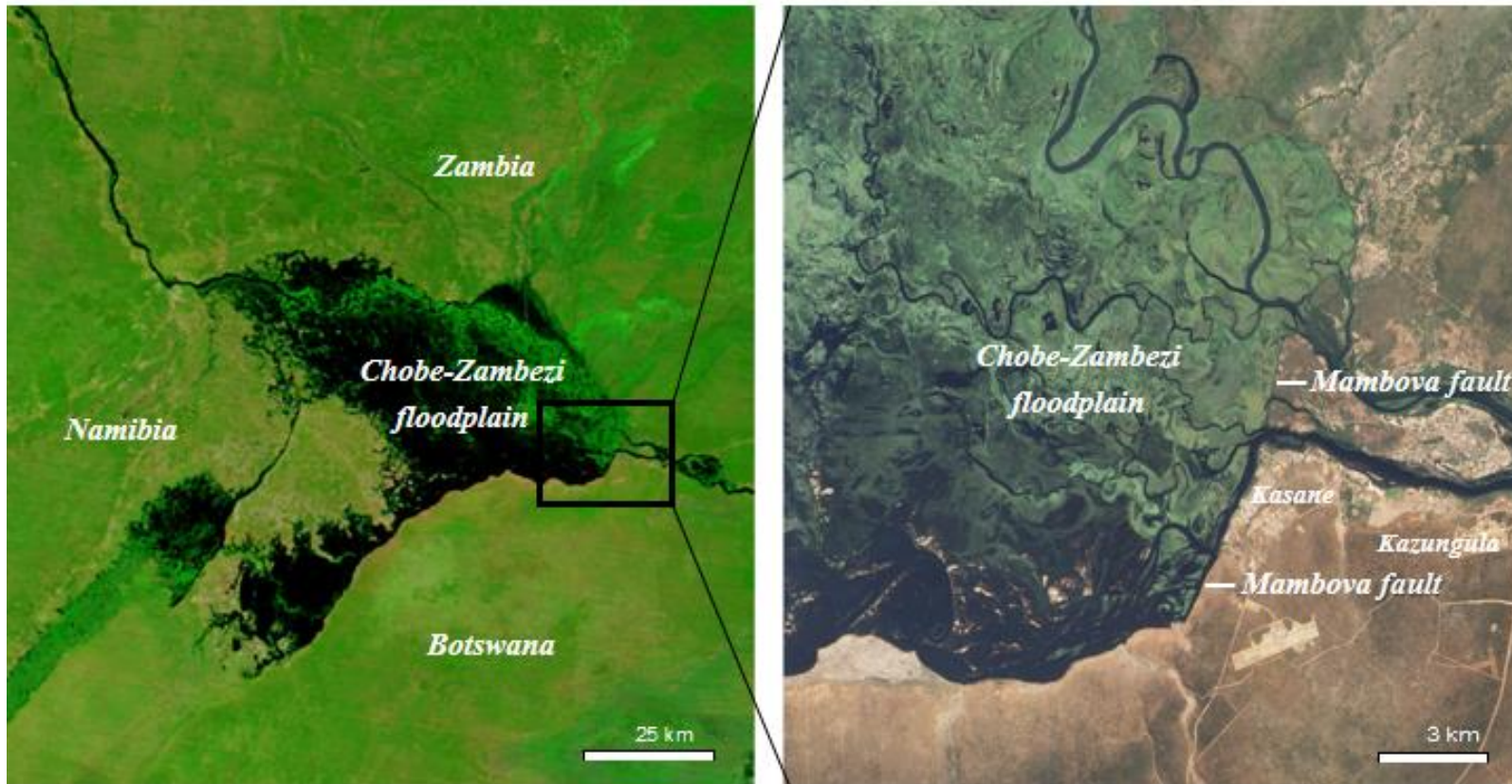


Figure 2-2. Landsat-based map of the Chobe River study area. Dominant land uses are shown within the three representative land use types, which include: Park (solid green line), Town (red), and Mixed-use (light blue). The Chobe National Park border is also shown (dashed black line), along with water quality transect points (black triangles) and the Kasane water purification facility (blue cross). Chobe River flow direction is indicated by the blue arrow.

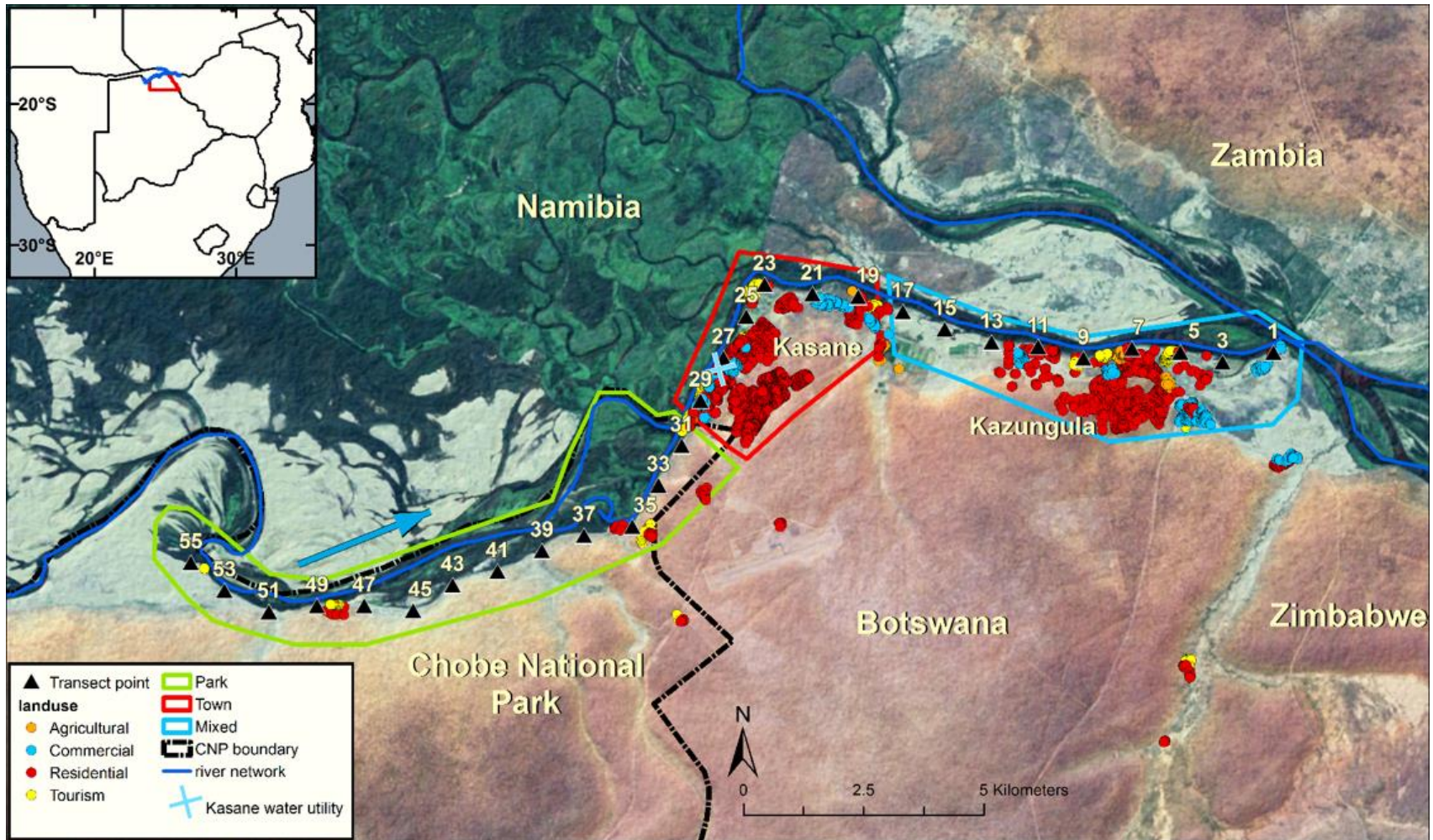


Figure 2-3. Seasonal relationships among water quality variables are summarized for the different land use classes. Red cells indicate that the mean value for each variable and land use is greater than the global mean for the study area, while blue symbolizes values below the global mean.

	Wet Season			Dry Season		
Variable	Park	Town	Mixed	Park	Town	Mixed
<i>E. coli</i> (CFU/100mL)	Red	Blue	Red	Red	Blue	Blue
TSS (mg/L)	Red	Blue	Red	Red	Blue	Blue
DO (mg/L)	Red	Blue	Blue	Red	Blue	Blue
Cond (mS/cm)	Red	Blue	Blue	Red	Blue	Blue
Temp (°C)	Red	Blue	Blue	Red	Blue	Blue

Figure 2-4. Box plots with outliers retained showing seasonal patterns of *E. coli* (CFU/100mL) and TSS (mg/L), in the Chobe River by land use class. Variability in the concentration data was high across all land use classes during both seasons, but was greatest within the Park and generally lower in Town and Mixed land use. Median wet season *E. coli* and TSS were similar to dry season median concentrations in Park and Town land use. In Mixed land use, median wet season concentrations were more than twice those observed during the dry season.

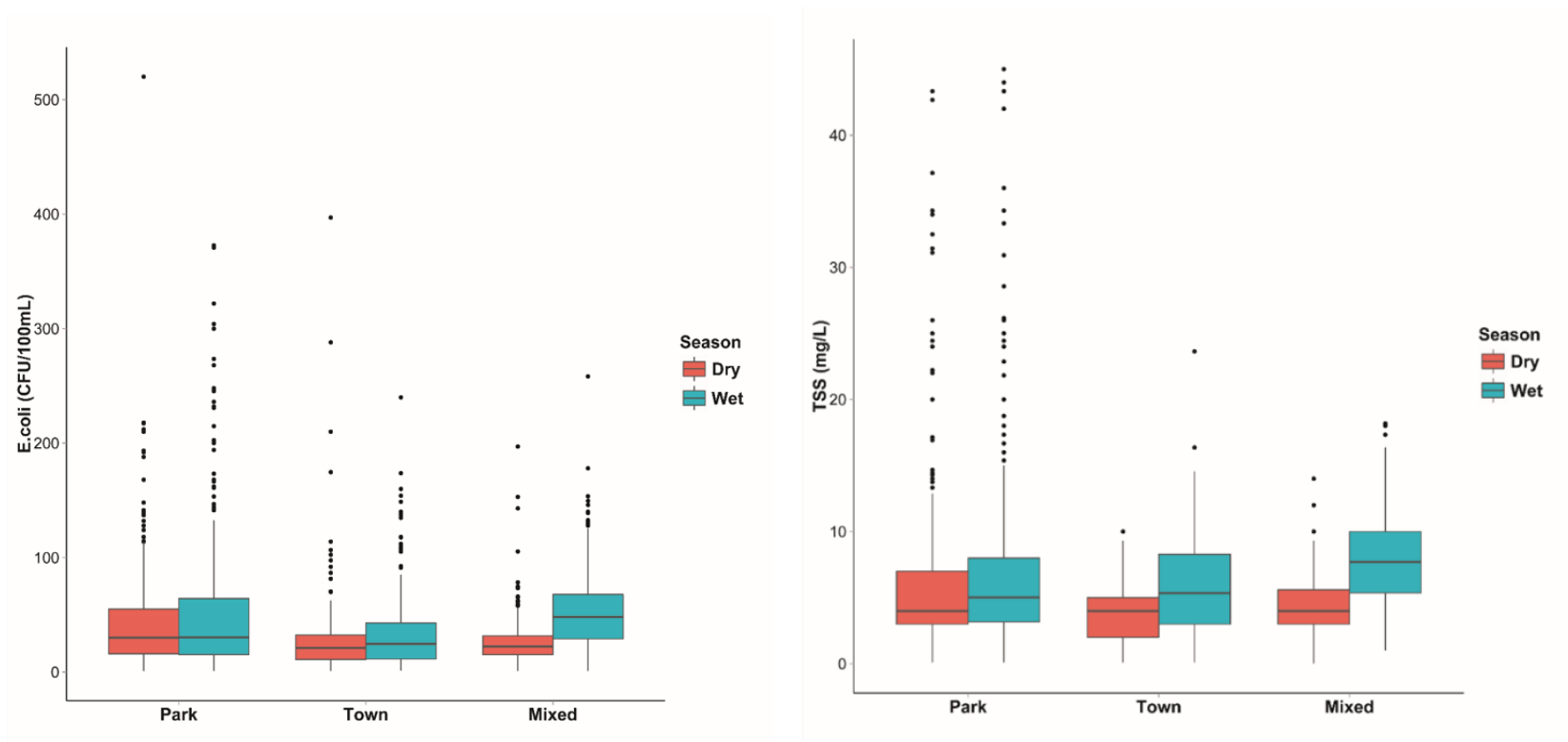


Figure 2-5. Box plots with outliers retained showing seasonal patterns of water temperature ($^{\circ}\text{C}$), dissolved oxygen (mg/L), and specific conductivity (mS/cm) in the Chobe River by land use class. Median values were similar across all three land use classes during the dry season, but differed substantially during the wet season. Median wet season DO was highest in the Park (despite having higher water temperature) compared to downstream levels, which may reflect greater primary productivity from vegetation in the Chobe River floodplain and its associated wetland systems. Median seasonal conductivity and interquartile range were highest in Park land use, with monthly median values ranging from a low of 0.04 mS/cm (May) at peak flood height, to a high of 0.42 mS/cm (October) when water levels were lowest. The range of observed seasonal values for water temperature, DO, and conductivity for the Chobe River were comparable to those recorded by Mackay et al. (2011) for the Okavango River Delta in 2006-2007 (Mackay et al. 2011).

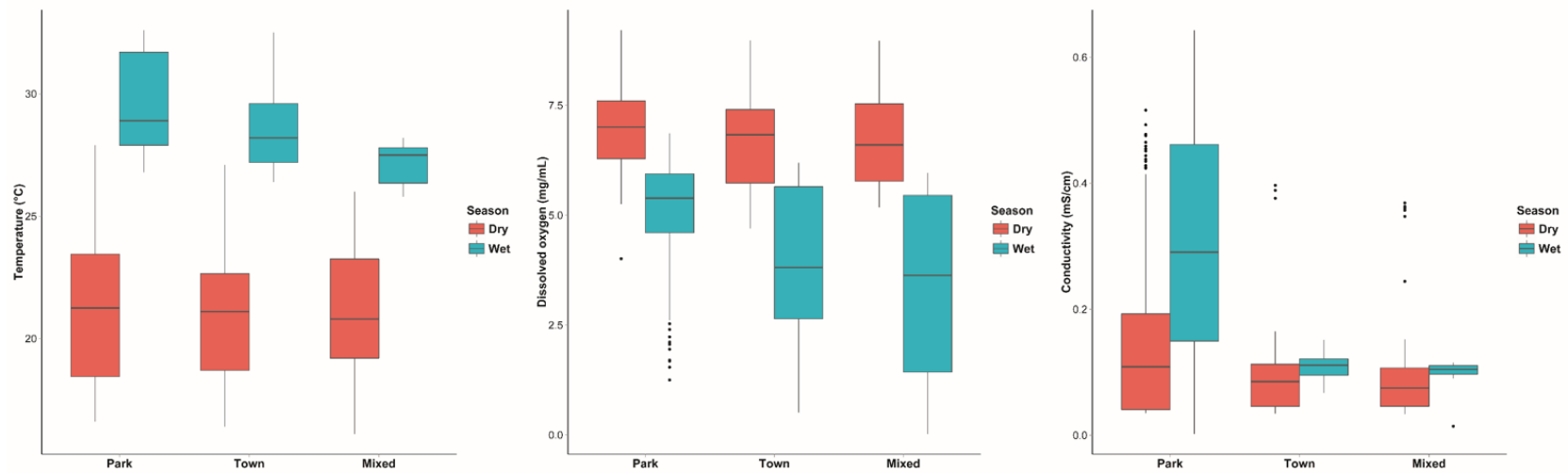


Figure 2-6. Monthly time series of bi-monthly water sampling data showing temporal and spatial variation of mean *E. coli* (CFU/100mL) and TSS (mg/L) concentrations with standard errors by month and land use class in relation to daily precipitation (mm), and Chobe River height (m).

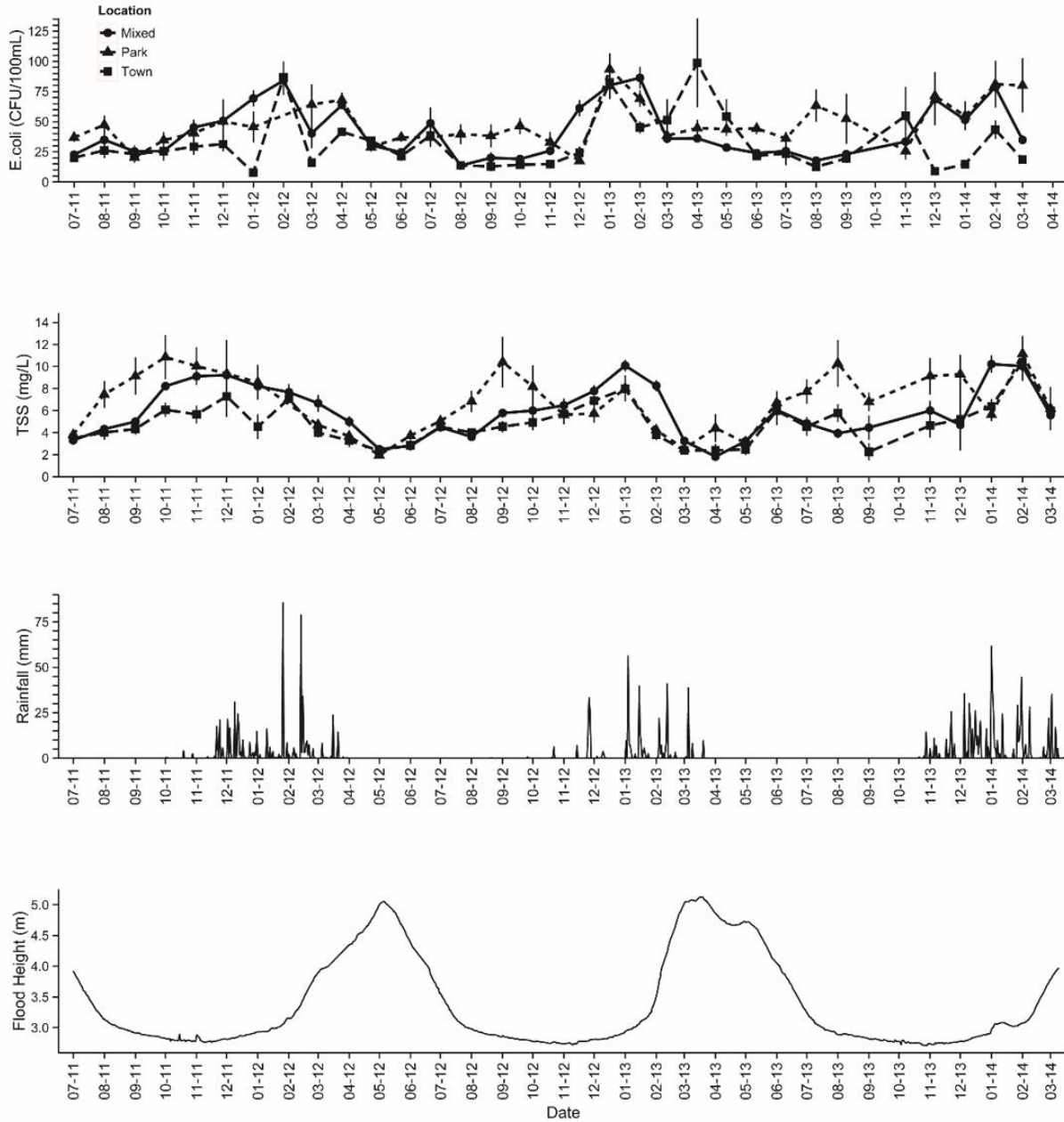


Figure 2-7. Arithmetic means of bi-monthly water sampling data by transect point showing seasonal and spatial variability of *E. coli* (CFU/100mL) and TSS (mg/L) concentrations with standard errors in relation to dry season mean fecal counts of elephant and other wildlife species. Transect points were assigned to three general land use types and proceed in an upstream direction from Mixed-use (1-17, Blue), Town (19-29, Red), Park (31-55, Green). Transect points where in-channel floodplain was present are indicated by the brown bracket.

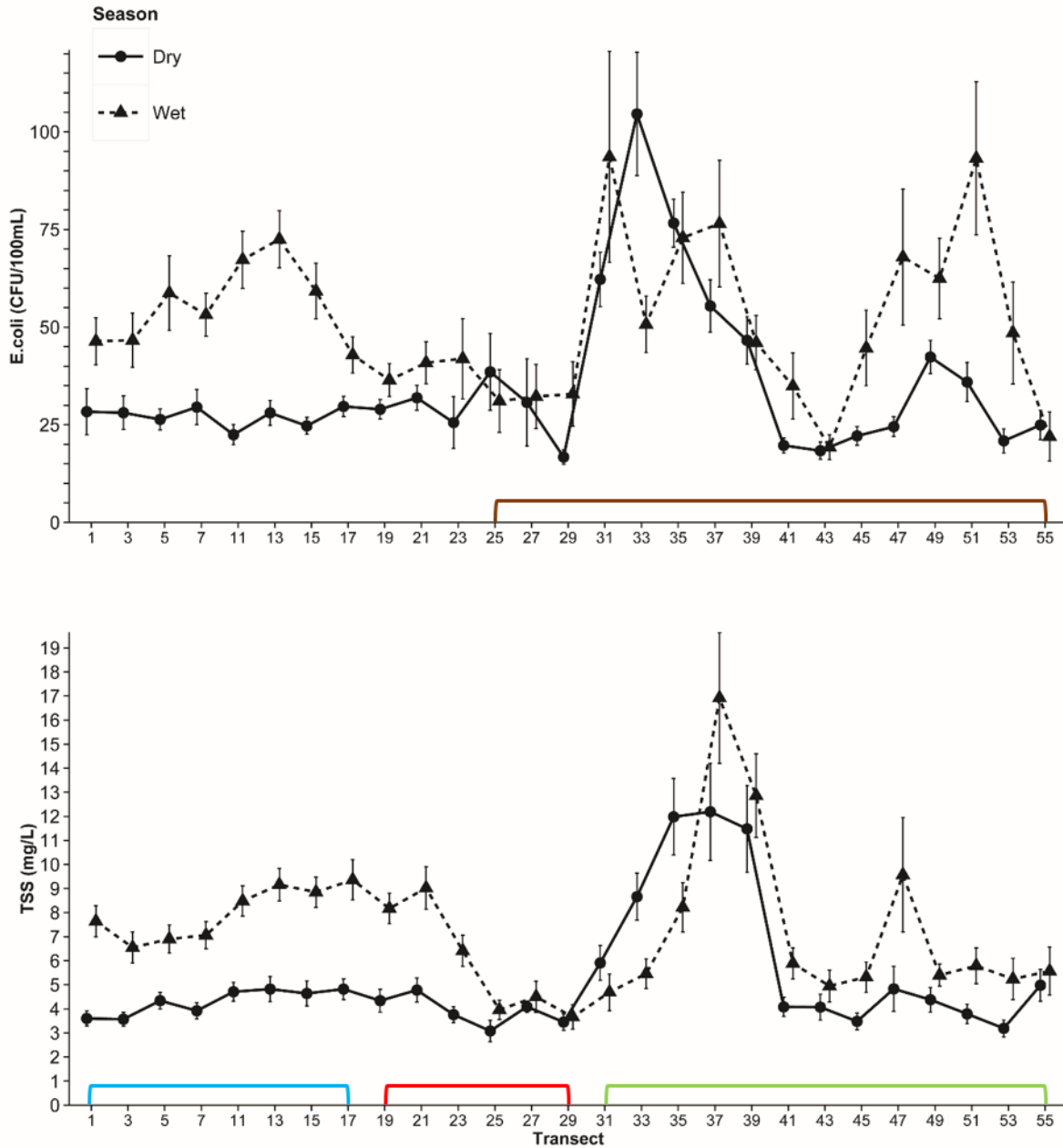


Figure 2-8. Mean *E. coli* (CFU/100ml) and TSS (mg/L) time series data by individual month and transect with standard errors. Monthly averages for the study area (all transect) are indicated by the red horizontal lines.

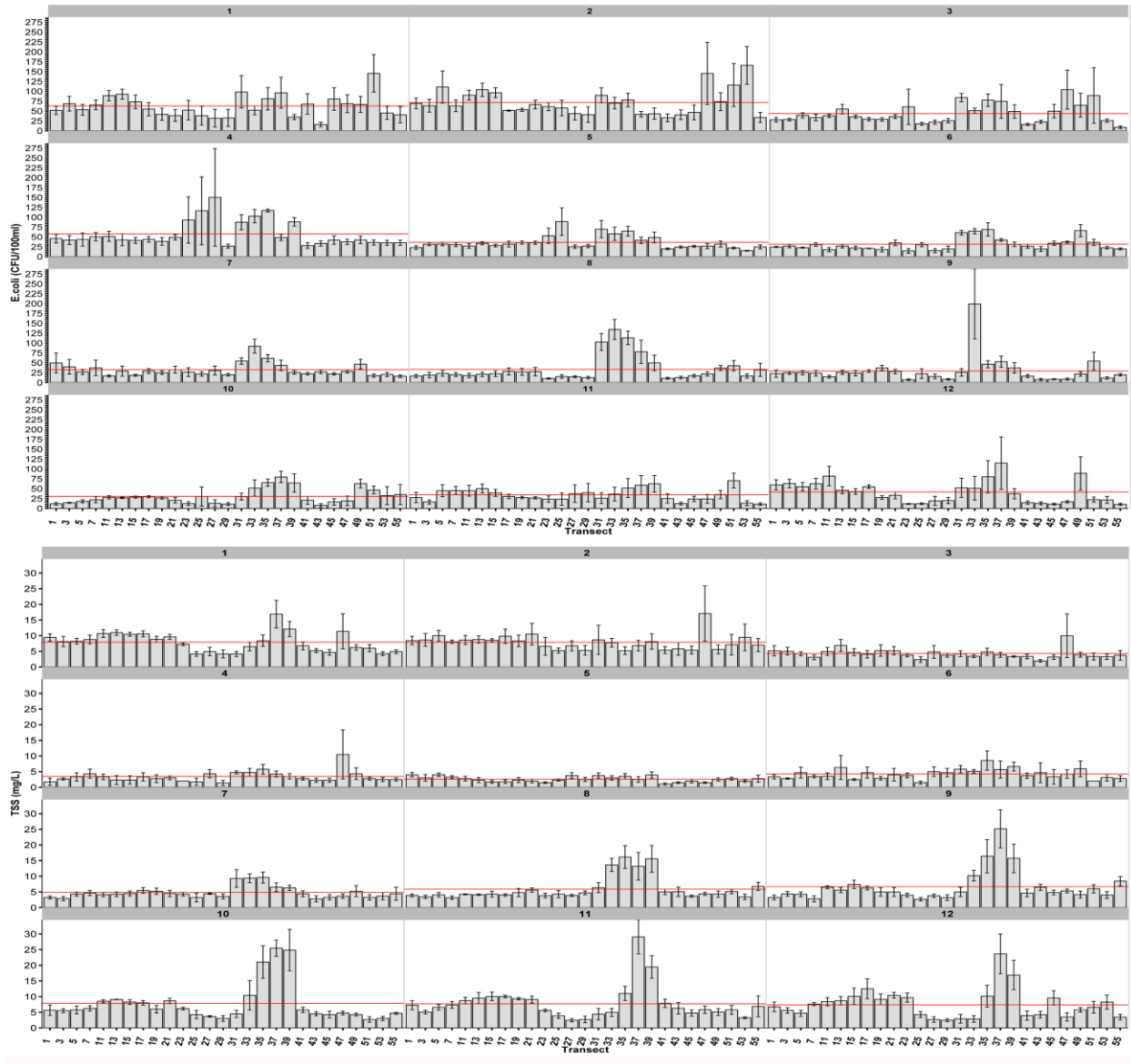


Figure 2-9. Seasonal and trend decomposition using loess (STL) for *E. coli*. and TSS water quality data collected bi-monthly from July 7, 2011 – March 19, 2014. Raw data are displayed in the top panel as averaged values for all transect points with a two week sampling frequency, followed by seasonal, trend, and residual components. Scale differs for each of the components so relative magnitude is indicated by the gray bars on the right side of the panels. The bar in the top panel represents a single unit of variation, with larger bars indicating a smaller amount of variation attributable to a particular component.

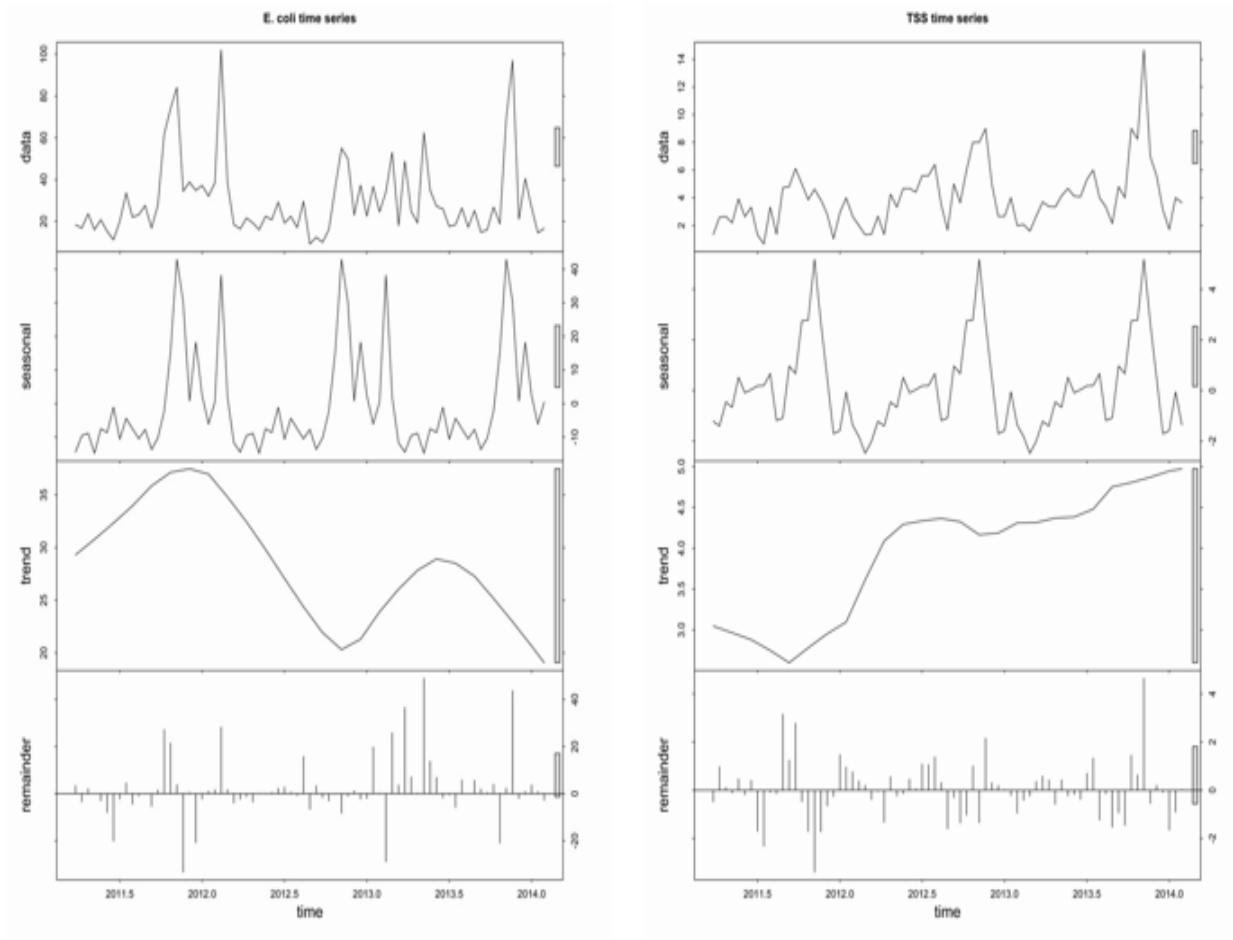
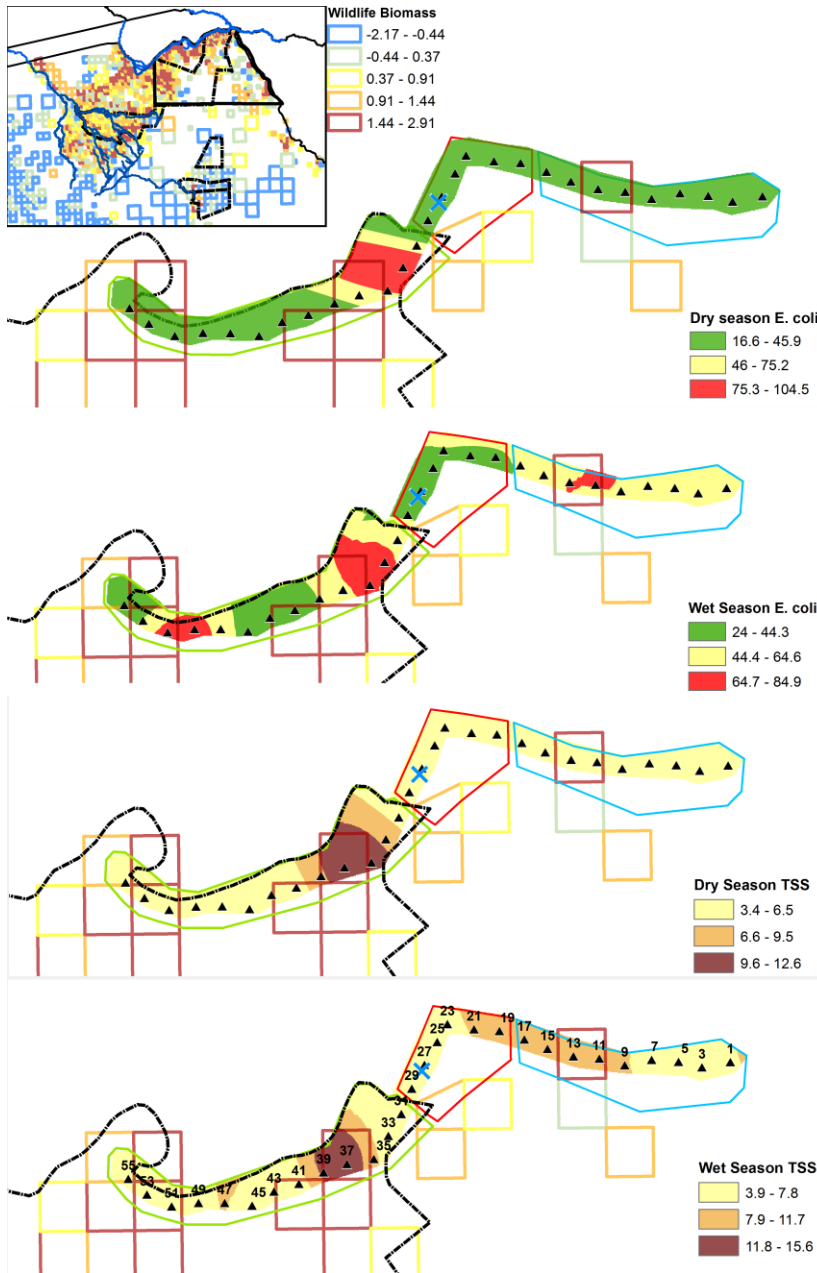


Figure 2-10. Raster surfaces of seasonal mean *E. coli* (CFU/100mL) and TSS (mg/L) estimated using ordinary kriging, overlaid with 2012 dry season aerial survey data showing log wildlife biomass (kg/km²). The Chobe National Park (dashed black line), Kasane water plant (light blue cross), transect points (triangles) and general land use classes: Park (green solid line), Town (red), and Mixed (light blue) are also shown. Close spatial overlap between areas of high and low *E. coli* and TSS concentrations can be seen during both wet and dry seasons.



Appendices

Appendix A. Geographical coordinates for water quality sampling transect points.

Transect	Latitude	Longitude
1	-17.79486	25.26083
3	-17.79657	25.25079
5	-17.79465	25.24252
7	-17.79385	25.23305
11	-17.79332	25.21464
13	-17.79243	25.20551
15	-17.78987	25.19636
17	-17.78654	25.18817
19	-17.78359	25.17946
21	-17.78300	25.17049
23	-17.78112	25.16112
25	-17.78713	25.15744
27	-17.79487	25.15289
29	-17.80288	25.14832
31	-17.81139	25.14456
33	-17.81878	25.13991
35	-17.82654	25.13472
37	-17.82814	25.12519
39	-17.83095	25.11691
41	-17.83475	25.10815
43	-17.83725	25.09935
45	-17.84194	25.09155
47	-17.84095	25.08192
49	-17.84087	25.07268
51	-17.84191	25.06321
53	-17.83781	25.05453
55	-17.83248	25.04798

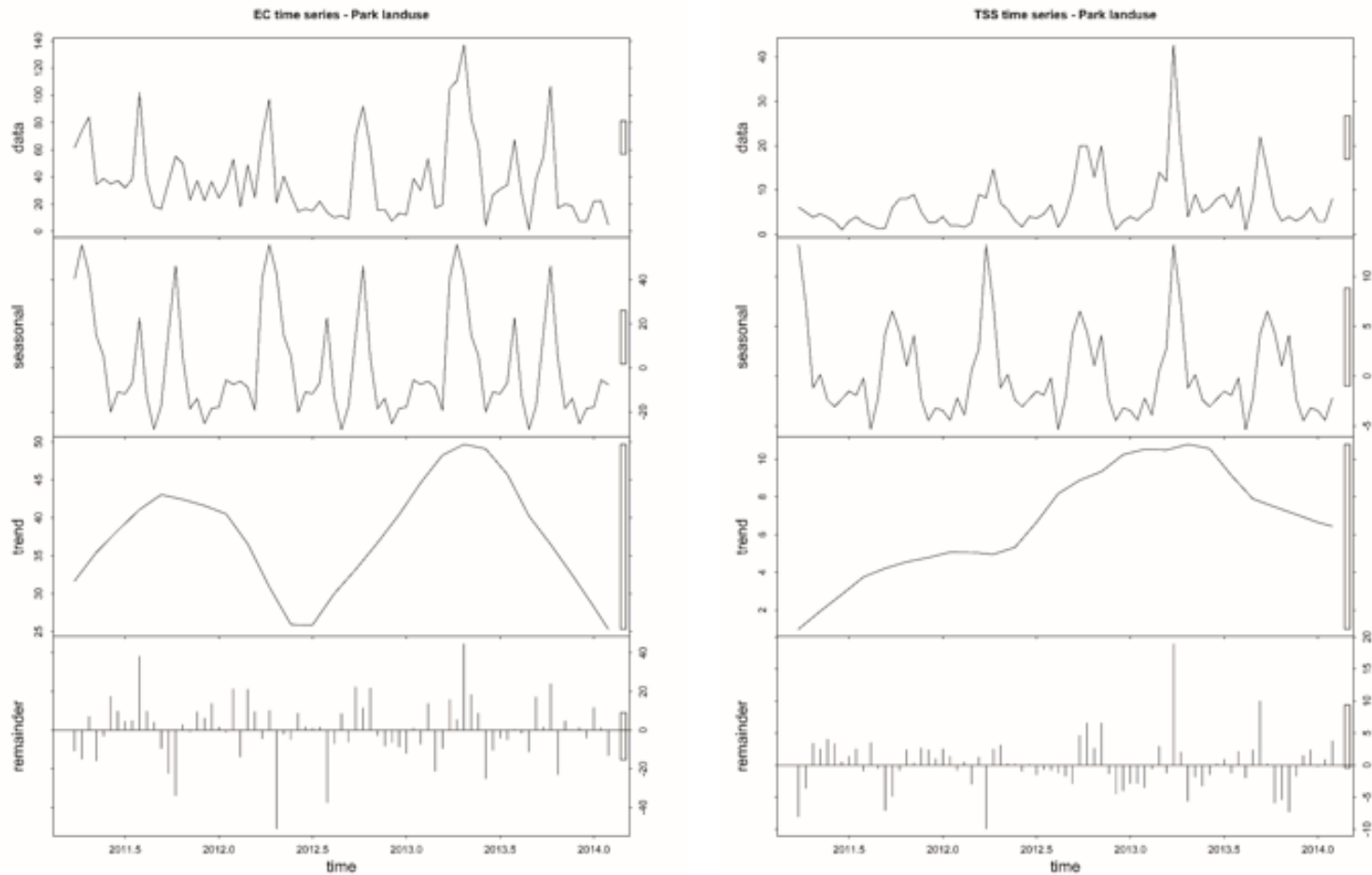
Appendix B. Moran's I test results for spatial autocorrelation in seasonal *E. coli* and TSS data.

Variable	Moran's I	E(X)	var(X)	z-score	P-value
Dry season <i>E. coli</i>	0.227395	-0.0011	5.9E-05	29.7514	< 0.0001
Dry season TSS	0.24419	-0.0012	7.1E-05	29.0642	< 0.0001
Wet season <i>E. coli</i>	0.031631	-0.0014	0.00002	7.42253	< 0.0001
Wet season TSS	0.202886	-0.0014	0.00011	19.7651	< 0.0001

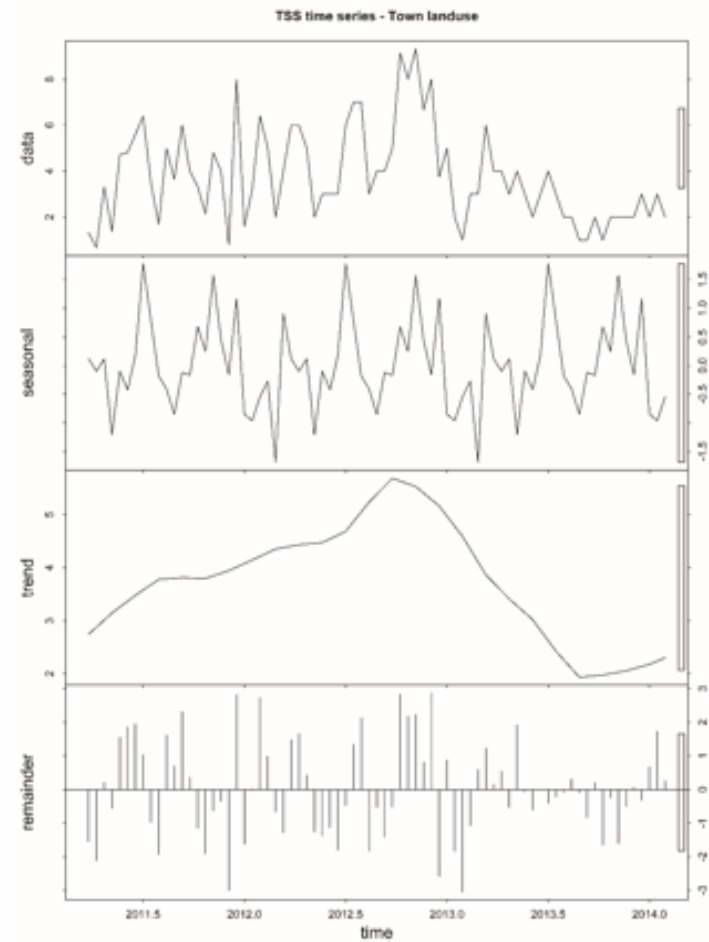
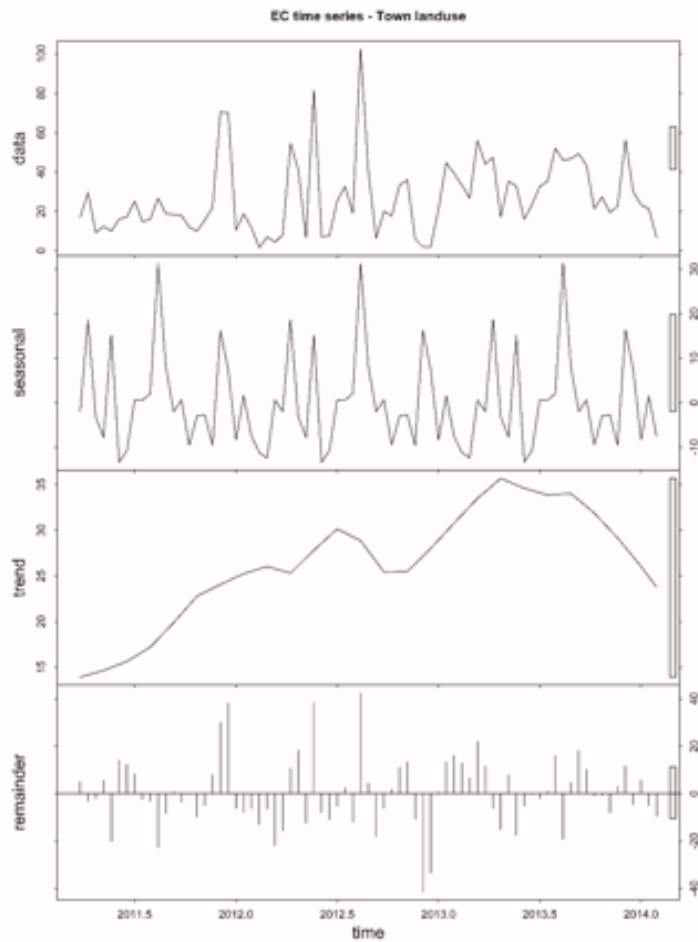
Appendix C. Cross-validation statistics for semivariogram models that best-predicted seasonal *E. coli* and TSS water concentrations.

Variable	Model	Root-Mean-Square Error	Average Standard Error	Root-Mean-Square Standardized Error
Dry_ <i>E. coli</i>	Gaussian	8.041	7.563	1.366
Wet_ <i>E. coli</i>	J-Bessel	17.126	17.435	1.057
Dry_TSS	Gaussian	1.112	1.151	1.022
Wet_TSS	J-Bessel	1.619	1.492	1.194

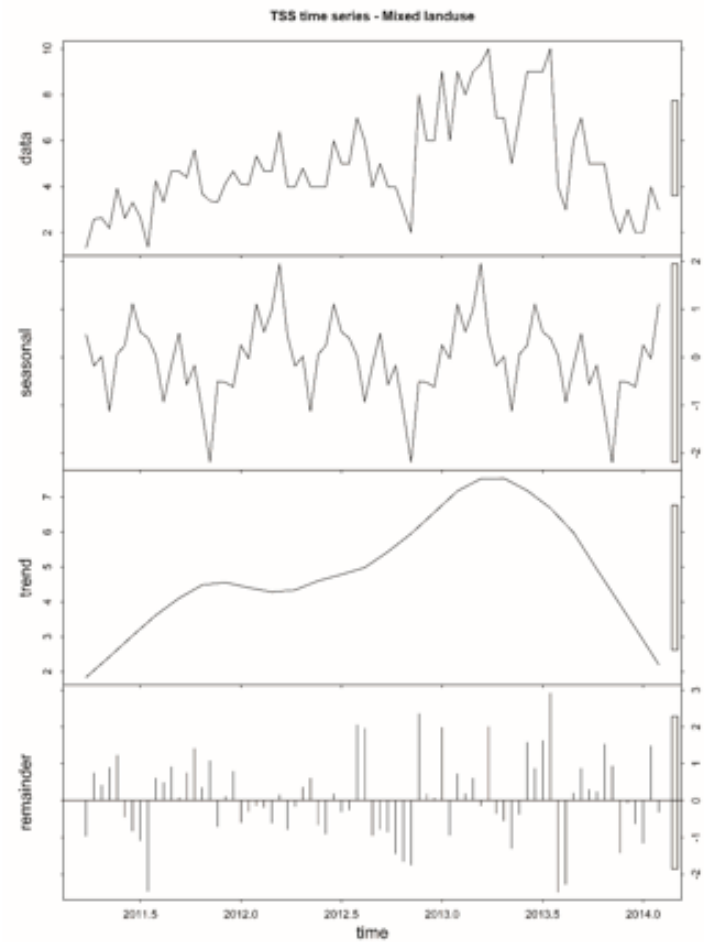
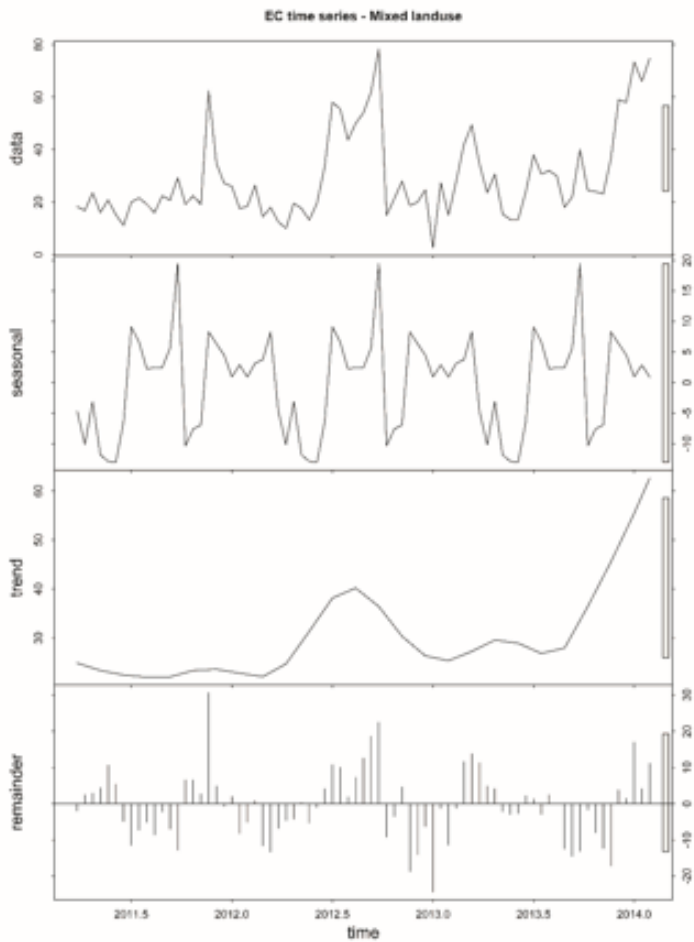
Appendix D. Seasonal and trend decomposition using loess (STL) of *E. coli.* and TSS water quality data collected over the period July 7, 2011 – March 19, 2014 in Park land use. Raw data are displayed in the top panel as averaged values for all transect points with a two week sampling frequency, followed by seasonal, trend, and residual components. Scale differs for each of the decomposed components so relative magnitude is indicated by the gray bars on the right side of the panels. The bar in the top panel can be considered as a single unit of variation, with larger bars indicating a smaller amount of variation attributable to a particular component.



Appendix E. Seasonal and trend decomposition using loess (STL) of *E. coli*. and TSS water quality data collected over the period July 7, 2011 – March 19, 2014 in Town land use. Raw data are displayed in the top panel as averaged values for all transect points with a two week sampling frequency, followed by seasonal, trend, and residual components. Scale differs for each of the decomposed components so relative magnitude is indicated by the gray bars on the right side of the panels. The bar in the top panel can be considered as a single unit of variation, with larger bars indicating a smaller amount of variation attributable to a particular component.



Appendix F. Seasonal and trend decomposition using loess (STL) of *E. coli*. and TSS water quality data collected over the period July 7, 2011 – March 19, 2014 in Mixed land use. Raw data are displayed in the top panel as averaged values for all transect points with a two week sampling frequency, followed by seasonal, trend, and residual components. Scale differs for each of the decomposed components so relative magnitude is indicated by the gray bars on the right side of the panels. The bar in the top panel can be considered as a single unit of variation, with larger bars indicating a smaller amount of variation attributable to a particular component.



Chapter 3: A multi-temporal remote sensing analysis of land cover change dynamics, recent fire history, and elephant browsing in the semi-arid savanna of northern Botswana.

Abstract

Savannas occupy a fifth of the earth's land surface, yet despite their ecological and economic significance understanding of the complex couplings and feedbacks that drive spatiotemporal patterns of land cover (LC) change is lacking. We evaluated LC changes occurring across the 21,000 km² Chobe District of northern Botswana using Landsat TM, ETM+, and OLI satellite imagery for 1990, 2003, and 2013. Net and gross LC changes were assessed for the Chobe National Park (CNP) and six protected forest reserves, as well as for buffer areas around seven towns and villages, and the riparian corridor of the Chobe River. An estimated 10892 km² (52%) of Chobe District land area experienced quantifiable LC changes during the study period. Woodland cover had a net decline of 1514 km² (16.2% of total woodland area) from 1990-2013 and shrubland had net expansion of (1305 km², 15.7%), while grassland also grew by 265.3 km² (20.3% of class total). Woodland losses were higher along the Chobe River than elsewhere in the Chobe District. While elephants are often cited as an important driver of woodland losses, particularly along the Chobe River corridor, we observed limited quantifiable changes in woodland cover associated with areas of high elephant biomass (Large Stock Units/km²) in 2003 and 2013. Dynamic couplings between precipitation and fire were evident in multi-decadal time series data. Analysis of daily active fire data from the Moderate Resolution Imaging Spectroradiometer (MODIS) showed that 2001-2013 fire frequencies were highly variable across the Chobe District. While detected fires were largely a dry season phenomenon, fire frequency and intensity were dynamic over time, with high fire years typically following years with fewer fires, and more fires in years with higher rainfall. This suggests greater plant biomass in years of high rainfall increase dry season fuel loads conducive to fire ignition and spread. The majority of active fires were located in wet/irrigated vegetation in 2003, while in 2013 woodland burned most frequently. Gettis-Ord GI* Hot Spot Analysis showed several significant clusters of fires associated with locations experiencing high rates of woodland change

Introduction

Savanna woodlands are a vital resource for wildlife and contribute to landscape heterogeneity by altering levels of soil moisture and nutrients which in turn impact the distribution of associated plant communities (Belsky et al. 1989). Woodlands, both natural and managed, benefit ecosystem functionality by providing essential habitat for a wide range of taxa, regulating decomposition processes, and nutrient cycling, limiting precipitation runoff and soil erosion and securing water quality (Anderson et al. 1976, Swift et al. 1979, Lowrance et al. 1997, McCulley et al. 2004). Water-restricted environments experiencing strong seasonal climate regimes are particularly vulnerable to natural and human-induced land cover (LC) changes (Wessels et al. 2004). An estimated 70% of dryland regions are affected by various forms of land degradation, with rural communities being particularly impacted (Dregne et al. 1991, Wily and Mbaya 2001). Knowledge of when and where changes have occurred across the landscape is essential to protecting plant and wildlife biodiversity, as well as traditional cultures and livelihoods. Yet, information remains scarce regarding the nature of long-term LC changes for much of southern Africa.

While most researchers agree that competition, population demographics, climate, and historical disturbance regimes all are present and interact in dynamic and complex ways to influence structure and function of savanna systems, considerable debate exists about whether these assumptions and mechanisms hold true under all conditions or are mutually exclusive under certain conditions (Sankaran et al. 2004). Vegetation patterns in savanna ecosystems are clearly shaped by climate variability and disturbances, while positive feedbacks from vegetation and nonlinearities present in the coupled plant-climate system influence the magnitude of plant community responses to external forcing (Zeng and Neelin 2000). A continental-scale analysis of tree cover in African savannas by Bucini and Hanan (2007) suggests the magnitude of a disturbance largely depends upon mean annual precipitation (MAP) regimes across rainfall zones. In semi-arid savannas (MAP 400-650mm) such as those in northern Botswana, MAP exerts a stronger control over maximum tree cover along with disturbances that act as strong modifiers. In mesic savannas (MAP >1600mm), precipitation no longer strongly limits tree cover, and disturbance impacts become more important in maintaining the system, while in arid savannas (MAP <400mm) the opposite is true (Bucini and Hanan 2007). While precipitation controls maximum realizable woody cover in arid savannas, disturbance dynamics control savanna structure in areas that receive MAP in excess of 650 ± 134 mm (Sankaran et al. 2005). In

these unstable “disturbance-driven savannas”, fire and herbivory are essential maintain both trees and grasses in the system by preventing woodlands from attaining a closed canopy state (Bond et al. 2003).

Studies of land cover changes in dryland areas such as the Chobe District have typically focused on short time spans and areas of less than 100 km² (Child 1968, Simpson 1975, Ben-Shahar 1993, Moe et al. 2009, Teren and Owen-Smith 2010, Rutina and Moe 2014, Skarpe et al. 2014a), or on LC change occurring solely in the Chobe National Park (Mosugelo et al. 2002). Global-scale initiatives including Global Land Cover Network’s (GLCN) Africover project and the European Space Agency’s Globcover mapping project are currently unavailable for Botswana or are coarse in scale. Global forest cover change assessments using automated processing chains often fail to identify open canopy savanna woodlands and accurately discriminate between grasslands and shrublands, particularly in semi-arid regions with strong rainfall seasonality (Bontemps et al. 2011, Hansen et al. 2013).

In this study, we classified and mapped savanna LC in the Chobe District, Botswana. Northern Botswana, which typifies semi-arid savanna in southern Africa, and serves as an important ecosystem model to evaluate influential factors driving landscape change across the region. We used 30-meter resolution imagery from Landsat Thematic Mapper (TM), Enhanced Thematic Mapper Plus (ETM+), and Operational Land Imager (OLI) satellites, in order to characterize patterns of landscape change between 1990 and 2013. In addition to identifying spatial and temporal changes on a regional scale, we quantified LC changes occurring within the boundaries of the National Park and six protected forest reserves, and in buffer areas surrounding major towns and villages and the riparian corridor of the only permanent surface water, the Chobe River. Finally, we evaluated the intensity of land cover change in the Chobe District and the nature of couplings and feedbacks between ecological, environmental, and anthropogenic components that influence long-term LC change patterns, with a particular focus on the effects of fire and browsing by elephants on woodland change dynamics.

Methods

Study area

The 21,000 km² Chobe District located in northeastern Botswana is a semi-arid savanna ecosystem which supports diverse assemblages of species and habitats of global conservation significance, including the largest elephant (*Loxodonta africana*) population on the African continent (Blanc, 2007). The region is characterized by highly variable seasonal rainfall, with nearly all annual precipitation (avg. 604 mm) falling during the summer wet season (December – April), followed by a general absence of rain from May to November. A mosaic of private, state, and tribal land use and management units exist within the Chobe District, (Fig. 1). Communal lands are typically utilized for livestock grazing and agriculture at lower intensity than other Botswana districts due to extensive crop raiding by wildlife and endemic livestock diseases like Foot-and-mouth (*Aphthae epizooticae*). Protected areas occupy approximately 58% of the District's total land area, of which the Chobe National Park (CNP) occupies 11,700 km², along with six protected forest reserves and extensions: Kazuma, Maikaelelo, Sibuyu, Chobe, and Kasane Forest Reserves, and the Kasane Forest Reserve Extension, with a combined land area of approximately 4550 km². The town of Kasane is the regional government seat (est. population 9,008), along with Kazungula (est. pop. 4,133) are the largest urban settlements in Chobe District (BCSO, 2011). Human population density is generally low outside of Kasane and Kazungula, with most of the districts villages located in the Chobe Enclave, a 1,690 km² communally-managed land holding located along the District's northern border with Namibia and completely enclosed by the Chobe National Park to the east and west, Chobe Forest Reserve to the south, and the Chobe River to the north. There are five main villages in the Enclave: Kachikau, Kavimba, Mabele, Satau, and Parakarungu, with a combined population of 7,500 people (BCSO, 2011). Approximately 30% of the population work outside of the Enclave, while within the Enclave, 85% of households engage in crop production and 75% own livestock (Painter 1997). Livestock are raised for family consumption or local sale as endemic diseases like foot and mouth prevent the movement and sale of animals to the Botswana Meat Commission (BCSO, 2011). A majority of households extract forest and wetland resources for subsistence purposes, including firewood, food and traditional medicine, thatching grass, reeds, poles and other materials for building and crafts (Jones 2002, Schuyt 2005).

Surface water resources

The Chobe River and its wetlands provide the only permanent source of surface water in the Chobe District. As a transboundary watershed, the Chobe River Basin is considered a core component of the Kavango-Zambezi (KAZA) Transfrontier Conservation Area, shared by Angola, Botswana, Namibia, Zambia, and Zimbabwe (Pricope 2013). The Chobe River enters Botswana from Namibia as the Kwando (Cuando) River, becoming the Linyanti River as it flows along the border between Botswana and Namibia's Caprivi Strip, becoming the Chobe River after exiting the seasonally-flooded Lake Liambezi. In high flood years, large areas of the Chobe Enclave are inundated as far upstream as Lake Liambezi, reaching its highest water levels in March and April. Flooding of the Chobe River during the dry season coincides with drying ephemeral water holes across the region, driving wildlife to congregate in very high densities along the riverfront, especially within the borders of the CNP (Omphile and Powell 2002, Alexander and Blackburn 2013). Elephant and impala in particular, have been often blamed for degrading the vegetation community and causing the disappearance of large *Acacia* and other mature trees in the Chobe riparian forest fringe (Mosugelo et al. 2002, Moe et al. 2009, Rutina and Moe 2014)

Protected woodlands

Woodlands in Botswana and southern Africa were heavily-utilized in the early 20th century for commercial logging, agriculture, livestock grazing, extraction of firewood and building materials, food, and traditional medicines (Schuyt 2005). Beginning in the 1930s, the Botswana government granted concessions to timber harvesting companies in the District's present day forest reserves in exchange for royalties on the lumber extracted and sold (Lepetu et al. 2010). Between the mid-1930s and the 1950s, concentrated commercial logging operation which targeted Bloodwood (*Pterocarpus angolensis*) and Zambezi teak (*Baikiaea plurijuga*) greatly reduced the areal coverage of woodlands in the Chobe District (Skarpe et al. 2014a). Vegetation surveys conducted in 1965 (Child 1968) and 1969-1971 (Simpson 1975) noted that the once dense woodlands had been reduced to isolated patches by intensive timber extraction and replaced by shrub-dominated savannah. Kasane Forest Reserve was established in 1968 under the National Forest Act for the expressed purpose of conservation and management of valuable forest resources. In 1980, the reserve system was greatly expanded, adding the Kazuma, Maikaelelo, Sibuyu, Chobe, and Kasane Extension Forest Reserves. With most raw timber being

exported to neighboring South Africa and Zimbabwe, growing concerns about the economic sustainability of these arrangements, along with a lack of concessionaire adherence to contractual agreements, led the government to suspend all commercial harvesting operations in 1993 (FAO 2010). Botswana's forest policies have subsequently seen a shift away from an emphasis on commercial logging to one of multiple use zoning and community-based management in order to better serve the needs of the local human population (Lepetu et al. 2010).

Climatological data

Daily precipitation data from Kasane spanning the period 1922-2014 were provided by the Department of Meteorological Services, Botswana. Singular spectrum analysis (SSA) implemented in the [rssa] statistical package in the open source integrated programming environment R (R Core Team, 2013) was used to analyze rainfall time series data (Golyandina et al. 2001, Golyandina and Stepanov 2005). SSA is a non-parametric statistical method of analysis involving decomposition of time series data into a sequence of multi-dimensional lagged vectors and eigenvalues. Diagonal averaging is used to identify and extract equal elements in the time series and reconstruct time series components from the resulting matrix (Wu and Chau 2011). In this way, it is possible to extract and decompose important elements and whole signals from time series, into simpler data structures that retain all the information, and visualize the underlying oscillatory, trend, and noise components contained in the original data set (Marques et al. 2006).

Satellite Image Data Sources

Landsat satellite images for Chobe District were obtained from the United States Geological Survey (USGS) for the years 1990 (Landsat 5 Thematic Mapper; TM), 2003 (Landsat 7 Enhanced Thematic Mapper Plus; ETM+), and 2013 (Landsat 8 Operational Land Imager; OLI) (Fig. 2). In order to mitigate seasonal effects on land cover we tried to minimize the time between images acquired by the satellites, with acquisition dates ranging from April 8-28 (Appendix G). Landsat TM, ETM+, and OLI sensors have a spatial resolution of 30-meters for the visible, shortwave infrared (SWIR) and near infrared (NIR) bands. Spectral band and spatial resolution characteristics of the different Landsat platforms are summarized in Appendices H-J. Images from each time step were integrated into a geographic information system (GIS) database in preparation for conducting a time series analysis of historical trends and drivers of forest resource change in Chobe District.

Image pre-processing

Satellite image-based change detection involves the quantification and evaluation of shifting temporal and spatial patterns of landuse between two or more time periods. Data acquired by satellites are affected by the sun zenith angle, earth-sun distance, atmospheric conditions, and area topography, in addition to the temporal characteristics of the land feature of interest. In order to utilize remote sensing data to evaluate actual changes occurring on the land surface, it is necessary to first reduce scene-to-scene variability in images from different sensors and time periods by standardizing data onto a common geographic and radiometric scale. Pre-processing also allows for isolation and removal of factors which may degrade the image quality, while making it possible to focus analysis solely upon temporal changes associated with land surface features of interest. Prior to analysis, Landsat images were geometrically co-registered to reduce distortions and pixel errors which might be interpreted as actual LC changes. Landsat TM and ETM+ images were processed to surface reflectance using the Ecosystem Disturbance Adaptive Processing System (LEDAPS), while Landsat OLI surface reflectance was calculated using the USGS L8SR algorithm.

Principal components analysis

Multi-spectral data often possess a high degree of correlation among adjacent spectral bands, and therefore, using methods to extract significant spectral information while eliminating redundancy can be helpful in LULC classification (Schowengerdt 1983, Eklundh and Singh 1993). Principle components analysis (PCA) has been frequently used in change detection studies due to its relatively simplicity and effectiveness in enhancing information and reducing redundancy of interrelated variables, while retaining all of the information contained in the original data (Yeh and Li 1997, Lu et al. 2004, Deng et al. 2008). In the present study, PCA was used to transform the original multi-band Landsat images in preparation for LC classification and change detection. The first three principal components were found to contain >98% of the original information contained in the multi-spectral datasets for 1990, 2003, and 2013, and were used for all LC classifications.

Land cover classification

As the majority of woody plant species in the region are deciduous and timing of leaf loss is highly variable, minimizing time between image acquisitions is extremely important to achieving accurate LC classification results. We observed poor performance of supervised methods of classification in differentiating between cover types in the highly heterogeneous landscape, particularly grassland and shrubland. Poor performance of maximum likelihood supervised classification methods has also been noted for other semi-arid savannah systems where environmental and ecological variability create a mosaic landscape of diverse plant community assemblages (Kiage et al. 2007). In this study, we used unsupervised Interactive Self-Organizing Clustering (ISO Cluster) analysis in ArcMap 10.2 (ESRI, Redlands, California) to classify LC in the PCA-transformed images. The ISO Cluster procedure is based on an iterative process that uses a migrating means technique to compute minimum Euclidean distance and assign each image pixel to one of a certain number of user-defined clusters. Upon each iteration, new means are calculated and each cell is assigned to the closest mean in multidimensional attribute space until migration of cells from one cluster to another becomes minimal. PCA-transformed image pixels were grouped into 45 spectral clusters using a sampling interval of 25 cells with a minimum class size of 150 cells, and a 3x3 majority filter applied to reduce noise and outliers. Spectral clusters from the unsupervised classification were then assigned to one of six land cover classes based on the following definitions:

Water: Inland water bodies including major rivers, water-filled pans, reservoirs, and watering holes

Wet/irrigated vegetation: Wetland, floodplain, and riparian vegetation; inundated grass/herbaceous cover; irrigated agricultural land and saturated vegetation surrounding ephemeral water pans

Grassland: Short and tall grass/herb-dominated ground cover sometimes interspersed with poorly-developed layer of bushes and shrubs or sparse low-growing trees occupying <10% cover; *Stipagrostis uniplumi*, *S. ciliaris*, *Eragostris pallens*

Woodland: Trees generally >3 meters in height with canopy cover of >30%; frequently intermixed with a shrub or grass understory; *Baikiaea plurijuga*, *Colophospermum mopane*, *Pterocarpus angolensis*, *Schinziophyton rautanenii*, *Guibourtia coleosperma*, *Burkea Africana*

Shrubland: Short woody vegetation with heights <3 meters in height; frequently occurring along sharp transition zones with woodlands; *Dichrostachys cinerea*, *Combretum spp.* *Capparis tormentosa*, *Terminalia sericea*, *Dicrostachys cinerea*, *Acacia mellifera*

Bare/impervious: Sandy and bare soils; rock outcrops; and impervious surfaces including dirt and tar roads, parking lots, and rooftops

Land cover class assignments were verified using the original multispectral images and high resolution Google Earth imagery, along with observer knowledge of the study area. Grid values associated with incorrectly identified polygons representing localized misclassifications were corrected prior to merging polygons of the same value in preparation for post-classification change analysis.

Classification accuracy assessment

We assessed classification accuracy for 2013 LC assignments using standard confusion matrix cross-tabulation methods in the [caret] package in R (Kuhn 2008) (Kuhn 2012). A total of 928 reference sites were selected using a random point generator and existing cover was validated through ground truthing and examination of high resolution orthophotography. Since we were unable to directly assess classification accuracies for 1990 and 2003 directly due to a lack of suitable reference data, we used the 2013 LC classification and ground truth data to calculate proportional error by dividing the number of misclassified cells by contingency table row totals. The proportional errors for each LC class were then multiplied by the nominal LC class area, and summed along columns to derive an adjusted LC area representing classification uncertainty intervals. We calculated overall classification accuracy with binomial 95% confidence intervals for accuracy rates by dividing the total number of correctly identified reference points by the total number of sample units in the matrix (Congalton and Green 2008). Individual class accuracies were computed in a similar manner and include measures of: sensitivity (producer accuracy), specificity (true negatives), positive predictive value (user accuracy), and negative predictive values. Positive and negative predictive values reflect probabilities that a true positive or true negative is correct given the prevalence of classes within the population. Typically, classification accuracy is expressed numerically in terms of the percentage of cases correctly allocated (Foody 2002). While no set accuracy standard exists within the remote sensing community, an overall accuracy of 85% with no class less than 70% accurate is commonly recommended as a target for accuracy assessment (Thomlinson et al. 1999). Detection rate and detection prevalence were also computed from the reference data (Kuhn 2012), along with an unweighted Cohen's Kappa statistic describing agreement of categorical data relative to what would be expected by chance, with values of 1 indicating perfect alignment.

We also calculated quantity disagreement and allocation disagreement between the 2013 LC map and reference data following methods described by Pontius Jr and Millones (2011). Quantity difference is the amount of disagreement that derives from a proportional difference between the number of cells of a particular land class in two maps, while allocation difference is the additional disagreement resulting from a less than optimal match in the spatial allocation of the categories (Pontius Jr and Santacruz 2014). Agreement between reference data and the classified map for each land class category were also evaluated in terms of omission and commission error. Greater omission error than commission error for a particular category indicates that the maps underestimated the quantity of that category, while higher commission error indicates overestimation of a category (Zhou et al. 2014).

LC change detection

Post-classification analysis of net and gross changes in Chobe District LC was conducted in ENVI version 4.8 (Exelis Visual Information Solutions, Boulder, Colorado) for each time step. We used ArcMap version 10.2 (Earth Science Research Institute, Redlands, California) to extract LC values for each time step and quantify LC changes occurring within a 10 km radius (314 km²) ring buffer around seven towns and villages: Satau, Kachikau, Kasane, Kavimba, Kazungula, and Parakarunga. Buffer areas were clipped to the Chobe District border, and thus varied in size for the different towns and villages. LC changes occurring within a 1 km wide buffer area spanning the riparian zone of Chobe River were assessed in a similar manner. The riparian buffer was clipped to the District boundary and area (km²) and percent LC were calculated. Land cover values were extracted separately for the entire length of the Chobe River within the District, as well as portions of the river within the boundaries of Chobe Enclave, Chobe National Park, and Chobe and Kasane Forest Reserves. We also quantified LC changes occurring within the District's seven protected areas: Chobe National Park, Sibuyu, Maikaelelo, Kazuma, Chobe, and Kasane Forest Reserves and the Kasane Reserve Extension, and the Chobe Enclave. Percent change in LC during the different time steps was calculated as:

$$\text{Percent change} = (\text{final state} - \text{initial state} / \text{initial state}) \times 100$$

In addition to net change, we estimated gross LC changes to provide a more complete understanding of dynamic spatiotemporal patterns of class gains and losses across the Chobe District. As gross change often exceed net change, only accounting for net changes may result in significant underestimation of change intensity occurring across a landscape (Fuchs et al. 2015), which can have serious implications for conservation and management activities and outcomes. We further assessed LC changes in terms of the mutually exclusive components of quantity and allocation to aid practical interpretation of changes occurring among the different land classes (Pontius Jr and Santacruz 2014). Allocation difference was further divided into the components of exchange and shift, caused by pairwise and nonpairwise confusion, respectively. Exchange occurs between pairs of pixels in a map when a pixel is classified as category “A” in the first map and as category “B” in the second map, while simultaneously the reverse is true (class “B” in map 1, and class “A” in map 2”); shift describes allocation difference other than exchange (Pontius Jr and Santacruz 2014). We also conducted three levels of Intensity Analysis including: time interval, category, and transition (Aldwaik and Pontius 2012). Intensity analysis compares the observed changes to a hypothetical uniform change in order to examine how the size and intensity of LC losses and gains vary among the different time periods, as well as how gains and losses vary within and across different cover classes. At each level, the method also tests for stationarity of patterns across time intervals. For a category to be stationary in terms of its gains and losses, change intensity must be either greater or less than the uniform line of change for all time intervals. Intensity analysis at the transition level indicates whether gains in category *a* either target or avoid category *b*, and evaluates whether the apparent change intensities are uniform (Zhou et al. 2014).

MODIS Active Fire Data

We estimated fire frequency and intensity for Chobe District and its protected areas, settlements, and riparian corridor using monthly active fire detections (MCD14ML Collection 5.1) for January 1, 2001-December 31, 2013 acquired by the Moderate Resolution Imaging Spectroradiometer (MODIS) on board the Earth Observing System (EOS) Terra and Aqua satellites. MODIS active fire products detect fires burning in 1 km pixels using a contextual algorithm that applies thresholds to observed mid-infrared and thermal infrared brightness temperature and rejects false detections by comparing them to values from neighboring pixels (Giglio et al. 2003). Estimates of fire intensity were derived from quantitative observations of Fire Radiative Power (FRP) measured for each active fire pixel representing the amount of

energy released by a fire into the atmosphere in megawatts (MW). Only fires with a detection confidence greater than 75% were included in the analysis. In addition to frequency and distribution of fires associated with classified land cover and change detection masks from 2003 and 2013, we conducted an optimized hot spot analysis of fire clusters using Getis-Ord G_i^* in ArcGIS (v. 10.3) following integration and event collection of fires occurring within a 1 km neighborhood. Fires in neighboring countries were also included in the analysis to assess fire spread into the Chobe District across its borders with Namibia, Zambia, and Zimbabwe. Hot spot analysis compares observed fire frequencies to expected values to identify statistically significant clusters of high and low fire frequency, along with non-significant fire clusters. A False Discovery Rate (FDR) Correction was applied in order to account for multiple testing and spatial dependence and to reduce critical p-values used to determine analysis confidence levels.

Elephant biomass and land cover

Elephant biomass estimates were derived from aerial wildlife survey data collected by the Botswana Department of Wildlife and National Parks (DWNP) during the 2003 and 2012 dry seasons, and are represented as Large Stock Units (LSU)/km² (Boshoff et al. 2002, DWNP 2014). DWNP aerial census data was collected using a stratified systematic transect sampling design and data generated from the surveys were analyzed using Jolly's method for sampling blocks of unequal size to obtain wildlife biomass estimates (Jolly 1969). Land cover values from 2003 and 2013 classification maps were extracted from cells associated with survey polygons containing elephant biomass >20 LSU. Locations of high elephant biomass were also examined in relation to land cover class transitions between 2003-2013.

Results

Chobe District LC change

Classification accuracy

Figure 3 shows LC classification maps for 1990, 2003, and 2013. Classification and ground truth results used in accuracy analysis, along classification accuracy indices are summarized in contingency tables (Tables 1 and 2). Overall classification accuracy was 86.6% (95% CI 0.843, 0.888) with a Kappa coefficient of 0.832. Sensitivity (producer accuracy) and positive prediction values (user accuracy) for individual classes ranged from 79% to 96% and 77% to 100%,

respectively. Specificity was high indicating low misclassification error among the different LC classes. Classification accuracy was highest for water and bare/impervious LC and lowest for woodland cover. Figure 4a summarizes the overall disagreement between the LC map in 2013 and the reference data. Total disagreement was just over 13% with the majority due to the allocation component. Agreement, omission disagreement, and commission disagreement by category for the 2013 LC map are summarized in Figure 4b.

Net LC change statistics

Estimated net LC changes in the Chobe District are summarized in Tables 7 and 8, and in Figure 5. Error bars in Figure 5 indicate upper and lower bounds of misclassifications and show the errors were lower than the estimated change associated with each LC class, except for wet/irrigated vegetation in all three time steps, and woodlands change between 2003 and 2013. LC changes from 1990-2013 were characterized primarily by a decrease in woodland and expansion of shrubland. While woodland was the dominant cover in 1990 (9,329 km², 44.1% of the District) in 1990, shrubland became the dominant LC class by 2013 (9622 km², 45.5%). Woodland losses in the first time step were followed by an insignificant gain from 2003-2013. Shrubbyland also declined from 1990-2003, but experienced a net expansion of 2189 km² (30%) from 2003-2013, for a net increase over the study period. Grassland experienced the largest gains during the first time step, along with bare/impervious cover however, both classes decreased by more than 40% between 2003 and 2013. For the study period, grassland increased by just over 265 km² (20%), while bare/impervious area decreased by 196 km² (11.5%). Changes in open water and wet/irrigated vegetation cover were small in regards to District land area, but highly variable.

Quantity and allocation indices

Figure 6a shows that the rate of overall change was nearly equal during the two time steps. Quantity difference accounted for less than a quarter of all change during each time interval, while exchange exceeded shift during both time steps. Figure 6b shows that during 1990-2003, woodland, grassland, shrubland, and bare/impervious all accounted for the quantity difference, with woodland and shrubland having a net loss and grassland and bare/impervious having a net gain. Shrubbyland and woodland accounted for the majority of exchange, while shrubbyland contributed most to the observed shift component. From 2003-2013, shrubbyland (net gain) and grassland (net loss) comprised the largest proportion of quantity difference. The majority of

exchange occurred between shrubland and woodland, while woodland and bare/impervious cover contributed most to the shift component.

Gross LC change statistics

Accounting for gross changes among the different classes highlights the complex and dynamic nature of LC in the Chobe Region (Table 5). A full accounting of gross changes among the different LC classes for each time step are included in Appendix K. Gross woodland change from 1990-2013 was greater than net change, with the majority of woodland cover transitioning to shrubland. Woodland expansion and succession during the study period, in turn, likely accounted for the majority of shrubland change. Class changes in bare/impervious cover were primarily represented by a shift to shrubland, while the majority of observed grassland change over the study period was in transition to wet/irrigated vegetation, with grassland gains primarily derived from loss of shrubland and wet/irrigated vegetation.

Between 1990 and 2003, woodland class changes totaled 4319 km² (46%), with the majority transitioning to shrubland (Table 5). Woodlands also expanded by 2342 km² (28%) into shrubland and 236 km² (14%) into bare/impervious. Substantial losses of shrubland to bare/impervious and grassland were also observed, while the majority of bare/impervious change occurred via transition to shrubland. From 2003-2013, gross woodland changes totaled 3515 km² (46%), with most lost to shrubland gains. In turn, shrubland lost 2797 km² (38%) to woodlands. Grassland lost 942 km² (33%) to shrubland, while the majority of change in bare/impervious cover was also attributable to the shrubland encroachment.

Change intensity analysis

Category-level intensity analysis of LC gains and losses (Fig. 7) indicate change intensity was higher from 2003-2013 than in the first time step. Woodland gains and losses were dormant and stationary during both time intervals, suggesting woodland change was generally less intense than those experienced by other LC classes. In contrast, gains and losses of shrubland, bare/impervious, and wet/irrigated cover were more intense than if the overall change rate was uniformly distributed across the landscape. Active shrubland gains were higher from 1990-2003, while shrubland losses were more intense during the second time step. Grassland experienced gains intensively from 1990-2003 and more intensive losses during 2003-2013. Interestingly, despite a large net expansion of grassland from 1990-2003 and decline from 2003-2013, change

intensities of the respective gains and losses were less than the uniform change intensity for the District. Transition-level changes among LC classes (Fig. 8) indicate woodland gains and losses were higher from 2003-2013 and intensively driven by the exchange with shrubland during both time periods. Transitions to and from shrubland were most actively targeted by exchange with bare/impervious cover and grassland from 1990-2003 woodland, while woodland exchange was the dominant process from 2003-2013.

Protected areas change

Estimated LC changes in protected areas are summarized in Figure 9 and Appendix L. Woodland was the most abundant LC class in 1990 in all protected areas except Chobe National Park. Woodland remained the dominant cover over the study in three of the seven protected areas, despite shrubland gains in all protected areas. From 1990-2003 woodland declined in five of the protected areas, with the highest losses in Kasane (-53%) and Sibuyu (-34%) FRs. The greatest net woodland losses as a percent of class area from 1990-2013 were in Maikaelelo (-76%), Kazuma (-63%), and Kasane (-43%) Forest Reserves. Woodland subsequently increased between 2003-2013 in several FRs, but continued to steeply decline in Kazuma FR (-68%), Maikaelelo FR (-68%), and the Kasane FRE (-42%). Grassland increased over the study period in all protected areas but Kasane Forest FR (-6%) and Maikaelelo FR (-70.8%), with most of the observed gains occurring in the first time step, and most losses occurring from 2003-2013. Kasane Maikaelelo FRs experienced the greatest increase in bare/impervious cover over the study period. Urban expansion appeared to drive bare/impervious gains in Kasane FR, while in Maikaelelo FR frequent fires in the eastern section of the reserve likely drove bare/impervious gains.

Chobe Enclave and Village change

Estimated LC changes the Chobe Enclave and settlement buffers are summarized in Figure 10 are presented in and Appendix M. Shrubland was the dominant cover in the Enclave, with a net gain of 327 km² (50%) from 1990-2013. Woodland decreased in the Enclave by 268 km² (50%) over the study period, despite gains of 60 km² (28%) from 2003-2013. Woodland was the dominant LC class in five of the seven village buffers in 1990, and four of the buffers in 2013, but decreased over the study period in all the settlement buffers except Satau, with the highest loss observed for Kachikau (-51%). The towns of Kasane and Kazungula experienced woodland

losses of more than 60% from 1990-2003; however, these losses were offset by substantial woodland gains during 2003-2013, for a net loss of approximately 33%. Bare/impervious area increased substantially around Kasane (19%) and Kazungula (25%) over the study period, in contrast to decreasing or stable patterns observed elsewhere.

Riparian cover change

Estimated LC changes in 1km riparian buffer are summarized in Figure 11 and Appendix M. Woodland losses between 1990 and 2013 totaled 49 km² (-63%) along the Chobe River, ranging from 69-74% in the protected areas. Woodland losses in the Chobe Enclave over the study period, however, were substantially lower (-39%). Shrubland area also declined in all riparian buffers except in the CNP, while bare/impervious area increased in all but the Enclave. Locations and patterns observed for water, wet/irrigated vegetation, and grassland suggest that variability in seasonal flood extent and inundated land area, along with frequent fires drove changes in these classes.

Rainfall

Mean annual precipitation (MAP) recorded at the Kasane Meteorological Station over the period 1922-2014 was 632mm ±181mm. This long-term average was exceeded in 34 of the 58 years preceding 1980, but only in 7 years from 1980-2014. During the first time step of the analysis rainfall exceeded the long-term average only in 1991, compared to three years of above average rainfall from 2003-2013. Between 1990 and 2003, MAP was 533 mm compared to 601 mm from 2004-2014. Rainfall totals in 2002 (329 mm) and 2003 (422mm) were among the lowest recorded in the nearly 100 years of precipitation records, while >1000mm fell in 2008 alone.

Singular spectrum analysis (SSA) provides a graphical display of the long term oscillatory and trend components present in the rainfall time series (Fig 12). A trend of declining mean monthly rainfall since the 1920s is evident in the time series, as are short oscillations between wetter and drier periods on the order of approximately 5 -10 years. These oscillations correspond closely to major ENSO events, with prevailing wet conditions associated with La Niña (wet) years, and drought conditions associated with El Niño (dry) years (Pricope and Binford 2012). Mean monthly rainfall increased over the period 1985-1990 preceding the first time step of the analysis, followed by a return to drought conditions between 1990 and 2000 (Fig. 12). Despite

several years of above average rainfall between 2000 and 2013, the general drying trend during this period was also evident.

Fire frequency

A total of 9288 fires with detection confidence >75% were recorded across the Chobe District over the 2001-2013 fire seasons, with >1000 fires recorded in 2006, 2008, and 2011 (Table 6). Fire activity peaked in September and October, with only 11 fires recorded between December-March (Fig. 13). Mean Fire Radiative Power (FRP) was similar across the District during low to high fire years. Area-weighted Annual Fire Index (AFI) values for the Chobe Enclave and Unprotected (UP) area were higher than in the Chobe District as a whole, although average FRP was approximately 24% lower within the Enclave. AFIs were lower or equivalent compared to the District in all settlement buffers except Parakarungu and Kachikau. AFIs were lower or equivalent compared to the District in all settlement buffers except Parakarungu and Kachikau. Kasane and Kazungula in particular had a combined total of only nine fires over the analysis period. Average FRP for settlements also tended to be lower than in protected areas and riparian buffers. The highest AFIs were observed in the riparian buffer in the Chobe Enclave, and in both Kazuma FR and Kasane FRE, which all has an average of over seven fires/km².

Fire frequencies in the Chobe District exhibited a distinct biennial cycle, in which high fire years were typically preceded by a year with comparatively few fires. Comparison of total annual precipitation with fire frequency (Fig. 14) shows higher rainfall was associated with increased fire frequency. This suggests that increased wet season plant biomass in high rain years resulting in greater dry season fuel loads may drive these observed patterns. Analysis of land cover-fire associations showed fires were concentrated in wet/irrigated vegetation and woodland in 2003 (Fig. 15). In 2013, woodland and shrubland burned most frequently, while grassland also fueled a greater proportion of fires. Mean fire intensity in grassland, however, was substantially lower than in woodland and shrubland in both 2003 and 2013.

Hot Spot analysis using Gettis-Ord Gi* showed several distinct significant clusters of high fire frequency across the region and in the District along the Chobe River in the Enclave, and in the Kasane FRE and unprotected land bordering the Kazuma, Maikaelelo, and Sibuyu FRs, extending into the agricultural fields of Pandamatenga (Fig. 16). Fires associated with agricultural areas tended to occur in late April and early May, while land to the west primarily

burned from mid-September to late October. Spatiotemporal patterns of the significant fire hot spots located west of Pandamatenga and in Kasane FRE indicate they were not driven by fires spreading into Botswana from neighboring Zimbabwe. However, the significant cluster of fire hot spots near the Chobe River in the north of the Enclave suggests many of these fires are started from burning reeds and floodplain vegetation on both the Botswana and Namibian banks of the Chobe River.

Elephant Biomass and Land Cover

Land cover values extracted from 2003 and 2013 classification maps in locations of high elephant biomass (>20 LSU) in 2003 and 2012 are shown in Figure 16 and LC values from 2003-2013 woodland change are summarized in Figure 17. Areas of high elephant biomass in both 2003 and 2012 were predominately associated with woodland and shrubland cover. However, the majority of woodland in these locations experienced no change from 2003-2013 (Fig. 18). In 2003, 922 km² of woodland in locations of high elephant biomass experienced no detectible change, while 236 km² saw a transition to shrubland. The same pattern was observed for 2013 LC and 2012 elephant biomass, with 916 km² of woodland cover experiencing no change, and 144 km² changed to shrubland from 2003-2013.

Discussion

Land cover changes in the semi-arid savanna of northern Botswana are influenced by complex and dynamic interactions among a mosaic of ecological and environmental factors. Couplings and feedbacks between rainfall and fire appeared to drive LC changes at the observed spatiotemporal scale. Fire frequency was observed to increase in years of higher total rainfall with low and high fire years tending to alternate biennially. Observed LC changes across the Chobe District were not strictly linear in nature, a characteristic which has also been noted for other dryland regions (Diouf and Lambin 2001). Estimated change rates were nearly identical from 1990-2003 and 2003-2013, with exchange between classes being the dominant form of LC change. Quantity differences in contrast, accounted for less than a quarter of all change observed in each time step. Transition-level intensity analysis of class changes indicated active bi-directional exchange between woodland and shrubland was a highly influential process in Chobe

District. Grassland transitions were primarily due to quantity change between water and wet/irrigated vegetation, but fire and herbivory likely also influenced the observed changes. The large cluster of fires in the north of the Chobe Enclave along the Chobe River is in an area where people are known to frequently set fires to clear land for livestock and agriculture across the border in Namibia's Caprivi Strip. Another large cluster of significant fire hot spots was located in unprotected land between Maikaelelo and Kazuma forest reserves where harvesting of thatch materials is permitted in the dry season from September through October (Alexander pers. com.). Analysis of fires frequency in relation to land cover showed that in 2003, fires occurred primarily in wet/irrigated vegetation and woodland. In 2013, woodland experienced the greatest proportion of fires, along with shrubland, and grassland. Estimates of elephant biomass from 2003 and 2012 aerial survey data (DWNP 2014) were highest in areas classified as woodland and shrubland in 2003 and 2013 LC maps. Although some conversion to shrubland was noted for these locations, the majority of associated woodlands in areas of high elephant biomass experienced no detectable change between 2003 and 2013.

Across savanna landscapes, the spatial pattern and structure of woody plant and grass communities are often determined by water and soil nutrient availability, and the frequency and intensity of disturbance from fire and herbivory (Scholes and Archer 1997, Ringrose et al. 1998, Scholes et al. 2002, Sankaran et al. 2005). Mean annual rainfall (MAP) places constraints on maximum tree cover (Swaine et al. 1992, Bond 2008), while interactions and feedbacks between fire and grazing limit recruitment of savanna tree saplings into adults, inhibiting formation of dense forest canopy (Bond and Midgley 2001, Archibald et al. 2005, Staver et al. 2009). In semi-arid savannas (MAP <650mm), MAP exerts a stronger control over maximum tree cover with disturbances acting as strong modifiers. In more mesic savannas (MAP <1600mm), precipitation no longer strongly limits tree cover, and disturbance impacts become more important in maintaining the system, while in arid savannas (MAP <400mm) the opposite is true (Bucini and Hanan 2007). Long term (>50 year) fire exclusion experiments in Kruger National Park and other locations in South Africa have shown that grasslands with annual rainfall >650mm tend to be colonized by fire-sensitive woodland species in the absence of fire, but no comparable invasion of woody species occurred at sites with lower rainfall (Bond et al. 2003). Time series analysis of rainfall patterns in the Chobe District from 1922-2014 showed average annual precipitation recorded at the Kasane Meteorological Station was 632mm ±181mm, ranging

between 301-1205mm. This suggests that tree-grass dynamics in the savanna of the Chobe District may alternate between greater responsiveness to climate-dependency in unusually dry periods and more fire-dependent during years of above average rainfall. These short term oscillations may have important long term implications for the structure and composition of Chobe savanna given the complex couplings and feedbacks between climate, fire, herbivory, and anthropogenic disturbance (Bond et al. 2003, Archibald et al. 2005, Staver and Levin 2012).

Protected Areas

Woodland decreased over the study period in all protected areas except Chobe National Park. Similar to trends observed across the District, woodland losses during the initial time step were offset by gains from 2003-2013 in four of the seven protected areas. In the three reserves where woodland decreased between 2003 and 2013 the losses were very high, with both Kazuma and Maikaelelo FRs experiencing declines of over 68%. Substantial loss of woodland area also occurred in the Kasane Forest Reserve Extension between 2003 and 2013 (194 km², -42%). Significant fire hotspots were also observed within the borders of Kasane FRE, Maikaelelo FR, and Kazuma FR. AFIs showed annual fire frequency per km² was higher for Kasane FRE and Kazuma FR than all but the riparian corridor of the Chobe Enclave. Substantial increases in bare/impervious area from 2003-2013 were also observed in the three reserves, as well as in Kasane FR. Much of the bare/impervious expansion in Kasane FR occurred in close proximity to the towns of Kasane and Kazungula, both of which grew substantially in population and urban land area over the study period. In addition to having an extensive and growing road network, a 30.6 km² portion of the Kasane FR was de-gazetted in 2002 for residential purposes and the expansion of the Kasane Airport (Lepetu et al. 2010).

Chobe Enclave and villages

Woodland area decreased over the study period in the Chobe Enclave and in all the settlement buffers except Satau, with the largest net losses observed for the village of Kachikau. Over the same period, shrubland expanded in all settlement buffers and in the Chobe Enclave. Woodland losses over the study period were generally higher for the Enclave and settlements than the Chobe District as a whole. However, despite substantial losses from 1990-2003, woodland gains were observed from 2003-2013 around most settlements, including the rapidly growing urban centers of Kasane and Kazungula. Bare/impervious area increased substantially in Kasane and Kazungula over the study period, likely driven by growth of urban and residential infrastructure.

Research in the Kalahari region of southern Botswana indicated that areas of degraded vegetation are often in close proximity to villages and boreholes with both bush product harvesting and livestock grazing leading to the transformation of dry savannah vegetation to woody weed development (Ringrose et al. 2002). Firewood remains one of the most important sources of household energy for many residents of the Chobe District and is by far the most common natural resource extracted from the region's woodland reserves (Lepetu et al. 2010).

Riparian buffer

Woodland losses were substantially higher in 1 km buffer along the Chobe River than in the Chobe District, protected areas, and settlement buffers. Although woodland experienced a net increase in the CNP over the study period, woodland area decreased by 74% within the CNP's riparian zone. Declines of similar magnitude were observed in the Kasane Forest Reserve (-72%) and Chobe Forest Reserve (-69%), most of which occurred during the first time step. Shrubland declined within the riparian zone for all areas except the Chobe National Park. Bare/impervious area increased by 35% along the length of the Chobe River, with the greatest expansion occurring in the Kasane Forest Reserve. Changes in bare/impervious, grassland, and wet/irrigated cover were likely due, in part, to differences in annual flooding and natural shifts owing to floodplain development over the study period. The riparian buffer of the Chobe Enclave had the highest average annual fire frequency per km² of any location in the study area, with fire hot spots clustered mainly in the western portion of the Enclave, extending into Namibia's Caprivi Strip, and are likely the result of widespread burning of reeds and other floodplain vegetation. Fires may be started by people in an effort to open and improve grazing or agricultural land, reduce insect loads, or to attract game to the nutritious regrowth of plants following a burn (Archibald et al. 2005)

Much of the research on LC changes in the Chobe District has focused on browsing impacts within the narrow riparian forest fringe of the Chobe River. Many herbivores, elephants in particular, concentrate their browsing activities within relatively close proximity to the Chobe River (Mosugelo et al. 2002). Riparian habitat provides concealment for herbivores and fertile alluvial soils provide high-quality forage, making it among the most heavily utilized of landscape components, especially in water limited environments (Naiman and Rogers 1997a, Wiegand et al. 2006). Research suggests elephant browsing may have a greater impact on the Chobe River's riparian tree community than on woodlands within the interior of the District (Mosugelo et al.

2002, Moe et al. 2009, Rutina and Moe 2014). This may be due, in part, to dietary preferences of elephants for *Acacia spp.*, which also have historically more abundant along the Chobe River than in woodlands within the interior of the District (Teren and Owen-Smith 2010). Dietary differences mediating feeding-patch choice between male and female elephants may also contribute to greater impacts of elephant browsing observed in riparian tree communities (Stokke 1999). Browsing by ungulates, especially impala, was also found to be highly influential in seedling survival and recruitment during the late dry season (June-September) (Moe et al. 2009). A positive association has also been noted between elephant browsing and the abundance and distribution of gallinaceous birds (Stokke et al. 2014), and consumption of seeds and seedlings by gallinaceous birds and rodents may affect regeneration and colonization rates along the Chobe riverfront (Rutina et al. 2005). However, the loss of mature trees within the riparian forest fringe may also be part of the return of the riparian tree community to a more open state of equilibrium after undergoing a significant expansion in the 19th century due to the near extirpation of elephants by the ivory trade, and the collapse of artiodactyl populations following a series of rinderpest outbreaks (Vandewalle 2003, Moe et al. 2009, Skarpe et al. 2014d). Environmental and ecological factors aside from elephant browsing may also be influential in the decline of mature trees observed in the Chobe's riparian forest. Surveys conducted by Wackernagel (1992) along the Chobe and Linyanti Rivers found a large proportion of damage within the riparian zone appeared to be caused more by wind throw than by elephants felling trees or removing bark. Coulson (1992) also found very little elephant damage within areas of high tree mortality in riparian woodlands along the Linyanti and Kwando Rivers, suggesting damage by other factors such as wind and fire.

A continental-scale analysis of tree cover in African savannas by Bucini and Hanan (2007) suggests the magnitude of disturbance effects largely depend upon mean annual precipitation (MAP) regimes across rainfall zones. In semi-arid and mesic savannas (MAP 400-1600mm) like those found in northern Botswana, MAP exerts a stronger control over maximum tree cover along with disturbances that act as strong modifiers. In more mesic savannas (MAP <1600mm), precipitation no longer strongly limits tree cover, and disturbance impacts become more important in maintaining the system, while in arid savannas (MAP <400mm) the opposite is true (Bucini and Hanan 2007). Long term (>50 year) fire exclusion experiments in Kruger National Park and other locations in South Africa have shown that grasslands with annual rainfall

>650mm tend to be colonized by fire-sensitive woodland species in the absence of fire, but no comparable invasion of woody species occurred at sites with lower rainfall (Bond et al. 2003). Time series analysis of rainfall patterns in the Chobe District from 1922-2014 (Fig. 11) showed long-term average annual precipitation recorded at the Kasane Meteorological Station was 632mm \pm 181mm, ranging between 301-1205mm. This suggests that tree-grass dynamics in the savanna of the Chobe District may alternate between greater responsiveness to climate-dependency in unusually dry periods and more fire-dependent during years of above average rainfall. Such short term oscillations can have important long term implications for Chobe savanna plant community structure and composition given the strong couplings and feedbacks between climate, fire, herbivory, and anthropogenic disturbance (Bond et al. 2003, Archibald et al. 2005, Staver and Levin 2012). Increasing fire frequency as a result of climate-induced changes across the southern African region (Milly et al. 2005, Pricope and Binford 2012) may have profound effects on the distribution of woodlands in savanna systems.

Conclusion

Our results highlight the dynamic and non-linear nature of LC change in northern Botswana. We observed a net decrease in woodland and net expansion shrubland and grassland in the Chobe District during the study period. Woodland losses were greatest in within the riparian zone buffer in the Chobe National Park, despite tending to be lower overall in the protected areas. Although Chobe District woodlands had a net loss of more than 16% from 1990-2013, many locations saw substantial woodland gains from 2003-2013. Analysis of LC class transition-level intensity indicated bi-directional exchange between woodland and shrubland was a highly influential process. Gross changes in woodland and shrubland were higher than net change and dominated by active exchange between the two classes during each time step. Changes in LC across the District appeared highly responsive to climatic fluctuations. This suggests that tree-grass dynamics in the savanna of the Chobe District may alternate between greater responsiveness to climate-dependency in unusually dry periods and more fire-dependent during years of above average rainfall. Fire frequencies were highly variable, with more active fires recorded in years with higher total rainfall, likely due to greater wet season plant biomass and resulting increase in dry season fuel loads. Analysis of active fire location in relation to classified land cover showed the majority of ignitions in 2003 were located in wet/irrigated vegetation, but in 2013 woodland burned more frequently than any other LC class. The location and timing of fires, most of which occurred late in the dry season before the arrival of large convective storms associated with

lightning production, suggests the majority of ignitions are anthropogenic in origin. We observed little evidence of unsustainable pressure on woodlands in the CNP from growing elephant populations. Comparison of aerial survey data with land cover showed that while elephant biomass was highest in woodlands in both 2003 and 2013, the majority of these same woodland areas experience no detectable change from 2003-2013. In Chobe National Park woodland grew by more than 20% despite increasing elephant populations over the same period. Observations of multi-decadal LC changes are essential to guide future conservation, management, and consumption activities of Botswana's limited forest resources. Identifying spatial and temporal LC changes further supports the development of an early warning framework to identify existing and emergent threats to forest resources and services, and reduce potential adverse impacts on livelihoods and health of local communities.

Literature cited

- Aldwaik, S. Z., and R. G. Pontius. 2012. Intensity analysis to unify measurements of size and stationarity of land changes by interval, category, and transition. *Landscape and Urban Planning* **106**:103-114.
- Alexander, K., and J. Blackburn. 2013. Overcoming barriers in evaluating outbreaks of diarrheal disease in resource poor settings: assessment of recurrent outbreaks in Chobe District, Botswana. *BMC Public Health* **13**:1-15.
- Anderson, H. W., M. D. Hoover, and K. G. Reinhart. 1976. Forests and water: effects of forest management on floods, sedimentation, and water supply.
- Archibald, S., W. Bond, W. Stock, and D. Fairbanks. 2005. Shaping the landscape: fire-grazer interactions in an African savanna. *Ecological Applications* **15**:96-109.
- Belsky, A., R. Amundson, J. Duxbury, S. Riha, A. Ali, and S. Mwonga. 1989. The effects of trees on their physical, chemical and biological environments in a semi-arid savanna in Kenya. *Journal of Applied Ecology*:1005-1024.
- Ben-Shahar, R. 1993. Patterns of elephant damage to vegetation in northern Botswana. *Biological Conservation* **65**:249-256.
- Bond, W., G. Midgley, F. Woodward, M. Hoffman, and R. Cowling. 2003. What controls South African vegetation—climate or fire? *South African Journal of Botany* **69**:79-91.
- Bond, W. J. 2008. What Limits Trees in C₄ Grasslands and Savannas? *Annual Review of Ecology, Evolution, and Systematics*:641-659.
- Bond, W. J., and J. J. Midgley. 2001. Ecology of sprouting in woody plants: the persistence niche. *Trends in Ecology & Evolution* **16**:45-51.
- Bontemps, S., P. Defourny, E. V. Bogaert, O. Arino, V. Kalogirou, and J. R. Perez. 2011. GLOBCOVER 2009-Products description and validation report.
- Boshoff, A., G. Kerley, and R. Cowling. 2002. Estimated spatial requirements of the medium-to large-sized mammals, according to broad habitat units, in the Cape Floristic Region, South Africa. *African Journal of Range and Forage Science* **19**:29-44.
- Bucini, G., and N. P. Hanan. 2007. A continental-scale analysis of tree cover in African savannas. *Global Ecology and Biogeography* **16**:593-605.
- Child, G. 1968. An ecological survey of northeastern Botswana. Food and Agricultural Organization.
- Congalton, R. G., and K. Green. 2008. Assessing the accuracy of remotely sensed data: principles and practices. CRC press.

- Deng, J., K. Wang, Y. Deng, and G. Qi. 2008. PCA-based land-use change detection and analysis using multitemporal and multisensor satellite data. *International Journal of Remote Sensing* **29**:4823-4838.
- Diouf, A., and E. Lambin. 2001. Monitoring land-cover changes in semi-arid regions: remote sensing data and field observations in the Ferlo, Senegal. *Journal of Arid Environments* **48**:129-148.
- Dregne, H., M. Kassas, and B. Rozanov. 1991. A new assessment of the world status of desertification. *Desertification Control Bulletin*:6-18.
- DWNP. 2014. Aerial census of wildlife and some domestic animals in Botswana. Department of Wildlife and National Parks. Monitoring Unit, Research Division. Gaborone.
- Eklundh, L., and A. Singh. 1993. A comparative analysis of standardised and unstandardised principal components analysis in remote sensing. *International Journal of Remote Sensing* **14**:1359-1370.
- FAO. 2010. Global forest resources assessment 2010: Main report. Food and Agriculture Organization of the United Nations.
- Foody, G. M. 2002. Status of land cover classification accuracy assessment. *Remote Sensing of Environment* **80**:185-201.
- Fuchs, R., M. Herold, P. H. Verburg, J. G. Clevers, and J. Eberle. 2015. Gross changes in reconstructions of historic land cover/use for Europe between 1900 and 2010. *Global Change Biology* **21**:299-313.
- Giglio, L., J. Desloîtres, C. O. Justice, and Y. J. Kaufman. 2003. An enhanced contextual fire detection algorithm for MODIS. *Remote Sensing of Environment* **87**:273-282.
- Golyandina, N., V. Nekrutkin, and A. A. Zhigljavsky. 2001. Analysis of time series structure: SSA and related techniques. CRC press.
- Golyandina, N., and D. Stepanov. 2005. SSA-based approaches to analysis and forecast of multidimensional time series. Page 298 *in* Proceedings of the 5th St. Petersburg Workshop on Simulation.
- Hansen, M. C., P. V. Potapov, R. Moore, M. Hancher, S. Turubanova, A. Tyukavina, D. Thau, S. Stehman, S. Goetz, and T. Loveland. 2013. High-resolution global maps of 21st-century forest cover change. *Science* **342**:850-853.
- Jolly, G. 1969. Sampling methods for aerial censuses of wildlife populations. *East African agricultural and forestry journal* **34**:46-49.
- Jones, B. T. 2002. Chobe Enclave. by: IUCN/SNV CBNRM Support Programme.
- Kiage, L., K. B. Liu, N. Walker, N. Lam, and O. Huh. 2007. Recent land-cover/use change associated with land degradation in the Lake Baringo catchment, Kenya, East Africa: evidence from Landsat TM and ETM+. *International Journal of Remote Sensing* **28**:4285-4309.

- Kuhn, M. 2008. Building predictive models in R using the caret package. *Journal of Statistical Software* **28**:1-26.
- Kuhn, M. 2012. The caret package.
- Lepetu, J., J. Alavalapati, and P. Nair. 2010. Forest dependency and its implication for protected areas management: A case study from Kasane Forest Reserve, Botswana. *International Journal of Environmental Research* **3**:525-536.
- Lowrance, R., L. S. Altier, J. D. Newbold, R. R. Schnabel, P. M. Groffman, J. M. Denver, D. L. Correll, J. W. Gilliam, J. L. Robinson, and R. B. Brinsfield. 1997. Water quality functions of riparian forest buffers in Chesapeake Bay watersheds. *Environmental Management* **21**:687-712.
- Lu, D., P. Mausel, E. Brondizio, and E. Moran. 2004. Change detection techniques. *International Journal of Remote Sensing* **25**:2365-2401.
- Marques, C., J. Ferreira, A. Rocha, J. Castanheira, P. Melo-Gonçalves, N. Vaz, and J. Dias. 2006. Singular spectrum analysis and forecasting of hydrological time series. *Physics and Chemistry of the Earth, Parts A/B/C* **31**:1172-1179.
- McCulley, R. L., S. Archer, T. Boutton, F. Hons, and D. Zuberer. 2004. Soil respiration and nutrient cycling in wooded communities developing in grassland. *Ecology* **85**:2804-2817.
- Moe, S. R., L. P. Rutina, H. Hytteborn, and J. T. du Toit. 2009. What controls woodland regeneration after elephants have killed the big trees? *Journal of Applied Ecology* **46**:223-230.
- Mosugelo, D. K., S. R. Moe, S. Ringrose, and C. Nellemann. 2002. Vegetation changes during a 36-year period in northern Chobe National Park, Botswana. *African Journal of Ecology* **40**:232-240.
- Naiman, R. J., and K. H. Rogers. 1997. Large animals and system-level characteristics in river corridors. *Bioscience*:521-529.
- Omphile, U. J., and J. Powell. 2002. Large ungulate habitat preference in Chobe National Park, Botswana. *Journal of range management*:341-349.
- Painter, M. 1997. DWNP's Monitoring and Evaluation Experience with the Natural Resources Management Project: Lessons Learned and Priorities for the Future. Natural Resources Management Project.
- Pontius Jr, R. G., and M. Millones. 2011. Death to Kappa: birth of quantity disagreement and allocation disagreement for accuracy assessment. *International Journal of Remote Sensing* **32**:4407-4429.
- Pontius Jr, R. G., and A. Santacruz. 2014. Quantity, exchange, and shift components of difference in a square contingency table. *International Journal of Remote Sensing* **35**:7543-7554.
- Pricope, N. G. 2013. Variable-source flood pulsing in a semi-arid transboundary watershed: the Chobe River, Botswana and Namibia. *Environmental Monitoring and Assessment* **185**:1883-1906.

- Pricope, N. G., and M. W. Binford. 2012. A spatio-temporal analysis of fire recurrence and extent for semi-arid savanna ecosystems in southern Africa using moderate-resolution satellite imagery. *Journal of Environmental Management* **100**:72-85.
- Ringrose, S., W. Matheson, and C. Vanderpost. 1998. Analysis of soil organic carbon and vegetation cover trends along the Botswana Kalahari Transect. *Journal of Arid Environments* **38**:379-396.
- Rutina, L. P., and S. R. Moe. 2014. Elephant (*Loxodonta africana*) Disturbance to Riparian Woodland: Effects on Tree-Species Richness, Diversity and Functional Redundancy. *Ecosystems* **17**:1384-1396.
- Sankaran, M., N. P. Hanan, R. J. Scholes, J. Ratnam, D. J. Augustine, B. S. Cade, J. Gignoux, S. I. Higgins, X. Le Roux, and F. Ludwig. 2005. Determinants of woody cover in African savannas. *Nature* **438**:846-849.
- Scholes, R., and S. Archer. 1997. Tree-grass interactions in savannas. *Annual Review of Ecology and Systematics*:517-544.
- Scholes, R., P. Dowty, K. Caylor, D. Parsons, P. Frost, and H. Shugart. 2002. Trends in savanna structure and composition along an aridity gradient in the Kalahari. *Journal of Vegetation Science* **13**:419-428.
- Schowengerdt, R. A. 1983. Techniques for image processing and classification in remote sensing. Academic Press New York.
- Schuyt, K. D. 2005. Economic consequences of wetland degradation for local populations in Africa. *Ecological Economics* **53**:177-190.
- Simpson, C. D. 1975. A detailed vegetation study on the Chobe River in north-east Botswana. *Kirkia*:185-227.
- Skarpe, C., J. du Toit, and S. R. Moe. 2014a. Elephants and savanna woodland ecosystems: a study from Chobe National Park, Botswana. John Wiley & Sons.
- Skarpe, C., H. Hytteborn, S. R. Moe, and P. A. Aarrestad. 2014c. Historical Changes of Vegetation in the Chobe Area. *Elephants and Savanna Woodland Ecosystems: A Study from Chobe National Park, Botswana*:43-60.
- Staver, A. C., W. J. Bond, W. D. Stock, S. J. Van Rensburg, and M. S. Waldram. 2009. Browsing and fire interact to suppress tree density in an African savanna. *Ecological Applications* **19**:1909-1919.
- Staver, A. C., and S. A. Levin. 2012. Integrating theoretical climate and fire effects on savanna and forest systems. *The American Naturalist* **180**:211-224.
- Swaine, M., W. Hawthorne, and T. Ogle. 1992. The effects of fire exclusion on savanna vegetation at Kpong, Ghana. *Biotropica*:166-172.

- Swift, M. J., O. W. Heal, and J. M. Anderson. 1979. *Decomposition in terrestrial ecosystems*. Univ of California Press.
- Teren, G., and N. Owen-Smith. 2010. Elephants and riparian woodland changes in the Linyanti region, northern Botswana. *Pachyderm*:18-25.
- Thomlinson, J. R., P. V. Bolstad, and W. B. Cohen. 1999. Coordinating methodologies for scaling landcover classifications from site-specific to global: Steps toward validating global map products. *Remote Sensing of Environment* **70**:16-28.
- Vandewalle, M. 2003. Historic and recent trends in the size and distribution of northern Botswana's elephant population. Pages 7-16 *in* *Effects of fire, elephants and other herbivores on the Chobe riverfront ecosystem*. Proceedings of a Conference organised by the Botswana-Norway institutional Cooperation and Capacity Building Project (BONIC). Gaborone: Government Printer.
- Wiegand, K., D. Saltz, and D. Ward. 2006. A patch-dynamics approach to savanna dynamics and woody plant encroachment—insights from an arid savanna. *Perspectives in Plant Ecology, Evolution and Systematics* **7**:229-242.
- Wily, L., and S. Mbaya. 2001. Land, people, and forests in eastern and southern Africa at the beginning of the 21st century: the impact of land relations on the role of communities in forest future. *lucn*.
- Wu, C., and K. Chau. 2011. Rainfall–runoff modeling using artificial neural network coupled with singular spectrum analysis. *Journal of Hydrology* **399**:394-409.
- Yeh, A. G. o., and X. Li. 1997. An integrated remote sensing and GIS approach in the monitoring and evaluation of rapid urban growth for sustainable development in the Pearl River Delta, China. *International Planning Studies* **2**:193-210.
- Zhou, P., J. Huang, R. G. Pontius, and H. Hong. 2014. Land Classification and Change Intensity Analysis in a Coastal Watershed of Southeast China. *Sensors* **14**:11640-11658.

Tables

Table 3-1. Contingency table results of LC classification accuracy assessment compared to reference data.

Predicted	Truth						Total	Commission error
	Water	Wet/irr. vegetation	Grassland	Woodland	Shrubland	Bare/imperv.		
Water	26	0	0	0	0	0	26	0
Wet/irr. veg.	0	76	11	0	0	0	87	0.126
Grassland	1	6	194	3	2	3	209	0.072
Woodland	0	4	1	122	26	2	155	0.213
Shrubland	0	0	16	29	199	13	257	0.226
Bare/imperv.	0	0	4	1	2	187	194	0.036
Total	27	86	226	155	228	205		
Omission error	0.037	0.116	0.155	0.213	0.131	0.088		

Table 3-2. Summary of accuracy assessment statistics by LC class. Individual class accuracies include measures of: sensitivity (producer accuracy), specificity (true negatives), positive predictive value (user accuracy), and negative predictive values. Positive and negative predictive values reflect probabilities that a true positive or true negative is correct given the prevalence of classes within the population.

	Water	Wet/irrigated vegetation	Grassland	Woodland	Shrubland	Bare/imperv.
Sensitivity	0.963	0.884	0.858	0.787	0.869	0.912
Specificity	1	0.987	0.978	0.957	0.917	0.990
Positive Predictive Value	1	0.874	0.928	0.787	0.774	0.964
Negative Predictive Value	0.999	0.988	0.956	0.957	0.955	0.976
Prevalence	0.029	0.093	0.244	0.167	0.247	0.221
Detection Rate	0.028	0.082	0.209	0.132	0.214	0.202
Detection Prevalence	0.028	0.094	0.225	0.167	0.277	0.209
Balanced Accuracy	0.981	0.935	0.919	0.872	0.893	0.951

Table 3-3. Estimated total area (km²) and percent land cover for the Chobe District.

	1990		2003		2013	
	km ²	%	km ²	%	km ²	%
Water	69.5	0.3	306.5	1.4	112.3	0.5
Wet/irrigated vegetation	428.6	2.0	319.9	1.5	525.8	2.5
Grassland	1,307.9	6.2	2,894.2	13.7	1,573.2	7.4
Woodland	9,329.1	44.1	7,672.3	36.3	7,815.3	36.9
Shrubland	8,317.1	39.3	7,432.9	35.1	9,621.6	45.5
Bare/impervious	1,701.1	8.0	2,527.6	11.9	1,505.1	7.1

Table 3-4. Estimated net land cover area (km²) and percent change for the Chobe District.

	1990-2003		2003-2013		1990-2013	
	km ²	%	km ²	%	km ²	%
Water	237.1	341.1	-194.2	-63.4	42.9	61.7
Wet/irrigated vegetation	-108.7	-25.4	206	64.4	97.2	22.7
Grassland	1586.3	121.3	-1321	-45.6	265.3	20.3
Woodland	-1656.8	-17.8	143	1.9	-1513.8	-16.2
Shrubland	-884.3	-10.6	2188.7	29.4	1304.5	15.7
Bare/impervious	826.5	48.6	-1022.5	-40.5	-196.1	-11.5

Overall accuracy: 0.8664 (95% CI 0.8428, 0.8876); No information rate: 0.2468; Cohen's Kappa: 0.8315

Table 3-5. Estimated total gross (class) changes in area (km²) and percent land for the Chobe District.

	1990-2003		2003-2013		1990-2013	
	km ²	%	km ²	%	km ²	%
Water	37	53.3	246.2	80.3	55.4	79.8
Wet/irrigated vegetation	302	70.5	174.2	54.5	194.9	45.5
Grassland	338.7	25.9	1721.9	59.5	385.2	29.5
Woodland	4319	46.3	3515.4	45.8	4843.2	51.9
Shrubland	4892	58.8	3396.3	45.7	4053.8	48.7
Bare/impervious	1197.5	70.4	1848.3	73.1	1359.1	79.9

Table 3-6. Summary of frequency and intensity of fires in the Chobe District, protected areas, settlements, and riparian buffers. Fire intensity is expressed as Fire Radiative Power (FRP) in megawatts (MW) of energy released to the atmosphere. Mean confidence for each location are included along with an area weighted Annual Fire Index (AFI), calculated by dividing average annual fire frequency by the total land area (fires*yr⁻¹/km²) of each feature, and represents a straightforward method of comparing fire intensity in analysis units of varying size.

Location	Area (km²)	Confidence	Total Fires	Avg Fires * year⁻¹	Annual Fire Index	Avg. FRP	Min FRP	Max FRP
Chobe District	21,153	91	9288	714	3.4	120.6	6.3	2456.4
UP	5,216	92	3167	244	4.7	118.9	6.8	2383.5
Chobe Enclave	1,581	89	1128	87	5.5	93.0	6.3	1651.6
Protected Area								
Chobe NP	10,168	92	2835	218	2.1	125.5	7.4	2456.4
Kasane FR	175	92	33	3	1.5	71.1	13.7	176.3
Chobe FR	1,455	89	326	25	1.7	79.4	10	392.2
Kazuma FR	173	91	151	12	6.7	111.4	9.6	948.2
Maikaelelo FR	510	91	310	24	4.7	96.4	9.9	648.1
Sibyuyu FR	1,185	92	726	56	4.7	130.5	8.7	1091.6
Kasane FRE	690	90	613	47	6.8	106.3	12.1	1179.9
Villages								
Mbele	163	91	58	4	2.7	94.8	19.8	330.4
Kazungugla	117	91	2	0.2	0.1	59.4	40.8	78.0
Kasane	144	92	7	1	0.4	33.9	17.5	70.0
Kavimba	223	87	47	4	1.6	61.3	10.0	396.9
Satau	248	86	106	8	3.3	56.9	11.4	314.3
Parakarungu	228	87	132	10	4.5	96.6	9.5	1651.6
Kachikau	313	88	154	12	3.8	67.9	10.0	536.1
Riparian								
Chobe River	243	90	154	12	4.9	107.8	9.6	1205.9
Chobe Enclave	117	89	128	10	8.4	102.1	9.6	1205.9
Chobe FR	22	-	0	-	-	-	-	-
CNP	82	92	26	2	2.4	136.0	21.2	458.3
Kasane FR	22	-	0	-	-	-	-	-

Figures

Figure 3-1. Landsat-based map of the Chobe District study area showing protected area boundaries (black border), including the Chobe National Park, forest reserves (FR), forest reserve extensions (FRE), along with the Chobe Enclave (white border), and major settlements.

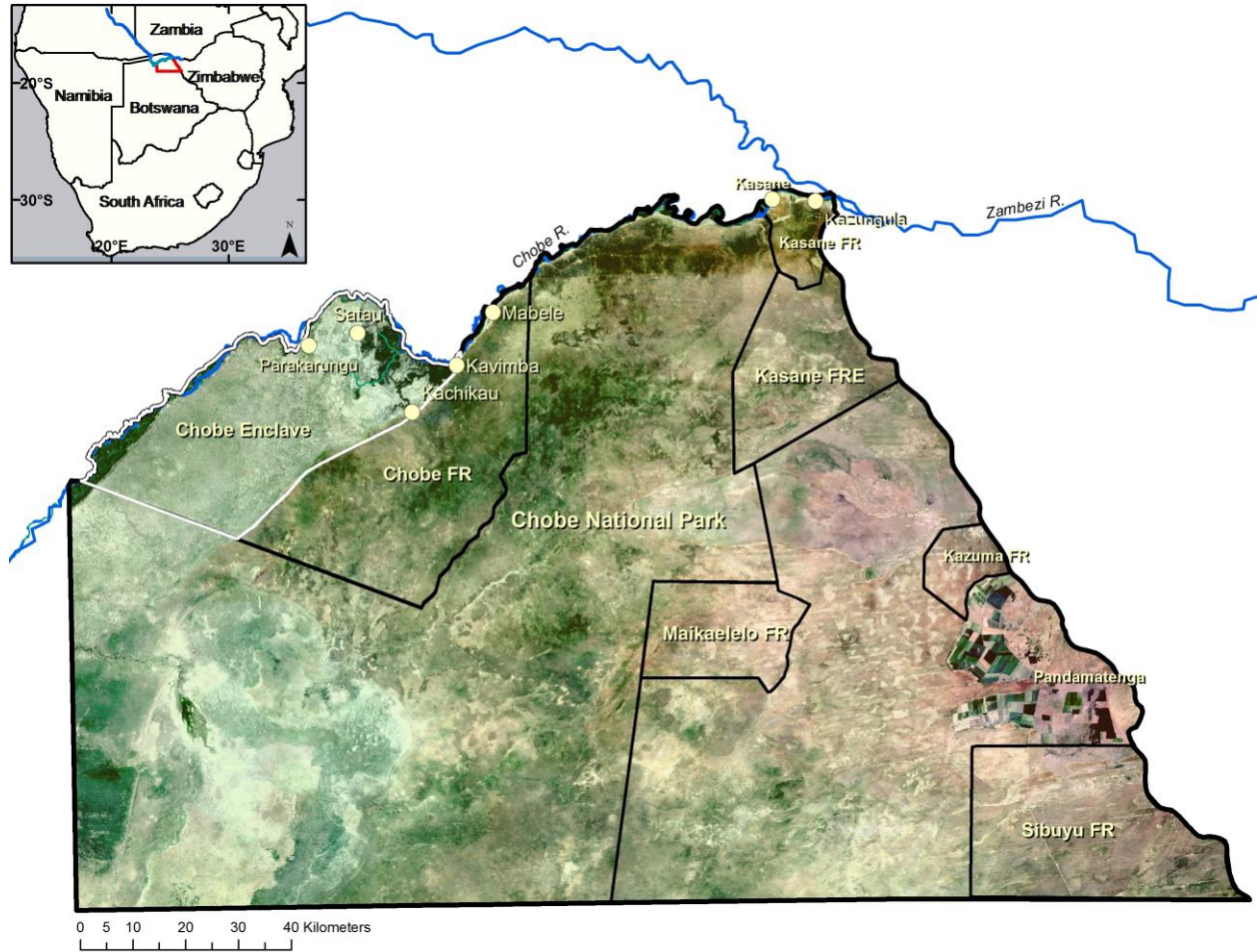


Figure 3-2. Landsat image mosaics clipped to the study area extent and displayed using a false color 7,4,2 band combination. Healthy vegetation appears as bright green and can saturate during periods of heavy growth, Grasslands appear green, pink areas represent barren soil, oranges and browns represent sparsely vegetated areas, sands and mineral soils appear in a multitude of different colors, and water appears blue to black.

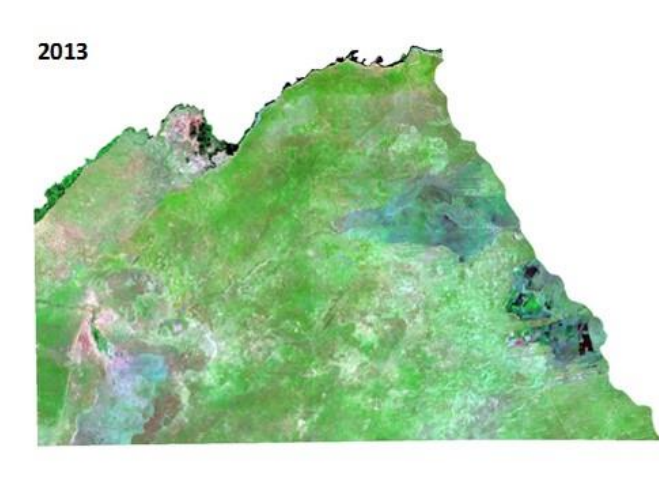
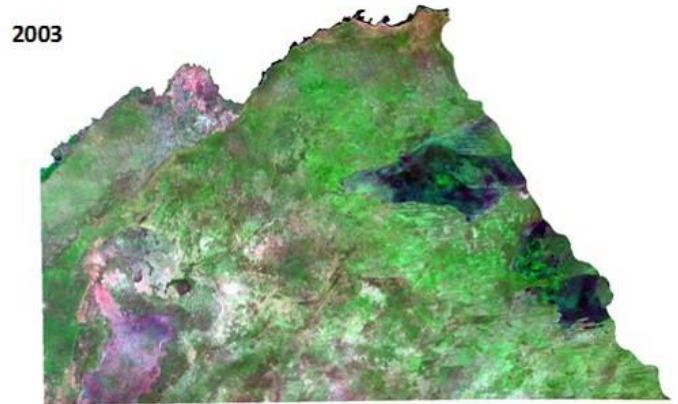
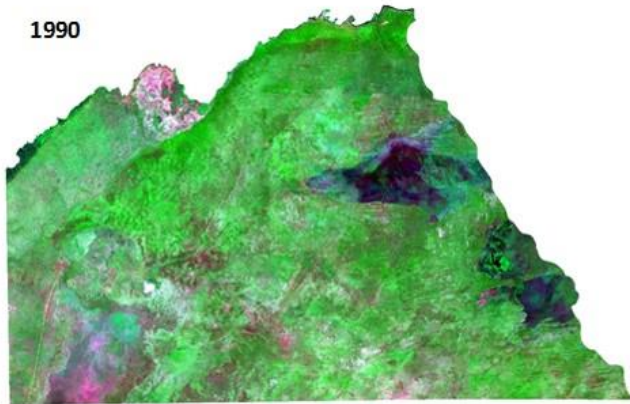


Figure 3-3. Land cover classification maps of Chobe District for 1990 (a), 2003 (b), and 2013 (c).

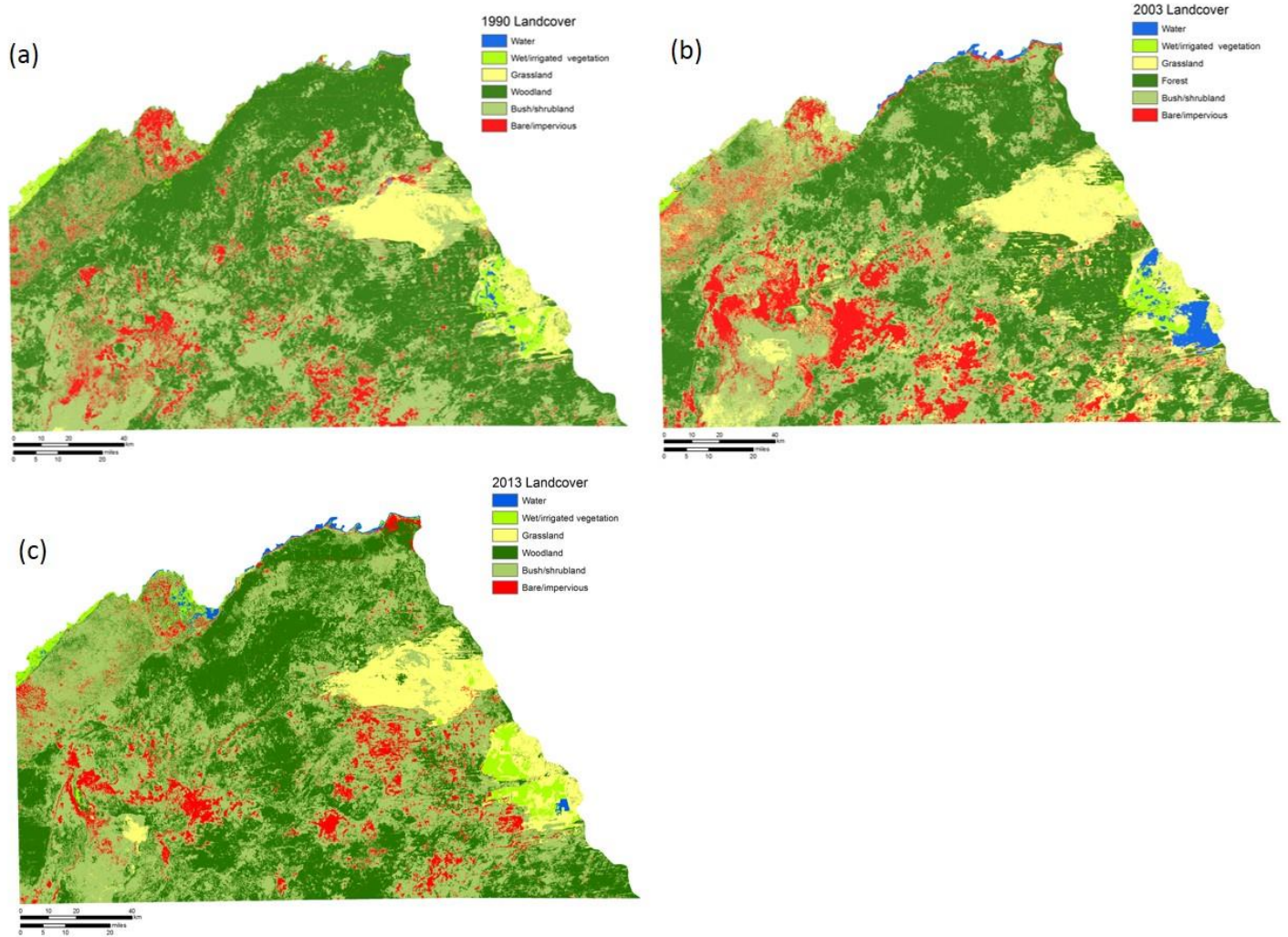


Figure 3-4. (a.) Summary of overall disagreement between the 2013 LC classification and reference data. (b.) Summary of agreement, omission disagreement, and commission disagreement by category for the 2013 LC classification

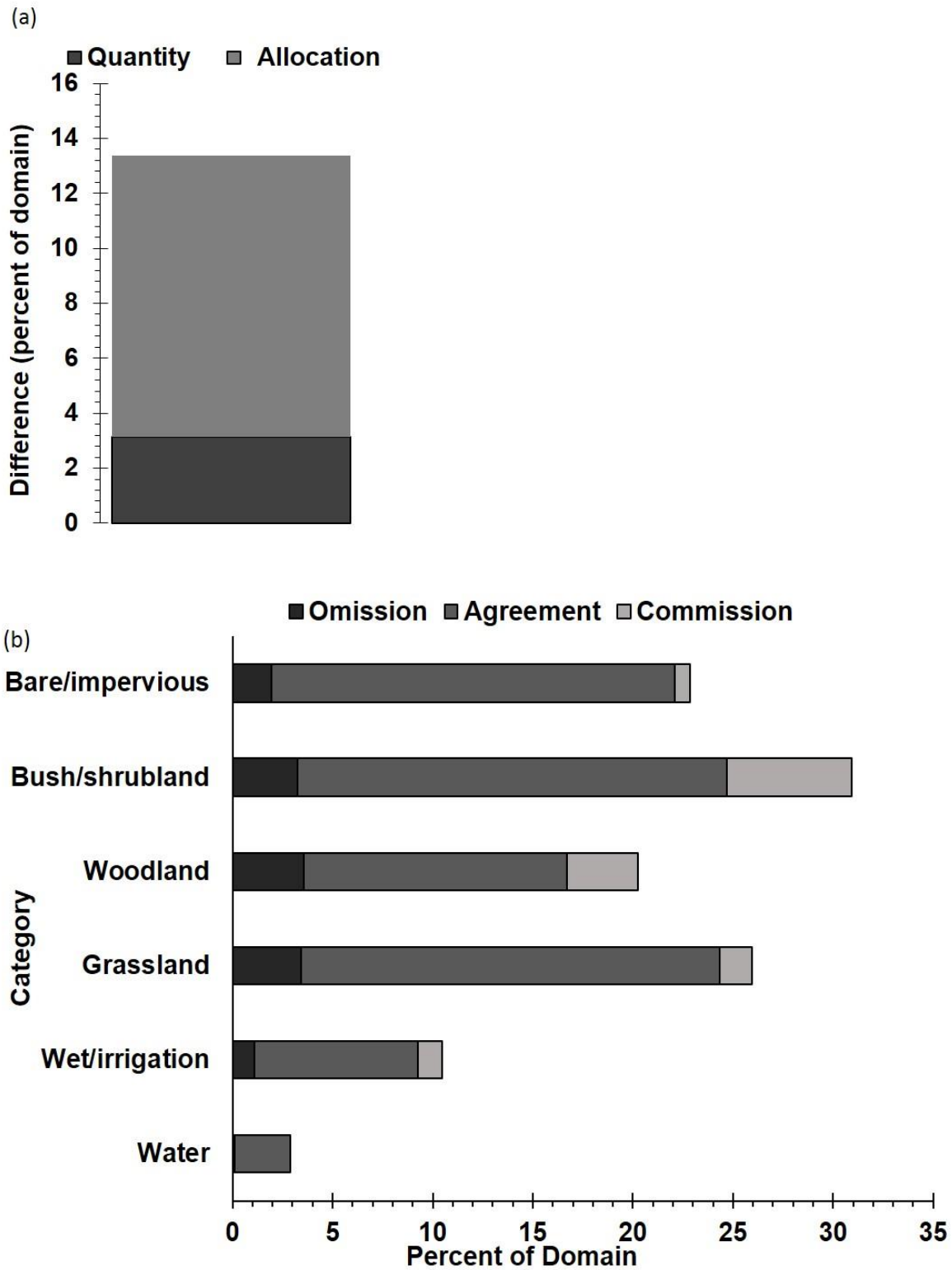


Figure 3-5. Changes in classified land cover area (km²) for each time step. Error bars for each LC class were calculated using 2013 LC classification and ground truth data by dividing the number of misclassified cells by contingency table row totals. We then multiplied the resulting proportional error for each LC class by the nominal LC class areas, and summed along each column to derive an adjusted LC area representing upper and lower classification uncertainty bounds for the three time steps. Errors were lower than the estimated change associated with each LC class, except for wet/irrigated vegetation in all three time steps, and woodlands change between 2003 and 2013.

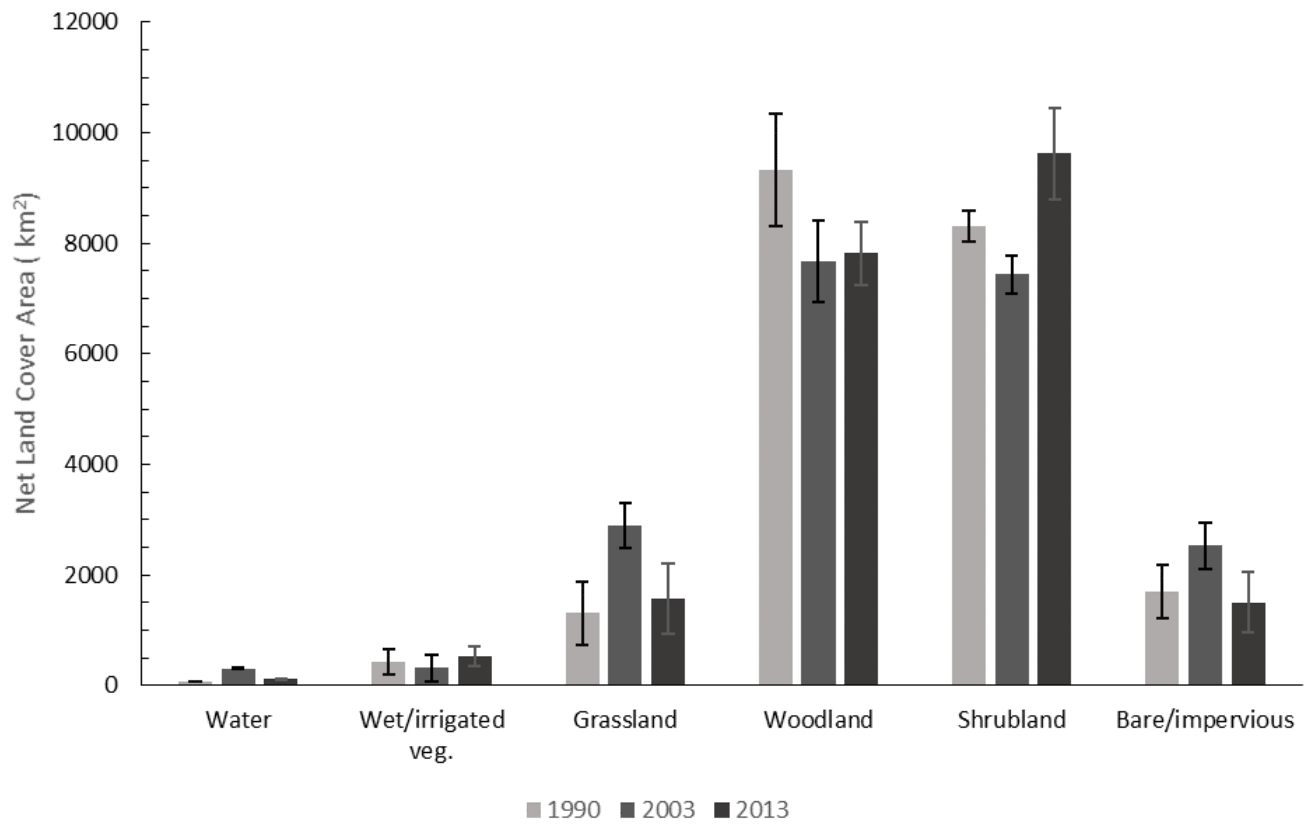


Figure 3-6. (a) Summary of the overall change during the two time steps in terms of quantity and allocation. **(b)** Category level summary of quantity and allocation indices for the period 1990-2003 and 2003-2013. The rate of overall change was nearly equal over the two time steps, and that quantity difference accounted for less than a quarter of all change during each time interval, and that exchange exceeded both quantity and shift in both time steps.

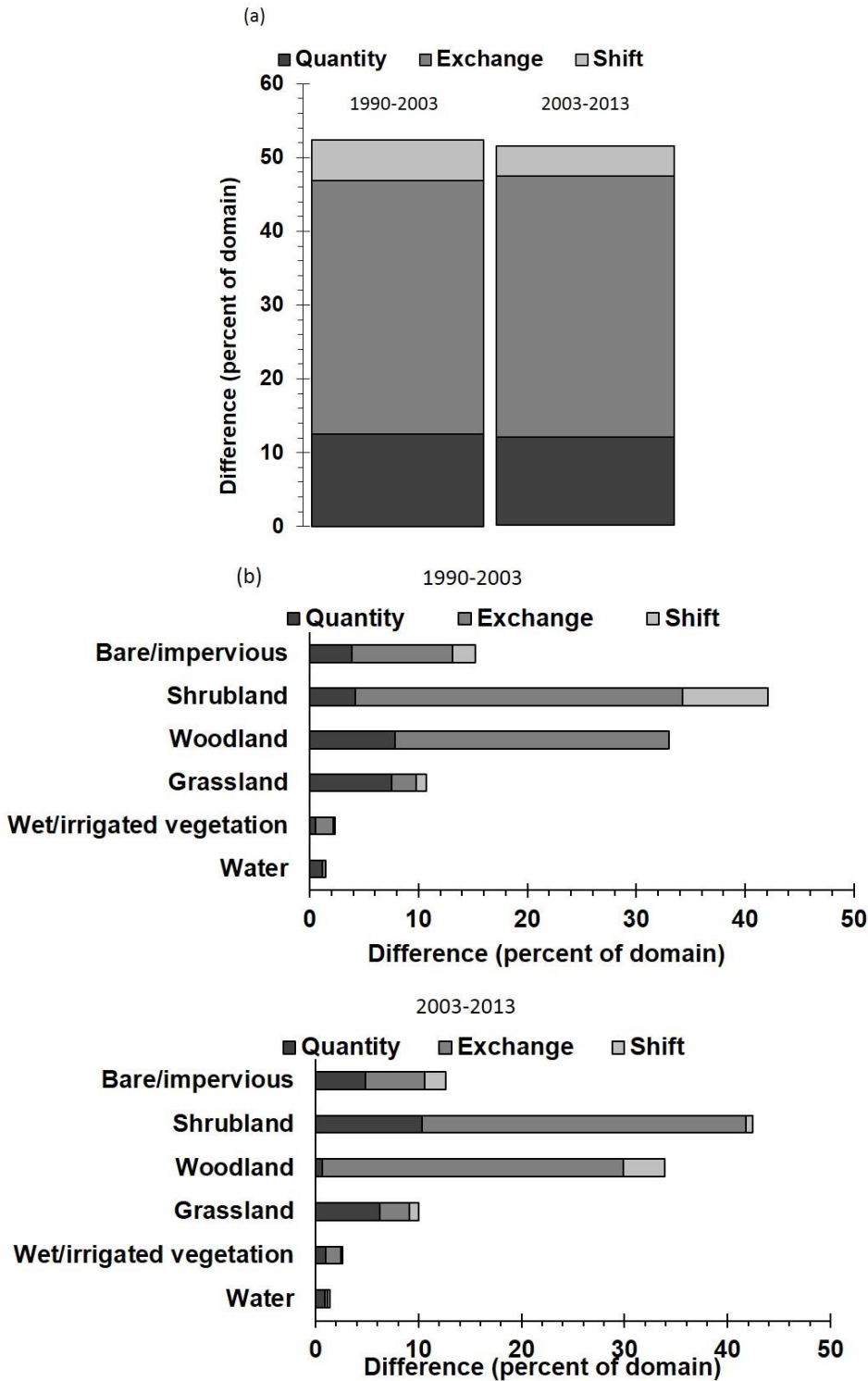


Figure 3-7. Category-level intensity analysis of gains and losses given observed changes in each time interval. Vertical axes show intensity of annual change during the time interval as a percent of the category. Horizontal (red) lines shows uniform intensity of annual change for the study area. Bars extending above the uniform line indicate change is relatively active for that category, while bars ending below the line indicate change is relatively dormant.

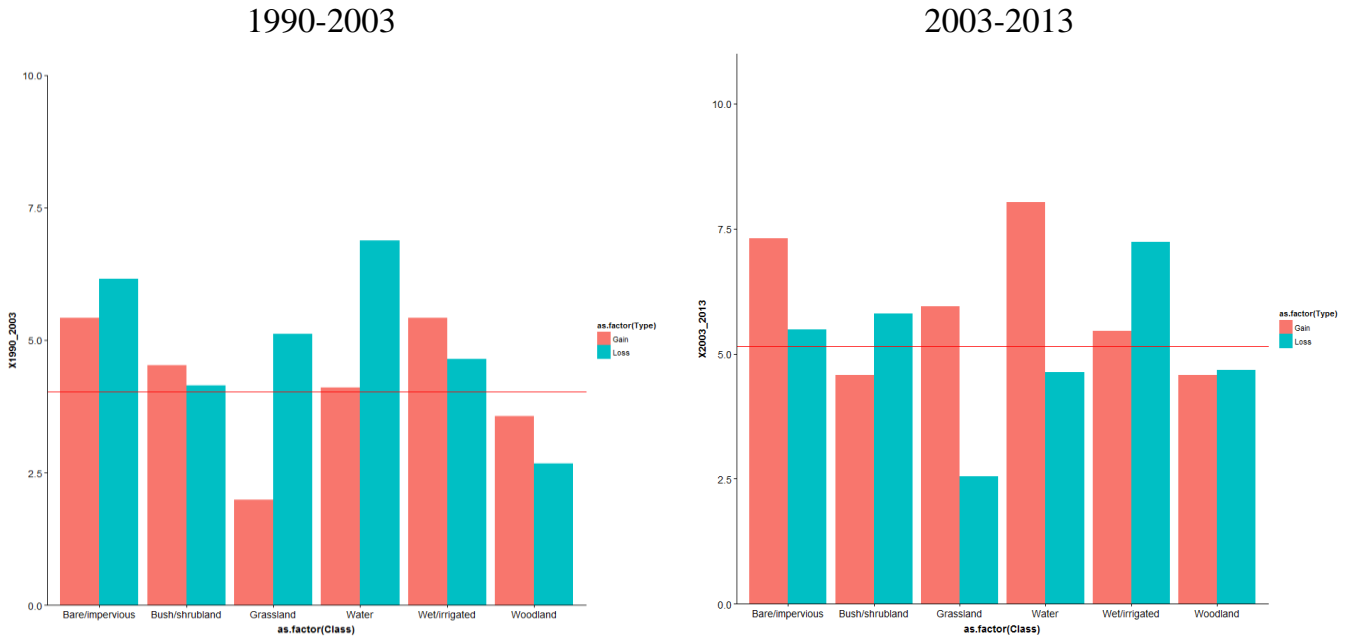


Figure 3-8. Transition-level changes among LC classes representing the intensity of Shrubland and Woodland gains (a) and losses (b) to other land cover classes in 1990-2003 and 2003-2013.

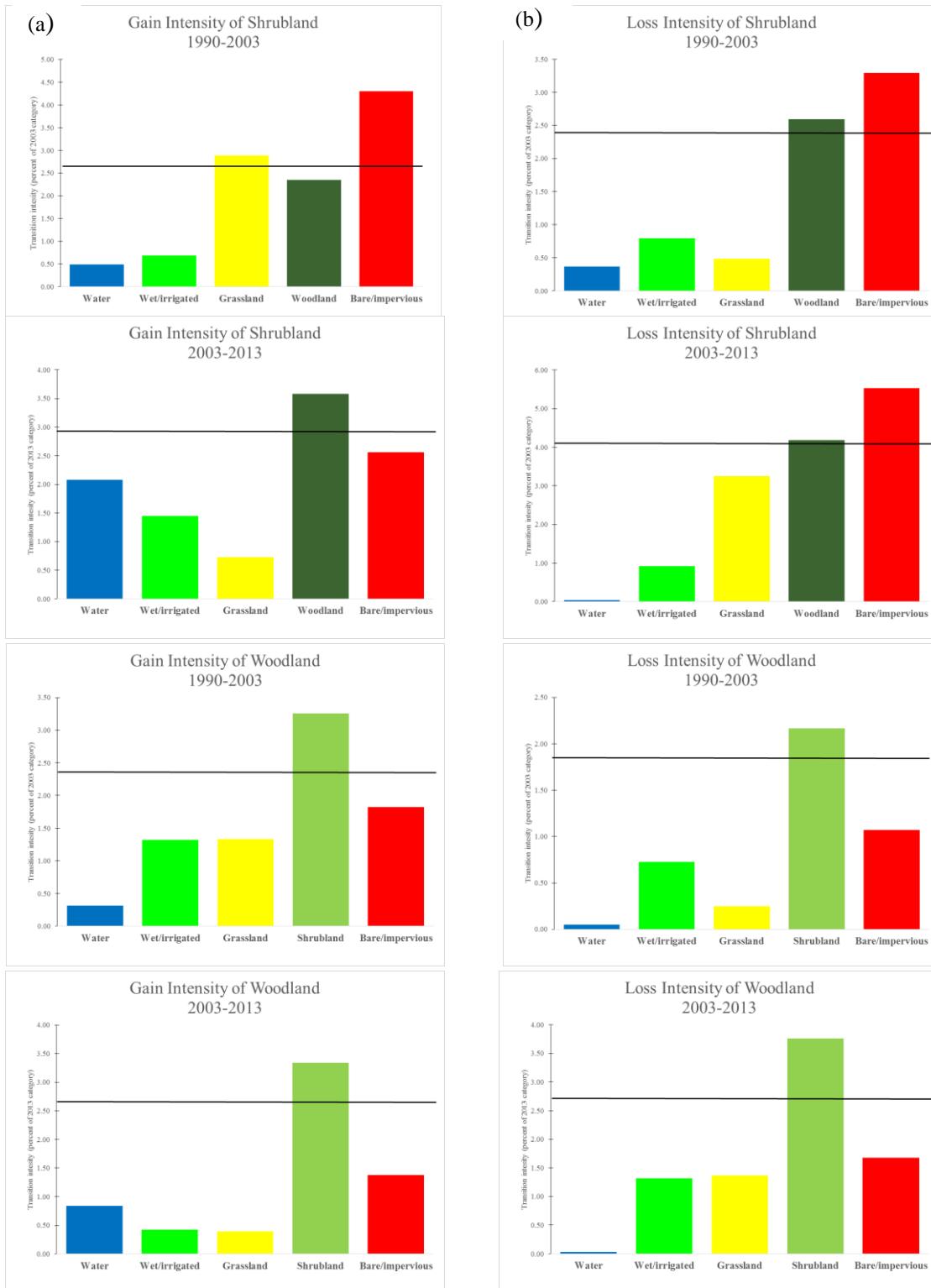


Figure 3-9. Land cover area (km²) for the three time steps in the Chobe District’s protected areas, including Chobe National Park (CNP) and six forest reserves (FR) and reserve extensions (RE).

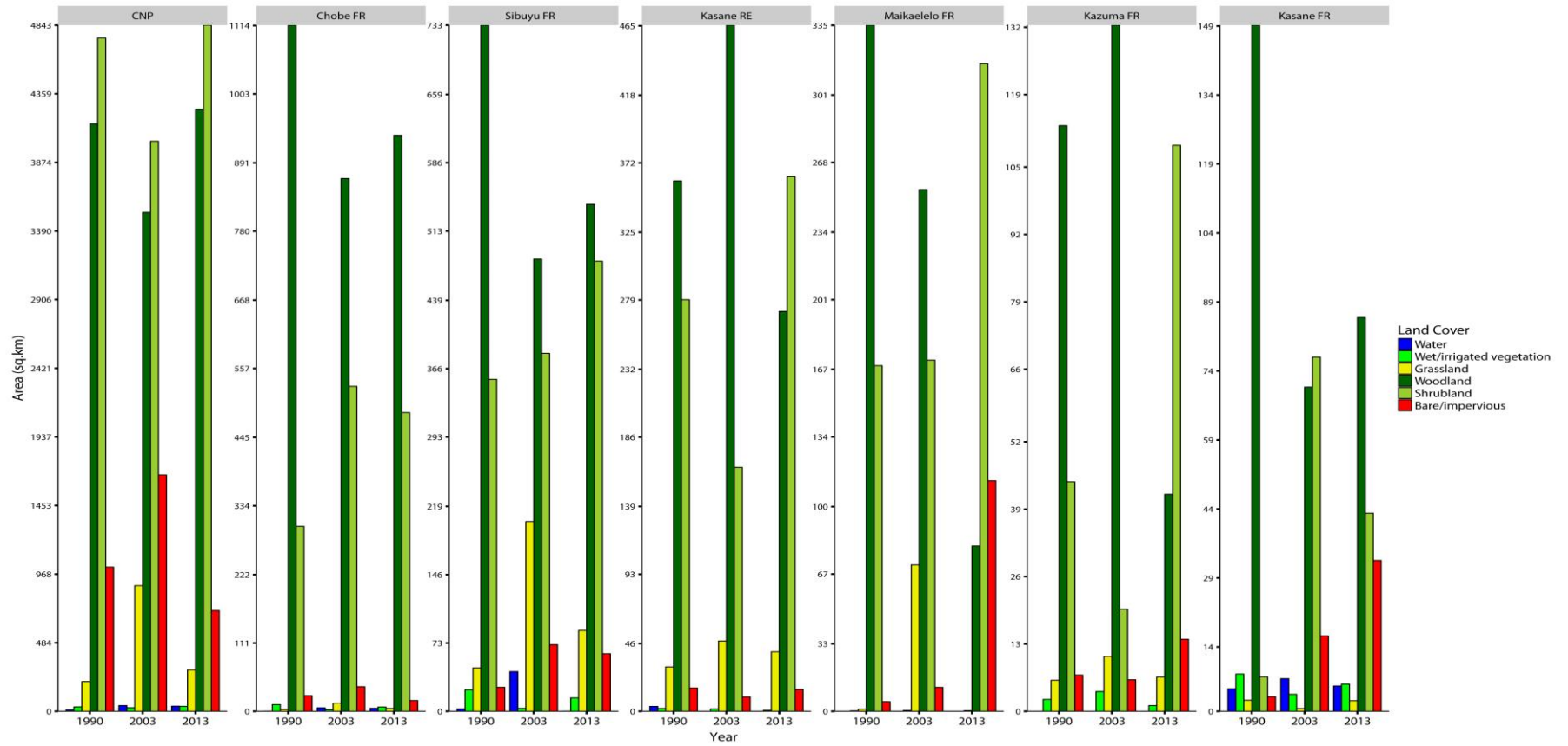


Figure 3-10. Land cover area (km²) for the three time steps in the Chobe District's settlement buffers and the Chobe Enclave.

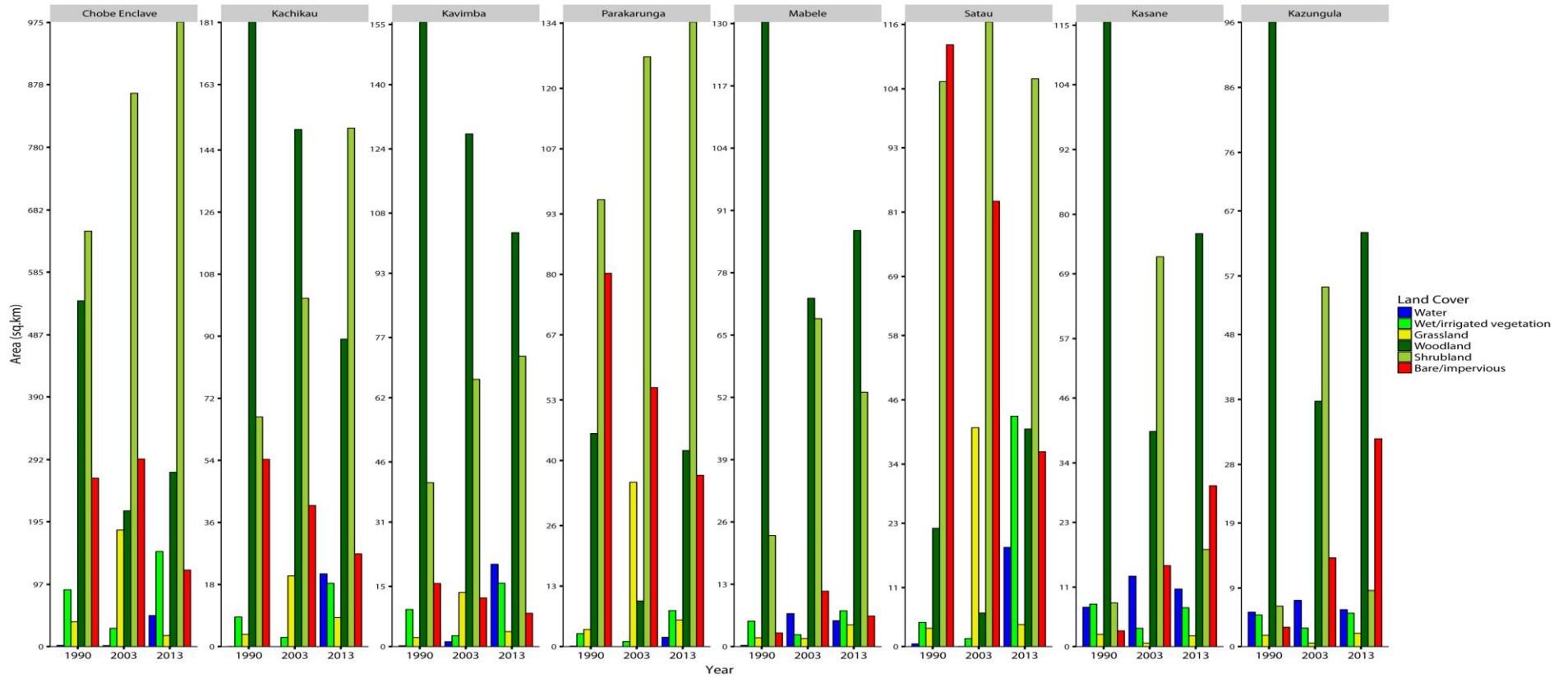


Figure 3-11. Land cover area (km²) for the three time steps within the 1 km² riparian buffer for the entire length of the Chobe River within the Chobe District, and portions of the river within the Chobe Enclave, Chobe National Park (CNP), and Chobe and Kasane Forest Reserves.

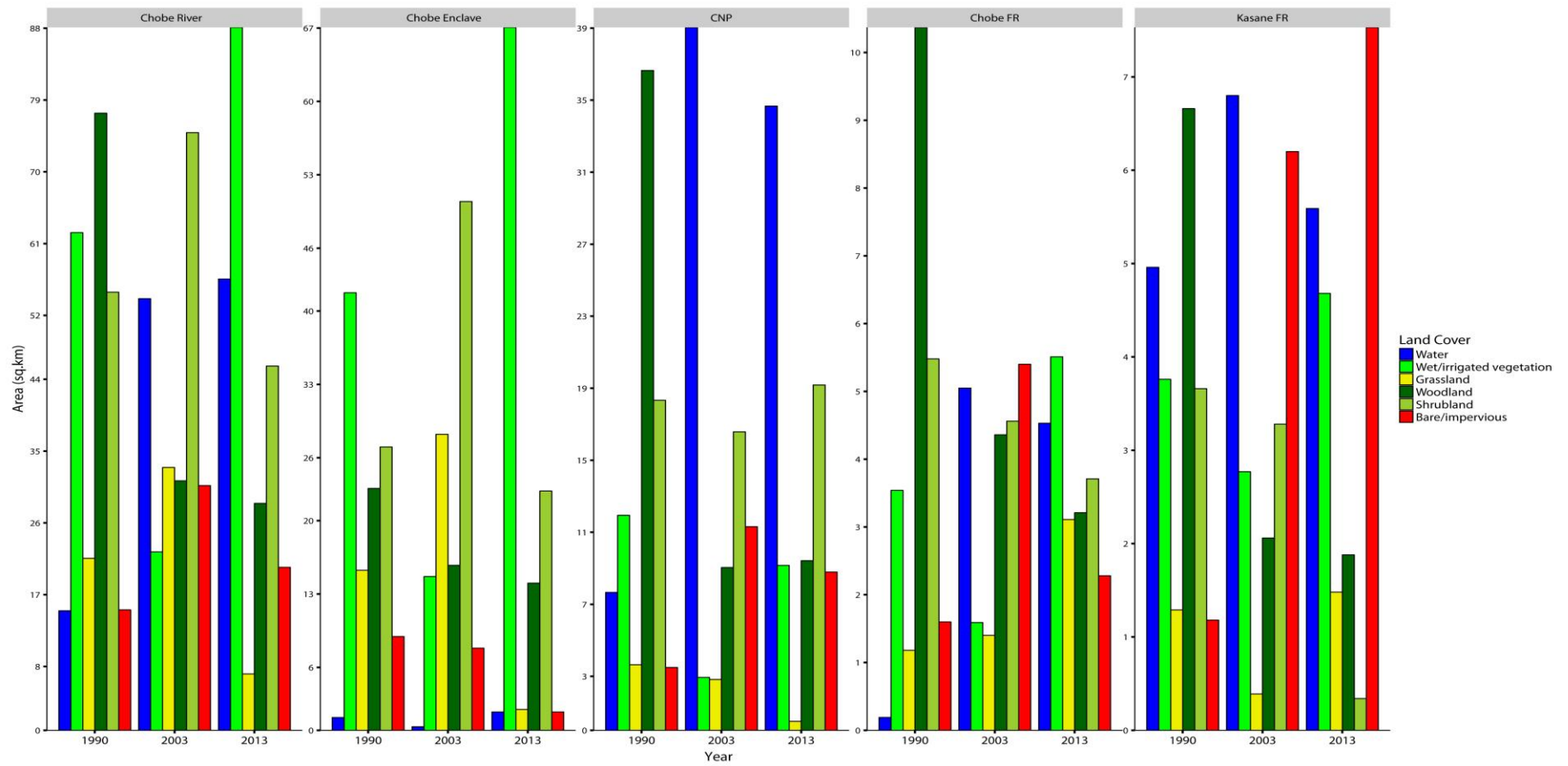


Figure 3-12. Single spectrum analysis (SSA) of mean monthly precipitation at the Kasane meteorological station between 1922 and 2014 showing the major oscillatory (blue) and long term trend components (red) of the rainfall time series data. The dashed black line indicates a period of missing data. A long-term trend of declining month precipitation is evident in the time series, as are shorter oscillations between wetter and drier periods on the order of approximately 5 -10 years, corresponding closely to the timing of major ENSO events. Mean monthly rainfall was higher in the period leading up to the first time step of the analysis, followed by a return to drought conditions after 1991 despite above average rainfall in 2008.

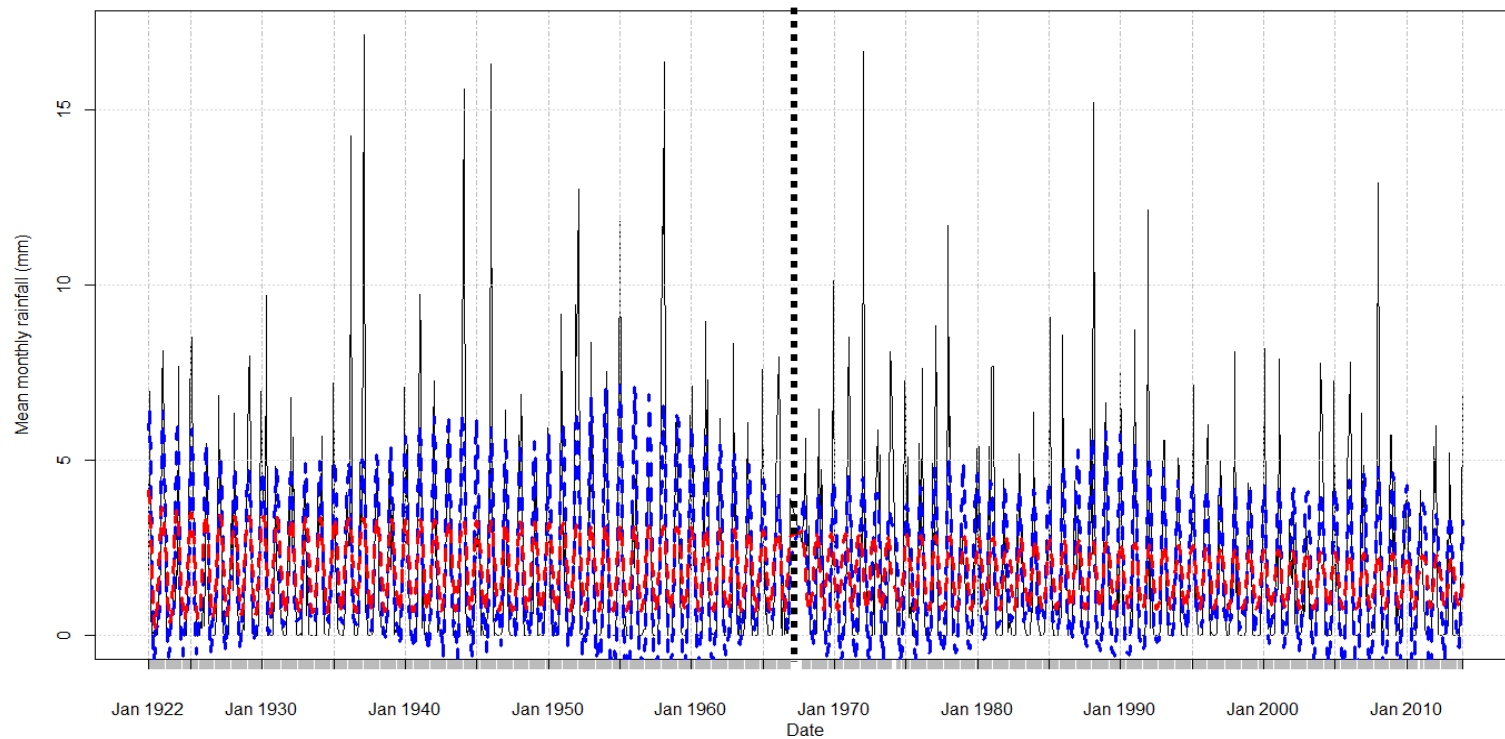


Figure 3-13. Total number of active fires recorded by the MODIS satellite in the Chobe District by month from 2011-2013. Fire is a dry season phenomenon in the system, with a total of 9288 fires were recorded across the Chobe District form 2001-2013.

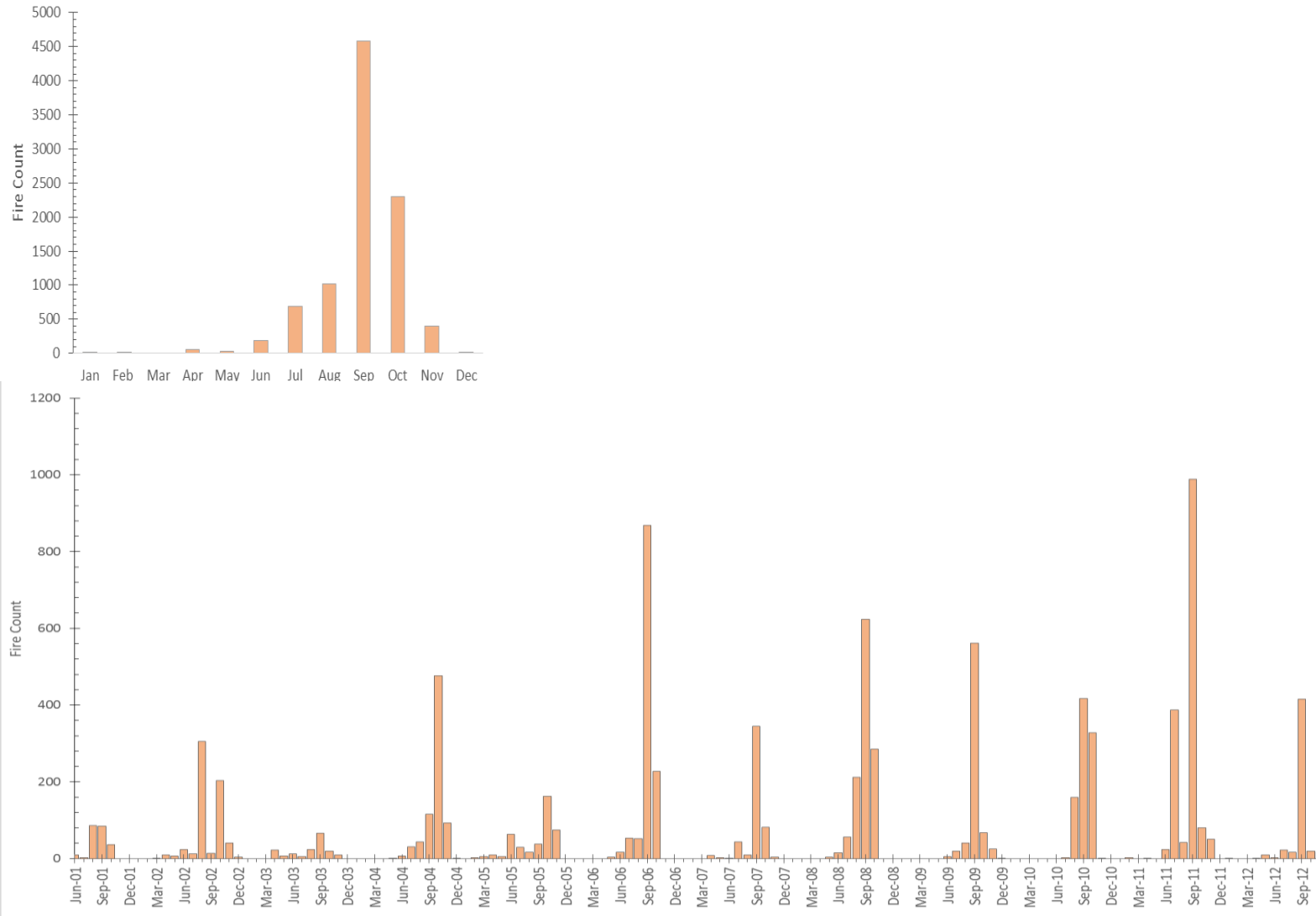


Figure 3-14. Comparison of total annual rainfall (mm) and active fires in the Chobe District, along with mean and maximum Fire Radiative Power (FRP) in megawatts. A total of 9288 fires were recorded across the Chobe District from 2001-2013, and fire frequency and intensity are dynamic over time. High fire years were typically preceded by a year with comparatively few fires, and fire frequency and intensity were greater in years with higher rainfall, which may seem contradictory, but suggests that increased wet season plant biomass in years with high rainfall results in greater dry season fuel loads conducive fire spread

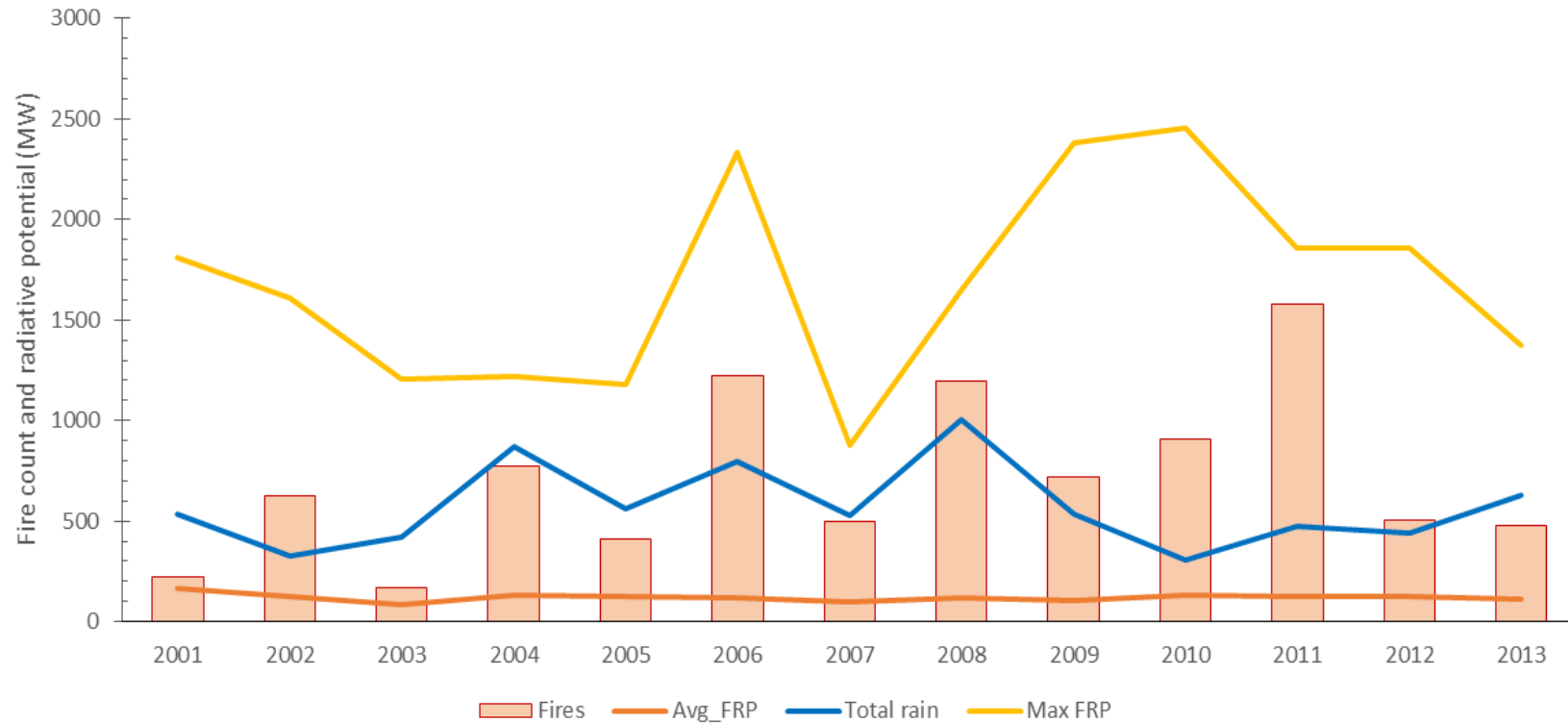


Figure 3-15. The total number and mean intensity (FRP, megawatts) of active fires in 2003 and 2013 in relation to classified land cover. Fires were concentrated predominately in wet/irrigated vegetation and woodland in 2003. In 2013, woodland and shrubland burned most frequently, while grassland also fueled a greater proportion of fires. Mean fire radiative power in grassland was lower than in woodland and shrubland in both 2003 and 2013. Expansion of shrubland in the region, may lead to a greater number of more intense fires across the District.

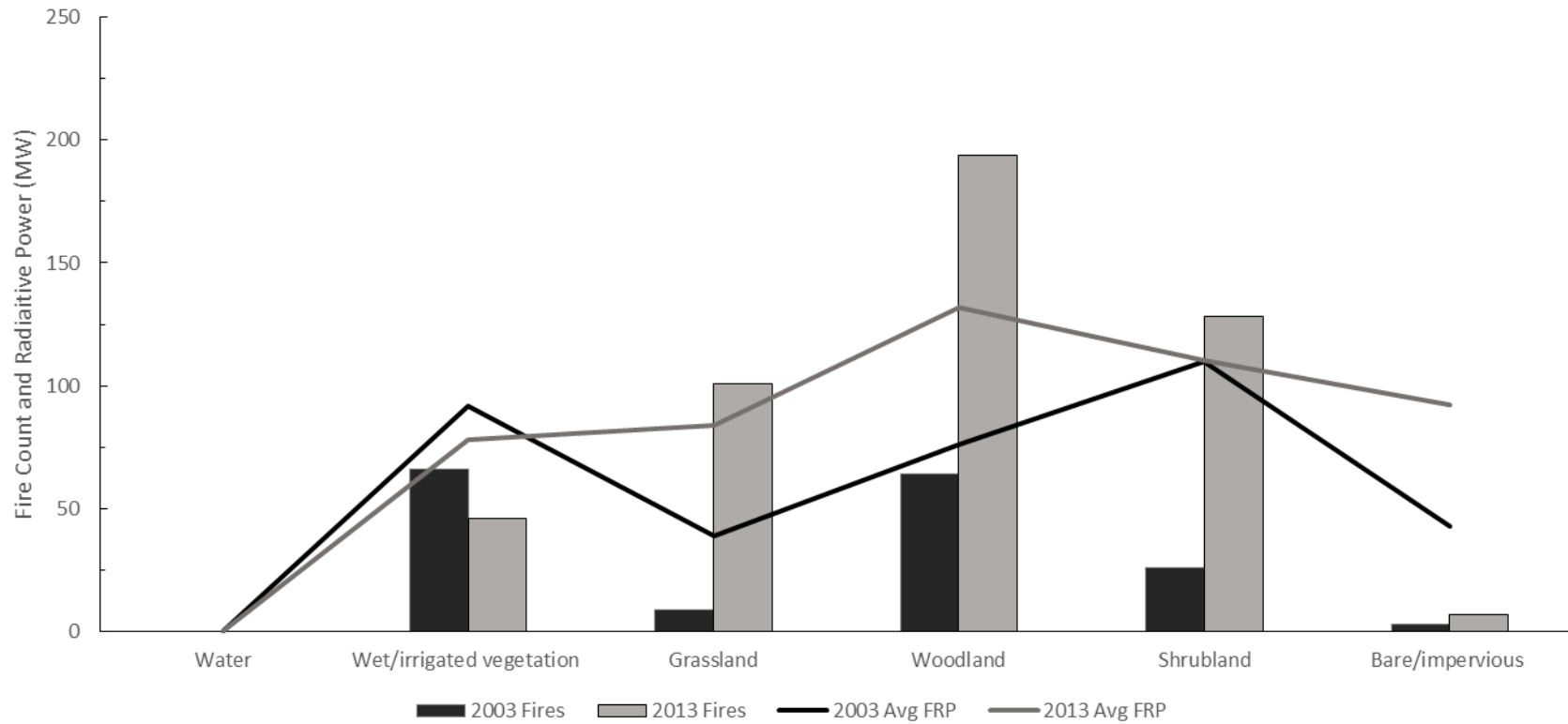


Figure 3-16. Gettis-Ord Gi* analysis of fire hot spots using MODIS active fire data from 2001-2013 overlaying 2013 land cover classification map. Significant clusters of high fire frequency were observed along the Chobe River in the Enclave, in the Kasane FRE, and in unprotected land bordering the Kazuma, Maikaelelo, and Sibuyu FRs, extending into neighboring agricultural fields. Fires associated with agricultural areas, however, tended to occur in late April and early May, while land to the west primarily burned from mid-September to late October. Spatiotemporal patterns of significant fire hot spots in the southeastern part of the District indicate they were not driven by fires spreading into Botswana from neighboring Zimbabwe. However, the significant cluster of fire hot spots near the Chobe River in the north of the Enclave suggests many of these fires are started from burning reeds and floodplain vegetation on both the Botswana and Namibian banks of the Chobe River.

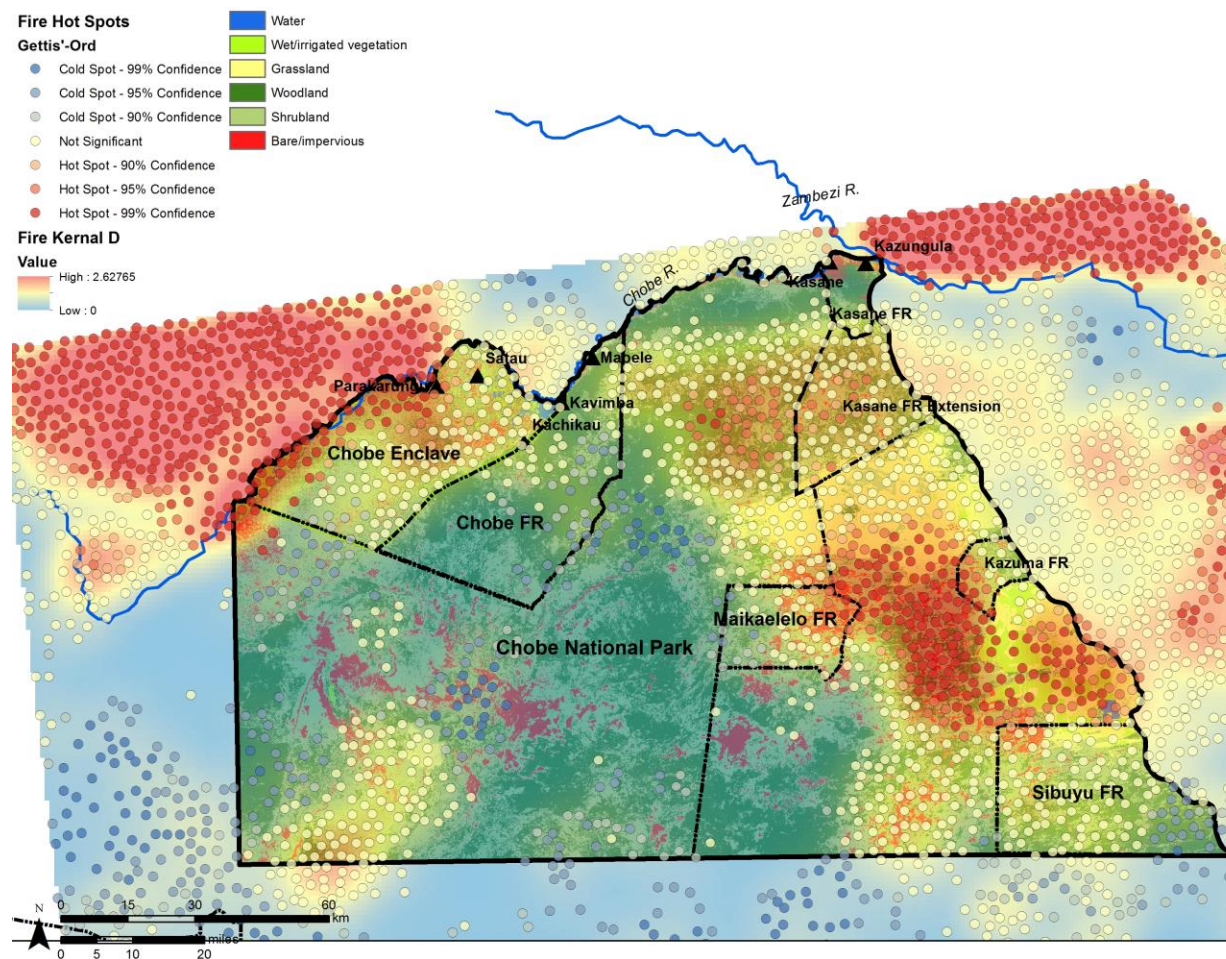


Figure 3-17. Associations between locations of high elephant density (>20 Large Stock Units/km²) and 2003 and 2013 land cover. Elephant biomass estimates were derived from aerial wildlife survey data collected by the Botswana Department of Wildlife and National Parks (DWNP) during the 2003 and 2012 dry seasons. Areas of high elephant biomass in both were predominately associated with woodland and shrubland cover in both years.

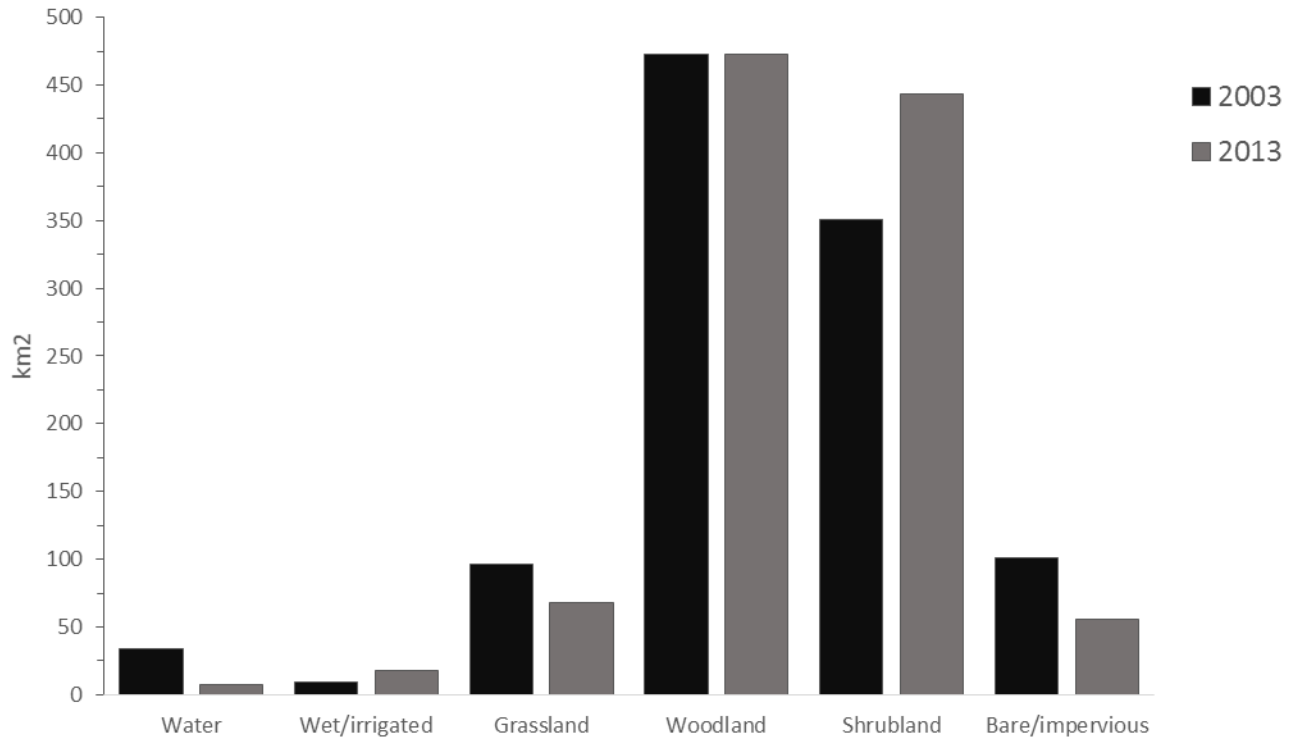


Figure 3-18. Associations between locations of high elephant density (>20 Large Stock Units/km²) and 2003-2013 changes from Woodland cover to other land cover classes. Elephant biomass estimates were derived from aerial wildlife survey data collected by the Botswana Department of Wildlife and National Parks (DWNP) during the 2003 and 2012 dry seasons. Despite locations of high elephant density in woodland and shrubland cover, the majority of woodland in these locations experienced no detectable change from 2003-2013.

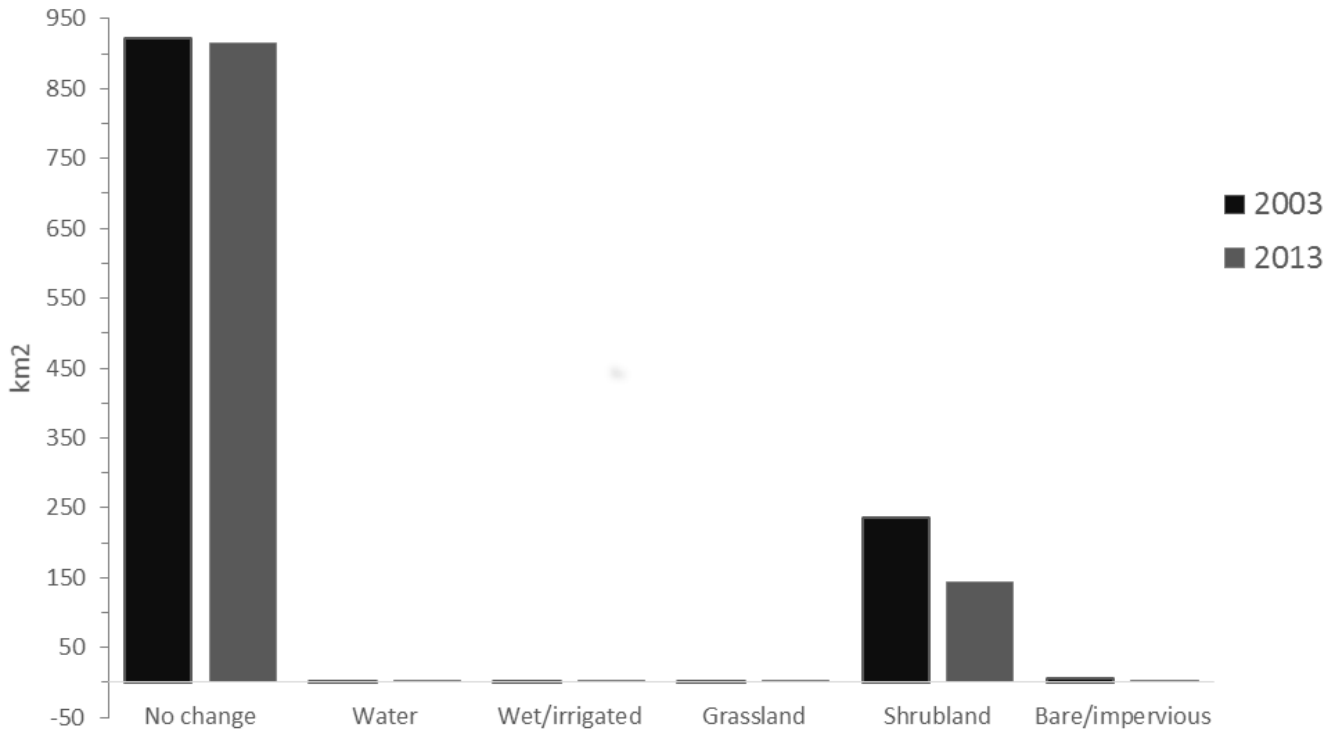
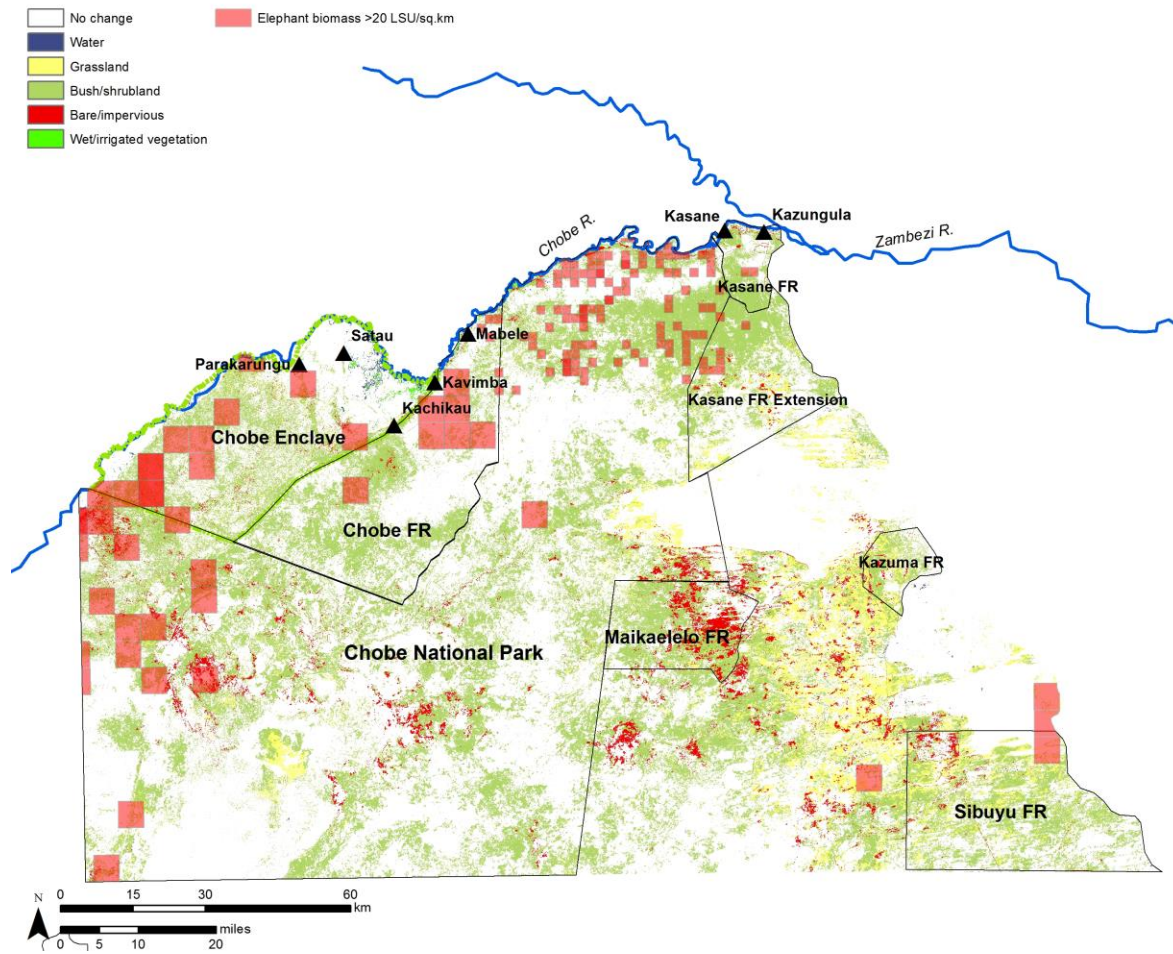


Figure 3-19. Map of locations of high elephant biomass (>20 Large Stock Units/km²) in relation to woodland cover class transitions from 2003-2013. Despite locations of high elephant density in woodland and shrubland cover, the majority of woodland in these locations experienced no detectable change from 2003-2013, while 236 km² saw a transition to shrubland. The same pattern was observed for 2013 LC and 2012 elephant biomass, with 916 km² of woodland cover experiencing no change, and 144 km² changed to shrubland from 2003-2013. of high elephant density (> 20 LSU) and 2003-2013 woodland cover change.



Appendices

Appendix G. Landsat data acquisition list by USGS scene designations indicating the Landsat sensor, the path/row, and year of acquisition.

Scene ID	Acquisition Date
LT51730721990099JSA00	09 April
LT51730731990099JSA00	09 April
LT51740721990106JSA01	16 April
LT51740731990106JSA01	16 April
LE71730722003111ASN00	21 April
LE71730732003111ASN00	21 April
LE71740722003118ASN00	28 April
LE71740732003118ASN00	28 April
LC81730722013114LGN01	24 April
LC81730732013114LGN01	24 April
LC81740722013105LGN01	15 April
LC81740732013105LGN01	15 April

Appendix H. Landsat TM spectral band and spatial resolution characteristics.

Band Number	Data	Spectral Resolution (μm)	Spatial Resolution (m)
Band 1	Blue	0.45 – 0.52	30
Band 2	Green	0.52 – 0.60	30
Band 3	Red	0.63 – 0.69	30
Band 4	NIR	0.77 – 0.90	30
Band 5	SWIR-1	1.55 – 1.75	30
Band 6	TIR	10.40 - 12.50	120
Band 7	SWIR-2	2.08 – 2.35	30

Appendix I. Landsat ETM+ spectral band and spatial resolution characteristics.

Band Number	Data	Spectral Resolution	Spatial Resolution
Band 1	Blue	0.45 – 0.52	30
Band 2	Green	0.52 – 0.60	30
Band 3	Red	0.63 – 0.69	30
Band 4	NIR	0.77 – 0.90	30
Band 5	SWIR-1	1.55 – 1.75	30
Band 6	TIR	10.40 - 12.50	60
Band 7	SWIR-2	2.09 – 2.35	30
Band 8	Pan	0.52 – 0.90	15

Appendix J. Landsat-8 (LCDM) spectral band and spatial resolution characteristics.

Band Number	Data	Spectral Resolution	Spatial Resolution
Band 1	Coastal/Aerosol	0.43 – 0.45	30
Band 2	Blue	0.45 – 0.51	30
Band 3	Green	0.53 – 0.59	30
Band 4	Red	0.64 – 0.67	30
Band 5	NIR	0.85 – 0.88	30
Band 6	SWIR-1	1.57 – 1.65	30
Band 7	SWIR-2	2.11 – 2.29	30
Band 8	Pan	0.50 – 0.68	15
Band 9	Cirrus	1.36 – 1.38	30
Band 10	TIR-1	10.60 – 11.19	100
Band 11	TIR-2	11.50 – 12.51	100

Appendix K. Complete accounting of estimated gross (class) changes in area (km²) and percent land cover in the Chobe District. Initial state class values are listed in columns and rows contain final state values. Land cover values in columns indicate how pixels in each Initial State image was classified in the Final State image. For example, the table shows from 1990-2003, a total of 3150 km² initially classified as woodland in 1990 had changed into shrubland in the 2003 final state image. The Class Changes row indicates the total area for each class in the initial state image that changed into a different class. Total area for each initial state class are shown in the Class Total row, while the Class Total column indicates area of each class in the final state image.

Final State	Initial State												Class Total
	Water		Wet/irrigated veg.		Grassland		Woodland		Shrubland		Bare/impervious		
	km ²	% cover	km ²	% cover	km ²	% cover	km ²	% cover	km ²	% cover	km ²	% cover	
1990-2003													
Water	32.5	46.7	123.5	28.8	115.7	8.8	12.5	0.1	19.5	0.2	2.9	0.2	306.5
Wet/irrigated veg.	17.3	24.9	126.6	29.5	91	7	54.9	0.6	28.7	0.3	1.3	0.1	319.9
Grassland	15.6	22.5	90.2	21.1	969.1	74.1	502.6	5.4	1087.5	13.1	229.1	13.5	2894.2
Woodland	0.5	0.7	40.5	9.4	42.5	3.2	5010.1	53.7	2342.2	28.2	236.6	13.9	7672.3
Shrubland	3.3	4.8	44.4	10.4	82.4	6.3	3150	33.8	3425.1	41.2	727.7	42.8	7432.9
Bare/impervious	0.3	0.5	3.4	0.8	7.1	0.5	599.1	6.4	1414.1	17	503.6	29.6	2527.6
Class Total	69.5	100	428.6	100	1307.9	100	9329.1	100	8317.1	100	1701.1	100	-
Class Changes	37	53.3	302	70.5	338.7	25.9	4319	46.3	4892	58.8	1197.5	70.4	-
2003-2013													
Water	60.3	19.7	3.9	1.2	14.6	0.5	9.4	0.1	23.4	0.3	0.8	0.0	112.3
Wet/irrigated veg.	131.7	43.0	145.7	45.5	139.9	4.8	22.0	0.3	76.1	1.0	10.6	0.4	525.8
Grassland	111.5	36.4	97.1	30.4	1172.3	40.5	61.3	0.8	114.3	1.5	16.6	0.7	1573.2
Woodland	1.0	0.3	42.2	13.2	394.9	13.6	4156.8	54.2	2797.4	37.6	423.0	16.7	7815.3
Shrubland	1.4	0.4	29.3	9.2	942.0	32.5	3215.0	41.9	4036.5	54.3	1397.3	55.3	9621.6
Bare/impervious	0.7	0.2	1.7	0.5	230.5	8.0	207.6	2.7	385.2	5.2	679.4	26.9	1505.1
Class Total	306.5	100.0	319.9	100.0	2894.2	100.0	7672.3	100.0	7432.9	100.0	2527.6	100.0	-
Class Changes	246.2	80.3	174.2	54.5	1721.9	59.5	3515.4	45.8	3396.3	45.7	1848.3	73.1	-

1990-2013

Water	14.0	20.2	18.7	4.4	19.4	1.5	22.9	0.2	33.6	0.4	3.7	0.2	112.3
Wet/irrigated veg.	33.1	47.6	233.7	54.5	142.1	10.9	34.5	0.4	77.2	0.9	5.3	0.3	525.8
Grassland	17.9	25.8	107.9	25.2	922.6	70.5	68.0	0.7	403.4	4.9	53.4	3.1	1573.2
Woodland	1.3	1.9	40.9	9.5	84.1	6.4	4485.9	48.1	2788.0	33.5	415.0	24.4	7815.3
Shrubland	2.6	3.8	24.3	5.7	132.4	10.1	4317.2	46.3	4263.4	51.3	881.8	51.8	9621.6
Bare/impervious	0.5	0.7	3.2	0.7	7.2	0.6	400.6	4.3	751.6	9.0	342.1	20.1	1505.1
Class Total	69.5	100.0	428.6	100.0	1307.9	100.0	9329.1	100.0	8317.1	100.0	1701.1	100.0	-
Class Changes	55.4	79.8	194.9	45.5	385.2	29.5	4843.2	51.9	4053.8	48.7	1359.1	79.9	-

Appendix L. Estimated area (km²) and percent (%) land cover for the three periods (1990, 2003, 2013) within the Chobe District's protected areas, the Enclave and buffer areas surrounding the district's settlements and the Chobe River riparian corridor.

	Water						Wet/irrigated vegetation						Grassland						Woodland						Bush/shrubland						Bare/imperious							
	1990		2003		2013		1990		2003		2013		1990		2003		2013		1990		2003		2013		1990		2003		2013		1990		2003		2013			
Protected areas	km ²	%	km ²	%	km ²	%	km ²	%	km ²	%	km ²	%	km ²	%	km ²	%	km ²	%	km ²	%	km ²	%	km ²	%	km ²	%	km ²	%	km ²	%	km ²	%	km ²	%				
CNP	9.5	0.1	40.5	0.4	36.4	0.4	30.7	0.3	24.9	0.2	35.1	0.3	210.1	2.1	886.7	8.7	292.0	2.9	4147.1	40.8	3521.8	34.6	4250.3	41.8	4752.7	46.7	4023.7	39.6	4843.6	47.6	1017.6	10.0	710.4	16.4	1669.3	7.0		
Kasane FR	4.9	2.8	7.1	4.1	5.5	3.2	8.1	4.6	3.7	2.1	5.9	3.4	2.4	1.4	0.6	0.4	2.3	1.3	149.2	85.1	70.5	40.2	85.6	48.9	7.5	4.3	77.0	43.9	43.1	24.6	3.2	1.8	32.8	9.3	16.4	18.7		
Kasane RE	3.3	0.5	0.0	0.0	0.0	0.0	1.9	0.3	1.6	0.2	0.7	0.1	30.1	4.4	47.7	6.9	40.4	5.9	359.8	52.1	465.5	67.4	271.3	39.3	279.2	40.5	165.6	24.0	363.0	52.6	15.8	2.3	14.8	1.4	9.8	2.1		
Chobe FR	0.2	0.0	5.6	0.4	4.8	0.3	10.9	0.7	2.7	0.2	7.0	0.5	3.1	0.2	13.4	0.9	4.6	0.3	1114.8	76.6	865.4	59.5	935.7	64.3	300.5	20.7	527.9	36.3	485.4	33.4	25.4	1.7	17.5	2.7	39.9	1.2		
Kazuma FR	0.0	0.0	0.0	0.0	0.0	0.0	2.3	1.3	3.8	2.2	1.1	0.6	6.0	3.5	10.6	6.1	6.6	3.8	113.0	65.5	132.4	76.7	41.9	24.3	44.3	25.6	19.7	11.4	109.2	63.3	7.0	4.0	13.9	3.5	6.1	8.1		
Maikaelelo FR	0.0	0.0	0.0	0.0	0.0	0.0	0.2	0.0	0.4	0.1	0.0	0.0	1.1	0.2	71.5	14.0	0.3	0.1	335.1	65.7	254.8	50.0	80.7	15.8	168.8	33.1	171.5	33.6	316.2	62.0	4.7	0.9	112.7	2.3	11.7	22.1		
Sibuyu	2.6	0.2	42.4	3.6	0.1	0.0	22.9	1.9	3.1	0.3	14.3	1.2	46.3	3.9	202.7	17.1	86.3	7.3	733.0	61.9	483.1	40.8	541.6	45.7	354.6	29.9	382.4	32.3	480.9	40.6	25.6	2.2	61.6	6.0	71.2	5.2		
Chobe Enclave and Villages																																						
Enclave	1.9	0.1	1.5	0.1	48.4	3.1	88.7	5.6	28.5	1.8	148.4	9.4	38.7	2.4	182.0	11.5	17.2	1.1	540.1	34.2	212.0	13.4	272.2	17.2	649.0	41.0	864.4	54.7	975.7	61.7	263.1	16.6	293.0	18.5	119.5	7.6		
Satau	0.5	0.2	0.0	0.0	18.5	7.4	4.5	1.8	1.5	0.6	43.0	17.3	3.4	1.4	40.8	16.5	4.1	1.7	22.0	8.9	6.2	2.5	40.6	16.3	105.3	42.5	116.4	47.0	105.9	42.6	112.2	45.2	83.0	33.5	36.3	14.6		
Mabele	0.2	0.1	6.9	4.2	5.4	3.3	5.3	3.2	2.5	1.5	7.5	4.6	1.8	1.1	1.7	1.0	4.5	2.8	130.3	79.6	72.7	44.4	86.8	53.0	23.2	14.2	68.4	41.8	53.1	32.4	2.8	1.7	11.5	7.0	6.4	3.9		
Kavimba	0.2	0.1	1.2	0.5	20.5	9.2	9.2	4.1	2.7	1.2	15.8	7.1	2.2	1.0	13.5	6.0	3.7	1.7	155.6	69.5	127.7	57.1	103.1	46.1	40.8	18.2	66.6	29.7	72.4	32.3	15.7	7.0	12.1	5.4	8.3	3.7		
Kazungula	5.3	4.5	7.1	6.1	5.7	4.9	4.9	4.1	2.8	2.4	5.1	4.4	1.7	1.5	0.5	0.5	2.0	1.7	96.0	82.0	37.7	32.2	63.7	54.4	6.2	5.3	55.3	47.2	8.6	7.4	3.0	2.5	13.6	11.6	32.0	27.3		
Kasane	7.3	5.1	13.0	9.0	10.6	7.4	7.8	5.5	3.4	2.3	7.2	5.0	2.3	1.6	0.6	0.4	2.0	1.4	115.6	80.3	39.8	27.7	76.4	53.1	8.1	5.6	72.1	50.1	18.0	12.5	2.9	2.0	15.0	10.4	29.8	20.7		
Kachikau	0.0	0.0	0.0	0.0	21.1	6.7	8.5	2.7	2.6	0.8	18.4	5.8	3.5	1.1	20.5	6.5	8.4	2.7	181.1	57.7	149.9	47.6	89.2	28.4	66.6	21.2	101.0	32.1	150.3	47.8	54.3	17.3	40.9	13.0	26.9	8.6		
Parakurunga	0.1	0.0	0.0	0.0	2.0	0.9	2.8	1.2	1.1	0.5	7.7	3.4	3.7	1.6	35.3	15.4	5.7	2.5	45.8	20.0	9.8	4.3	42.1	18.4	96.1	42.0	126.8	55.5	134.3	58.7	80.2	35.1	55.7	24.3	36.8	16.1		
Riparian Zone																																						
Chobe River	15.0	6.1	54.1	22.0	56.6	23.0	62.4	25.3	22.4	9.1	88.1	35.8	21.6	8.8	32.9	13.4	7.1	2.9	77.3	31.4	31.3	12.7	28.4	11.6	54.9	22.3	74.9	30.4	45.7	18.5	15.1	6.1	30.7	12.5	20.4	8.3		
CNP	5.0	9.4	6.8	47.8	5.6	42.4	3.8	14.6	2.8	3.6	4.7	11.2	1.3	4.5	0.4	3.5	1.5	0.6	6.7	44.8	2.1	11.1	1.9	11.5	3.7	22.4	3.3	20.3	0.3	23.5	1.2	4.3	6.2	13.8	7.5	10.8		
Enclave	7.7	1.0	39.0	0.3	34.7	8.2	11.9	35.6	2.9	12.5	9.2	57.2	3.6	13.0	2.8	24.1	0.5	1.7	36.6	19.7	9.0	13.4	9.4	12.0	18.3	23.0	16.6	43.0	19.2	19.5	3.5	7.6	11.3	6.7	8.8	1.5		
Kasane FR	0.2	23.1	5.0	31.6	4.5	26.0	3.5	17.5	1.6	12.9	5.5	21.8	1.2	6.0	1.4	1.8	3.1	6.9	10.4	31.0	4.4	9.6	3.2	8.8	5.5	17.0	4.6	15.3	3.7	1.6	1.6	5.5	5.4	28.9	2.3	35.0		
Chobe FR	1.2	0.8	0.3	22.6	9.6	20.3	41.7	15.8	14.7	7.1	67.1	24.6	15.3	5.3	28.2	6.2	2.0	13.9	23.1	46.4	15.7	19.5	14.0	14.4	27.0	24.5	50.5	20.4	22.8	16.6	8.9	7.2	7.8	24.1	1.7	10.2		

Appendix M. Estimated net change in land cover area (km²) and percent (%) change in land cover area for each class during the periods (1990-2003, 2003-2013, and 1990-2013) within the Chobe District's protected areas, the Enclave and 10 km (314 km²) buffer areas surrounding the district's settlements, and 1 km riparian buffer along the Chobe River.

	Water						Wet/irrigated vegetation						Grassland						Woodland						Bush/shrubland						Bare/impervious						
	1990-2003		2003-2013		1990-2013		1990-2003		2003-2013		1990-2013		1990-2003		2003-2013		1990-2013		1990-2003		2003-2013		1990-2013		1990-2003		2003-2013		1990-2013		1990-2003		2003-2013		1990-2013		
Protected areas	km ²	%	km ²	%	km ²	%	km ²	%	km ²	%	km ²	%	km ²	%	km ²	%	km ²	%	km ²	%	km ²	%	km ²	%	km ²	%	km ²	%	km ²	%	km ²	%	km ²	%			
CNP	31.0	324.5	-4.1	-10.2	26.8	281.0	-5.9	-19.1	10.2	41.2	4.3	14.1	676.6	322.1	-594.7	-67.1	81.9	39.0	-625.3	-15.1	728.4	20.7	103.1	2.5	-729.0	-15.3	819.9	20.4	90.9	1.9	651.8	64.1	-958.9	-57.4	-307.1	-30.2	
Kasane FR	2.2	44.0	-1.6	-22.2	0.6	12.0	-4.4	-53.7	2.2	58.7	-2.2	-26.6	-1.8	-73.5	1.6	254.1	-0.1	-6.0	-78.7	-52.8	15.2	21.5	-63.5	-42.6	69.5	930.3	-33.8	-43.9	35.7	477.5	13.2	410.6	16.4	100.2	29.6	922.3	
Kasane RE	-3.3	-100.0	0.0	0.0	-3.3	-100.0	-0.3	-13.8	-0.9	-56.3	-1.2	-62.3	17.6	58.4	-7.3	-15.2	10.3	34.2	105.6	29.4	-194.2	-41.7	-88.5	-24.6	-113.6	-40.7	197.4	119.2	83.7	30.0	-6.0	-38.2	5.0	51.3	-1.0	-6.5	
Chobe FR	5.4	2759.2	-0.8	-13.7	4.6	2367.0	-8.1	-74.8	4.3	155.5	-3.9	-35.6	10.3	332.0	-8.9	-66.1	1.4	46.4	-249.4	-22.4	70.3	8.1	-179.2	-16.1	227.3	75.6	-42.5	-8.1	184.8	61.5	14.5	57.1	-22.4	-56.1	-7.9	-31.0	
Kazuma FR	0.0	0.0	0.0	0.0	0.0	0.0	1.5	65.3	-2.8	-72.5	-1.3	-54.6	4.6	75.7	-4.0	-37.9	0.6	9.1	19.4	17.2	-90.5	-68.4	-71.1	-62.9	-24.5	-55.4	89.4	453.6	64.9	146.7	-0.9	-13.2	7.9	129.6	6.9	99.2	
Maikaelelo FR	0.0	310.0	0.0	0.0	0.0	0.0	0.1	56.1	-0.3	-92.7	-0.2	-88.5	70.4	6611.1	-71.2	-99.6	-0.8	-70.8	-80.3	-24.0	-174.1	-68.3	-254.4	-75.9	2.7	1.6	144.7	84.4	147.4	87.3	7.1	151.0	101.0	860.7	108.0	2311.2	
Sibuyu	39.9	1563.8	-42.3	-99.7	-2.4	-95.4	-19.8	-86.6	11.3	366.7	-8.5	-37.4	156.4	337.6	-116.4	-57.4	40.0	86.3	-249.8	-34.1	58.5	12.1	-191.3	-26.1	27.8	7.8	98.5	25.8	126.3	35.6	45.6	178.3	-9.6	-13.5	36.0	140.9	
Chobe Enclave and Villages																																					
Enclave	-0.3	-18.7	46.9	3110.4	46.5	2509.1	-60.2	-67.9	120.0	421.5	59.8	67.4	143.3	370.4	-164.8	-90.6	-21.5	-55.6	-328.1	-60.7	60.2	28.4	-267.9	-49.6	215.4	33.2	111.3	12.9	326.8	50.4	29.9	11.3	-173.5	-59.2	-143.7	-54.6	
Satau	-0.5	-96.4	18.5	102595.0	18.0	3561.1	-3.0	-67.3	41.5	2817.1	38.4	852.7	37.4	1099.0	-36.7	-90.0	0.7	20.4	-15.8	-71.7	34.3	549.5	18.5	83.9	11.1	10.5	-10.6	-9.1	0.5	0.5	-29.2	-26.0	-46.7	-56.2	-75.9	-67.6	
Mabele	6.6	2750.7	-1.5	-21.3	5.2	2142.2	-2.8	-53.2	5.0	201.3	2.2	40.9	-0.2	-8.4	2.9	171.2	2.7	148.4	-57.6	-44.2	14.1	19.4	-43.5	-33.4	45.3	195.4	-15.3	-22.4	29.9	129.2	8.7	309.2	-5.2	-44.7	3.6	126.2	
Kavimba	1.0	518.9	19.3	1596.8	20.3	10401.4	-6.5	-70.9	13.1	487.4	6.5	70.9	11.3	505.0	-9.8	-72.3	1.5	67.3	-27.9	-17.9	-24.6	-19.3	-52.5	-33.7	25.8	63.1	5.8	8.7	31.5	77.3	-3.6	-23.0	-3.8	-31.6	-7.4	-47.3	
Kazungula	1.8	34.1	-1.4	-19.9	0.4	7.4	-2.0	-41.6	2.3	80.8	0.3	5.5	-1.2	-69.3	1.5	286.7	0.3	18.6	-58.3	-60.7	26.0	68.8	-32.4	-33.7	49.1	788.6	-46.7	-84.4	2.4	38.6	10.7	358.8	18.3	134.4	29.0	975.3	
Kasane	5.8	79.1	-2.4	-18.2	3.4	46.4	-4.5	-56.9	3.8	112.4	-0.7	-8.5	-1.6	-72.0	1.4	214.8	-0.3	-11.9	-75.8	-65.6	36.6	92.0	-39.2	-33.9	64.1	792.4	-54.2	-75.1	9.9	122.2	12.1	416.3	14.8	98.8	26.9	926.3	
Kachikau	0.0	-100.0	21.1	100.0	21.0	51937.8	-5.9	-69.2	15.7	596.3	9.8	114.8	16.9	477.9	-12.1	-59.0	4.8	136.7	-31.2	-17.2	-60.8	-40.5	-92.0	-50.8	34.4	51.6	49.3	48.8	83.7	125.6	-13.4	-24.6	-14.0	-34.3	-27.4	-50.5	
Parakurunga	-0.1	-99.2	2.0	221100.0	1.9	1698.4	-1.7	-61.2	6.7	621.6	5.0	179.9	31.6	862.2	-29.6	-83.8	2.0	55.7	-36.0	-78.6	32.3	330.1	-3.7	-8.0	30.7	32.0	7.5	5.9	38.2	39.8	-24.6	-30.6	-18.8	-33.9	-43.4	-54.1	
Riparian Zone																																					
Chobe River	39.1	261.2	2.5	4.6	41.6	277.7	-40.0	-64.1	65.7	294.0	25.7	41.2	11.4	52.8	-25.9	-78.5	-14.5	-67.2	-46.1	-59.6	-2.8	-9.0	48.9	-63.2	20.0	36.4	-29.3	-39.1	-9.3	-16.9	15.6	103.2	-10.2	-33.4	5.3	35.3	
Enclave	31.4	409.4	-4.4	-11.2	27.0	352.4	-9.0	-75.4	6.2	212.1	-2.8	-23.2	-0.8	-22.5	-2.3	-82.1	-3.1	-86.2	-27.6	-75.3	0.4	4.2	-27.2	-74.3	-1.8	-9.6	2.6	15.7	0.8	4.6	7.8	223.6	-2.5	-22.3	5.3	151.5	
CNP	1.8	37.2	-1.2	-17.8	0.6	12.8	-1.0	-26.4	1.9	69.3	0.9	24.6	-0.9	-69.5	1.1	276.0	0.2	14.5	-4.6	-69.1	-0.2	-8.4	-4.8	-71.7	-0.4	-10.2	-2.9	-89.6	-3.3	-90.7	5.0	426.7	1.3	21.3	6.3	538.9	
Kasane FR	4.9	2621.8	-0.5	-10.2	4.3	2343.7	-1.9	-55.1	3.9	246.5	2.0	55.7	0.2	18.0	1.7	123.0	1.9	163.2	-6.0	-57.9	-1.2	-26.4	-7.2	-69.0	-0.9	-16.7	-0.9	-18.7	-1.8	-32.3	3.8	236.9	-3.1	-57.7	0.7	42.6	
Chobe FR	-0.9	-72.3	9.3	2760.2	8.4	691.2	-27.1	-64.9	52.4	357.2	25.3	60.7	13.0	84.9	-26.3	-93.0	-13.3	-87.0	-7.3	-31.8	-1.7	-10.8	-9.0	-39.2	23.4	86.7	-27.6	-54.8	-4.2	-15.5	-1.1	-12.3	-6.1	-77.7	-7.2	-80.5	

Chapter 4: Quantifying wildlife-source contributions to terrestrial and aquatic fecal loadings using a Distance sampling approach

Abstract

Spatially-distributed river basin-scale models like the Soil and Water Assessment Tool (SWAT) are increasingly utilized by a wide range of environmental and conservation stakeholders to quantify and predict the impacts of land management decisions on bacterial water quality in large and complex river systems. However, predicting fecal indicator bacteria (FIB) concentrations in surface waters remains the most uncertain parameter in regards to disagreement of modelling results with values observed in the field. Improved tools and methods of FIB-source characterization are needed to better estimate loading contributions from animal populations. Wildlife-source fecal bacteria contributions, in particular, have remained difficult to estimate because of the considerable spatiotemporal variability in animal density, habitat resource utilization, and diet in large river basins. In this study, we present a straightforward and low-cost, standardized method for estimating wildlife-source fecal loading on the landscape using Distance-sampling of dung piles along line transects in riparian habitat. Wildlife-source fecal density was estimated along 55 transects spaced 500 m apart along a 27.5 km reach of the Chobe River in northeastern Botswana. Fecal density estimates were stratified by protected (Chobe National Park, CNP) and unprotected (UP) land, as well as by transect. Average estimated fecal densities in the CNP ranged from 18.5-180.9 dung piles/ha. (%CV 19.4-35.0) in the wet season and 22.0-185.1 dung piles/ha. (%CV 16.4-42.3) in the dry season and were significantly higher than fecal densities in UP land ($p < 0.0001$). Wildlife fecal loads were consistently lower for transects located closer to human settlements and were highest at the same locations in the CNP during both wet and dry seasons. Regression analysis indicated a significant positive association between mean dry season fecal density and average waterborne concentrations of the FIB *Escherichia coli* (*E. coli*) in both the dry season ($p=0.042$) and the first three months of the wet season ($p=0.027$). Degree bank slope ($p=0.011$) and percent grass cover ($p=0.014$) were also influential in the wet season.

Introduction

Hydrological modeling is a powerful tool for planning and developing sustainable, long-term watershed management strategies and pollution guidelines, including Total Maximum Daily Loads (TMDLs) for fecal bacteria required by the US Clean Water Act. Developing accurate predictions of how complex natural processes and land use and management scenarios impact bacterial surface water quality within a watershed remains a significant challenge. Watershed modeling is inherently uncertain, as it involves using a simplified or reduced number of variables to represent complex environmental phenomena, selecting appropriate functional forms for potential interactions among many different variables, and assigning proper boundaries for model components (Suter II et al. 1987, Benham et al. 2006, Parajuli et al. 2009). While accurate simulations of the deposition, fate, and transport of fecal bacteria originating from agricultural and livestock sources have been undertaken with success, the influence of free-ranging wildlife populations on bacterial water quality dynamics remains largely unexplored (Benham et al. 2006, Baffaut and Sadeghi 2010).

Physically-based, spatially-distributed hydrologic models like the Soil and Water Assessment Tool (SWAT) rely on a detailed understanding of energy, mass, and momentum of water and sediments, in addition to watershed characteristics such as vegetation cover, soil, and topography, and generally require large amounts of input data for a wide range of parameters that often cannot be easily optimized (Ferguson et al. 2003, Srinivasan et al. 2010). Decay of fecal bacteria in aquatic systems is controlled by a number of biotic and abiotic processes for which accurate measurements are not often available. The majority of watershed models assume that FIB decay follow first-order kinetics, although some studies in natural systems have observed *E. coli* populations initially undergoing a rapid first-order decay, followed by a second, slower period of decay (Auer and Niehaus 1993). Most approaches to modeling fecal bacteria dynamics in natural surface waters consider only a net decrease in fecal bacteria concentration over time based upon experimental measurements using culture-based methods. Empirical determination of fecal bacteria decay rates using laboratory microcosms or field experiments represent both FIB death as well as loss of cultivability, but not their potential regrowth in sediments, on submerged aquatic vegetation, or in the water column (Bordalo et al. 2002, Jamieson et al. 2005b, Badgley et al. 2011, de Brauwere et al. 2014).

While many potential sources of pathogenic loadings to natural surface water exist, wildlife can represent a major source of aquatic contamination in watersheds where they occur at high population densities. Although wildlife dung may be considered beneficial as a fertilizer in systems that are nutrient-limited (Hobbs 1996, Augustine et al. 2003), high rates of fecal deposition can increase the risk of surface water contamination from excess nutrients and pathogenic organisms such as *Cryptosporidium*, *Salmonella*, and *Escherichia coli* (*E. coli*). In watersheds with large wildlife populations, improved knowledge of wildlife-source fecal loading may help increase accuracy of model predictions for fecal bacteria concentrations. Availability of agricultural land use data including livestock numbers, grazing and stocking densities, manure application rates and associated bacteria concentrations, often allows for accurate estimation of agricultural-source fecal bacterial loadings within a watershed. In contrast, wildlife-source fecal loadings are rarely quantified, therefore land use and cover data are frequently used to indirectly estimate wildlife numbers and distributions based on likelihood of animal occurrence in a particular habitat (Chapra 2008). Wildlife population estimates may be derived from either aerial or direct ground survey, hunting or road kill records, although standardized and agreed upon methods for quantification using the latter sources are currently lacking (Baffaut and Sadeghi 2010). For the purpose of hydrological modelling, wildlife population data are frequently distributed equally across all potential habitat for each species (Benham et al. 2006), ignoring potentially important aspects of landscape connectivity and spatiotemporal variability of wildlife habitat use and distribution across heterogeneous landscapes (Turner 1989). This approach may also result in high predictive uncertainty when modeling bacteria concentrations in watersheds where distinct variations in seasonal conditions, habitat, land use, or landscape features influence wildlife to aggregate disproportionately at high densities in certain locations along a watercourse.

Previous research in the Chobe River system of northern Botswana, identified significant associations between seasonal *E. coli* concentrations and dung counts from elephant (*Loxodonta africana*) and other wildlife in both the dry season and in the following wet season (Fox and Alexander 2015). Wildlife occupying semi-arid and arid ecosystems are often constrained to foraging within a relatively short distance of perennial surface water sources, particularly during the dry season (Redfern et al. 2003). Natural landscape heterogeneity and patterns of human

land use and development may further restrict and concentrate wildlife in certain locations where they may directly impact water quality through defecating into the watercourse, or indirectly through mobilization and runoff of fecal bacteria associated with dung and surrounding soil.

Building upon previous research on water quality dynamics in the Chobe River, we present a standardized, Distance sampling method for quantifying wildlife-source contributions to fecal bacterial loading of surface waters. This Distance-based method is especially useful for developing knowledge of how wildlife fecal loadings vary across a landscape or particular land use, either seasonally or during major phenological changes in vegetation. While dung surveys have been used to estimate population size for a wide range of species and habitats (Jachmann and Bell 1984, Jachmann 1991, Newey et al. 2003, Ellis and Bernard 2005, Anderson et al. 2013), to date little attempt has been made to use these data to inform the development and improve the accuracy of hydrologic water quality models. Here, we suggest a method which allows small teams of field technicians with minimal training to collect reliable wildlife fecal loading data at little cost, and at any desired spatial scale and temporal resolution within a watershed. We also evaluate the utility of Distance sampling methods to: 1) derive seasonal fecal loading estimates for wildlife in protected and unprotected land; 2) provide a simple, standardized method to estimate riparian fecal loading for use in distributed hydrological water quality models; and 3) answer questions about complex drivers and patterns of water quality variability in a semi-arid southern African river system.

Methods

Study site

The Chobe River in northern Botswana is the only permanent surface water source within the 21,000 km², semi-arid Chobe District (Fig. 1). A dominant feature in the region is the Chobe National Park (CNP), which is Botswana's second largest protected area (11,700 km²) and home to the largest elephant population in Africa, along with a diversity other wildlife species. Since the 1960s, the elephant population in the Chobe region has grown at an estimated mean annual rate of between 5.5% and 7% (Calef 1988, Vandewalle 2003), and currently number over 200,000 individuals (DWNP 2014). Human population density is generally low within the Chobe

District, although the towns of Kasane, the regional government seat (est. population 9,008), and Kazungula (est. pop. 4,133) have recently experienced rapid population growth along with associated expansion of urban, residential, and tourist infrastructure (BCSO, 2011). Agricultural land use along the Chobe River is constrained by crop raiding and destruction by wildlife, while livestock production is largely subsistence-based. Rainfall and availability of surface water resources greatly influence patterns of wildlife distribution and habitat utilization across the dryland savanna ecosystem. Precipitation is highly variable, with nearly all annual rainfall (avg. 604 mm) occurring during the summer wet season (November – April), with typically no rain during the dry winter months (May – October). Most rainfall events are high intensity, short duration convective storms in which rainfall depth may frequently exceed available storage of the predominantly shallow, sandy clay soils. Rainfall in excess of the soil infiltration capacity is quickly converted into surface runoff following classic Hortonian overland flow. Soil crusting or sealing typical of soils in semi-arid regions may also contribute to greater precipitation runoff (Perroll and Sandström 1995). Heavy and sustained rainfall during the wet season fills shallow pans and ephemeral channels across Chobe District, causing wildlife to disperse away from the permanent water sources across the landscape. Disappearance of temporary water holes as the dry season progresses forces movement of elephants and other water-dependent wildlife species back towards the Chobe River, where they concentrate at high densities in the riparian corridor and floodplain.

Fecal transect design and sampling protocol

Dry season accumulation of wildlife dung in the Chobe riparian zone and floodplain followed by wet season mobilization and transport, together with direct deposition of dung into the river channel, can have a significant influence on seasonal *E. coli* concentrations in the river system (Fox and Alexander 2015). Therefore, wildlife fecal count data were collected at points along a series of 55 line transects, each 50m in length and spaced 500m apart perpendicular to the Chobe River (Fig. 1). The first transect was located furthest downstream (east) at a random start point near the confluence of the Chobe and Zambezi Rivers. Transects 1-30 proceeded in an upstream direction and were located in unprotected land spanning a mosaic of undeveloped, residential, developing urban, and urban (transects 18-30) land use. Transects 31-55 were all located inside the boundaries of the Chobe National Park. Any transect obstructed either visually or by wildlife

was shifted by standard increments of 100m to the west until it could be successfully completed, while the predetermined distance to the next transect remained unchanged. Monthly sampling was conducted during 2012 in January, February, and April (wet season), and July-September (dry season), with a full sampling event taking approximately one week. Fecal transects were begun by taking a GPS bearing with the observer's back to the river, and this bearing was maintained throughout the duration of the transect. Visual scans for dung piles were conducted at one meter intervals with the observer looking directly left and right from the transect to spot all feces in line with that meter of the transect, as far as the eye can see. With the observer remaining on the transect line, a laser range finder was used to determine the distance in meters to each observed dung pile. Species of origin and approximate age of dung piles were determined by an experienced Basarwa tracker, and only dung piles <30 days of age were included in the analysis. Limiting the analysis to recently-deposited dung helped reduce problems associated with double counting of dung piles, since all but the April surveys were conducted in consecutive months. Furthermore, release of *E. coli* into surface water from dung piles show significantly decline with increasing age of fecal deposits, and while dung piles older than 30 days may remain a potential source of fecal bacteria, the quantity released is typically lower compared to that released from fresher manure (Springer et al. 1983, Kress and Gifford 1984).

Density analysis using Distance

We used the Distance program (version 6.2) (Buckland et al. 1993) to estimate wildlife fecal density from transect fecal counts. Distance sampling is a widely-used, quantitatively robust technique comprising a set of methods in which perpendicular distances from a line or point to a target object are used to model probability of detection in order to estimate the density of a population (Thomas et al. 2010). Target objects usually consist of individuals or groups of animals, but may include animal cues (e.g. vocalizations) or sign, such as dung or nests. Distance sampling does not assume that all target objects are detected with the exception of those located on the transect line (i.e. zero distance). Thomas et al. (2010) provide a thorough review of distance sampling, including design and analysis of transect data using Distance software. We compared the fit of four detection function models in each of the analyses, including: 1) uniform + cosine adjustments (also known as the Fourier series), 2) hazard rate + simple polynomial adjustments, 3) half-normal + cosine adjustments, and 4) half-normal + hermite polynomial

adjustments. Truncation distances and cut points were interactively determined through examination of global detection function plots and diagnostics. Models within delta-AIC of 2.0 were designated as competing models and the simplest top model was selected based on Akaike's Information Criterion (AIC) and Chi-square goodness of fit tests. We analyzed fecal transect data by month to examine seasonal differences in fecal loading. Spatial variability of wildlife fecal loading was also examined by stratifying the analysis by non-protected (transects 1-31) and protected land (Chobe National Park; transects 31-55), and by individual transects in order to evaluate finer-scale variation occurring across the landscape. Wildlife fecal loading values from each even-numbered, upstream transect point were combined with values from the nearest odd-numbered, downstream point in order to downscale data for graphical comparisons with bi-monthly mean *E. coli* (# colony forming units (CFU)/100mL), which were measured at 1000m intervals. Water quality grab samples for *E. coli* were collected bi-monthly from July 7, 2011 to March 19, 2014 (n=1630) and processed following standard United States Environmental Protection Agency methods 1103.1 (USEPA 2000) and 1604 (Oshiro 2002), previously described by Fox and Alexander (2015). Briefly, water grab samples were vacuum-filtrated through sterile gridded nitrocellulose membrane filters (0.45 µm pore size; Thermo Fisher Scientific, Waltham, Massachusetts, USA). Following filtration of each sample, the sides of the funnel were rinsed twice with 20–30 mL of sterile reagent-grade de-ionized (DI) water. Filters were then aseptically transferred to the surface of a RAPID'E.coli2 (BIORAD, Hercules, California, USA) agar plates, and incubated at 37 °C for 24 hours prior to colony enumeration.

Ground cover survey

Ground cover was measured at 1km intervals coinciding with water quality sampling locations using a modified step-point method. The step-point method has a simple theoretical basis and provides a rapid, accurate, and objective means of determining the proportion of ground cover over a particular site (Goodall, 1952; Evans and Love, 2006). Each step-point transect began at the river edge and extended 50m perpendicular to the river course. Percent ground cover was estimated in the riparian zone as the number of "hits" relative to the total number of points sampled.

Statistical analysis

Statistical comparisons were conducted in the open source R programming environment (R core Team, 2013). Paired and unpaired Welch's two sample t-tests for unequal variances were used to compare wet and dry season fecal loads for transects within protected and unprotected land, and between land uses, respectively. Associations between wet and dry season log mean *E. coli* concentrations, mean dry season fecal density (dung piles/ha), riparian ground cover, and degree bank slope were examined using multiple linear regression. An all possible regressions approach was used in variable selection and partial least squares regression was also used to evaluate percent variance explained by predictor variables. A natural log transformation was applied to mean *E. coli* concentration (CFU/100ml) prior to analysis to better approximate a normal distribution prior to fitting regression models.

Results

Wildlife fecal loading

A total of 2,544 fecal deposits <30 days of age were recorded during the study period, with 495 observations in the wet season, and 2,049 observations during the dry season. Maximum distance for dung piles spotted during the survey was approximately 30 m in the dry season and 20 m in the wet season. Truncation distances used to model Distance detection functions and eliminate potential outliers ranged from 14-20 meters in the dry season and 10-14 meters in the wet season (Appendix N), and excluded approximately 5% of observations. Wildlife fecal density estimates (dung piles/ha) for unprotected (UP) and protected (CNP) land, together with associated 95 percent confidence intervals and coefficients of variation are presented in Table 1 and Figure 3. Species for which too few dung piles were recorded or fecal density estimate %CV was >50% were lumped and modelled as a single source (Fig. 2) Wet season riparian fecal densities ranged from 2.2-25.4 dung piles/ha in UP land, and 18.5-180.9 dung piles/ha in the CNP, with the lowest fecal loads recorded in February and the highest in April for both unprotected and protected land. Dry season wildlife fecal density estimates varied from 10.3-113.3 dung piles/ha in unprotected land, and 22.0-185.1 dung piles/ha in the CNP. Dry season elephant fecal loading estimates were highest in September for both the CNP and UP land.

Fecal density estimates varied significantly both within and between seasons and land use (Table 2.). Dry season fecal loads were significantly higher than those in the wet season in both the CNP ($t=7.45$, $df = 74$, $p < 0.0001$) and UP land ($t=4.68$, $df = 89$, $p < 0.0001$). Dry season fecal loading was also significantly higher in the CNP compared to UP land in both the wet ($t=4.68$, $df = 89$, $p < 0.0001$) and dry seasons ($t=7.92$, $df = 89$, $p < 0.0001$). Wildlife tended to cluster in similar locations in both wet and dry seasons, albeit at much higher densities during the dry season (Fig. 4). Fecal loadings were consistently lower at transect points in and near the town of Kasane and highest between transects 35-39 in the CNP. Scatterplots comparing downscaled mean dry season fecal density estimates versus mean *E. coli* concentrations in both the dry and the wet season (December-February), by transect point (Fig. 4), show that average *E. coli* concentrations in water samples generally increased with higher fecal loading. All possible regressions identified mean fecal density, degree bank slope, and percent grass and shrub cover as variables that minimized model BIC. Results of OLS regression showed a significant positive association between mean dry season fecal density and log mean *E. coli* concentration in both the dry season ($\text{adj}R^2 = 0.113$, $p = 0.042$) and the first three months (December-February) of the wet season ($\text{adj}R^2 = 0.378$, $p = 0.027$) (Table 3). In the wet season, coefficients for degree bank slope ($p = 0.011$) and percent grass cover ($p = 0.014$) were also statistically significant. Partial least squares regression showed that in the dry season, mean fecal loading was responsible for approximately 18.5% of the variation in log mean *E. coli* concentration (Table 4). In the wet season, mean dry season fecal density explained 9.9% of the variance in log mean *E. coli*, while bank slope and grass cover explained 20.8% and 16.4%, respectively.

Discussion

Bacterial fate and transport are the least-explored components of mechanistic watershed models, especially in regards to wildlife-source contributions to concentrations of fecal indicator bacteria (FIB) in natural surface waters (Parajuli et al. 2009). Using well-established line transect survey and Distance sampling techniques, we quantified wildlife-source riparian fecal loads along a 27.5 km reach of the Chobe River spanning national park and unprotected land. Elephant and impala (*Aepyceros melampus*) were the largest contributors to terrestrial fecal loads in the Chobe National Park, with densities exceeding 185 and 160 dung piles per hectare in September, respectively. Impala fecal densities in the Chobe National Park exceeded those of elephant in

both July and August. Radio tracking studies of impala have shown that individuals tend to congregate at high density along the riverfront, especially in shrubland vegetation that is heavily impacted by elephant (Moe et al. 2014). In contrast, impala were essentially absent from locations outside of the park boundaries throughout the entire study period, although elephant were a major source of fecal loadings in unprotected land, along with other wildlife species, including baboon (*Papio ursinus*), warthog (*Phacochoerus africanus*), and hippopotamus (*Hippopotamus amphibious*). Domestic cattle (*Bos taurus*) were also found to be an important source of fecal loading in unprotected area, despite the generally low density of livestock across the study area.

Wildlife fecal densities increased over the three months of dry season sampling, with highest fecal loading observed in September at a time when the disappearance of water in temporary pans drives animals to forage close to the Chobe River in increasingly higher numbers. The grassy floodplains of the Chobe River represent an important food resource for herbivores during the dry season, when grass cover is typically limited elsewhere, and many animals also cross the river at shallow points along the river in order to take advantage of vegetation growing on low-lying channel islands. Significantly lower wet season fecal loads, in turn, likely reflect animal dispersal away from the Chobe River as water and food availability improve throughout the region, as well as increased mobilization and transport of dung material by precipitation runoff. While only dung piles less approximately 30 days of age were considered in the Distance analysis, heavy rainfall before and during wet season sampling likely caused considerable runoff of soil and accumulated dung. Dung beetles, which are typically more active during the warm, rainy season, also likely contributed to removal of fresh fecal material in between wet season sampling events (Doubé et al. 1991). Rainfall totals for January and February, 2012 recorded by the Kasane Meteorological Station were 126.4 mm and 167.6 mm, respectively, while in contrast, only 0.8mm of rainfall was recorded in Kasane between April and September. This near complete lack of rainfall across the region during the winter dry season likely means bacterial transport within the Chobe riparian zone is limited or absent between April and November. Comparison of dry season fecal densities with mean wet and dry season concentrations of *E. coli* (CFU/100ml) (Fig. 4), helped to identify several locations along the Chobe River where substantial indirect inputs via runoff of dung and associated fecal bacteria potentially occur.

Transects in the CNP with both high dry season fecal density and high mean *E. coli* concentrations suggest areas of direct wildlife fecal deposition into the river channel, as there was no precipitation available for mobilization and transport of material overland during this period. Conversely, transects where dry season fecal loads were high but mean *E. coli* concentrations were comparatively low reflect locations where direct, in-channel deposition of fecal material by wildlife is likely relatively limited. Interestingly, dry season *E. coli* concentrations at transects located in Kasane were higher than expected given the lack of fecal loading (Fig. 4, transects 25 and 27), which indicates bacterial input from other sources. Such comparisons were possible only due to the distinct seasonal differences in rainfall typical of southern Africa and other dryland systems (Tooth 2000), and would likely not be possible in more temperate regions where the timing of rainfall more consistent throughout the year..

Stratifying the analysis by transect allowed us to identify finer-scale spatiotemporal variations in wildlife fecal density driven by seasonal changes in climate, land use, and physical landscape characteristics. The observed seasonal differences in fecal loading highlight the benefit of repeating dung surveys over an extended period in order to better understand the movements, distributions, and habitat occupation of different wildlife species in a watershed. Examining finer-scale variation in wildlife fecal loading along the Chobe River transect indicates that much of the observed difference between protected and unprotected areas is likely attributable to the near complete absence of wildlife in riparian habitat at points in and near the town of Kasane (Fig. 3). Several points in unprotected land use had fecal density estimates well above the global mean for the study area, and in these areas, wildlife access to the Chobe River, floodplain, and wetlands has largely remained unobstructed by urban and residential development. Elephant presence, in particular, increased dramatically in September at many transects outside of the national park.

Distance-based methods proved to be a simple, cost-effective, and statistically-robust way to estimate wildlife fecal densities, and have several advantages compared to other methods for estimating wildlife distributions for use in watershed models (Barnes 2001). The ability to describe actual riparian fecal loading represents a major improvement beyond simply assuming equal distribution of fecal loading by wildlife across a watershed or river basin for modelling

purposes. The use of aerial or ground population survey data or hunting and road kill records to derive fecal loading estimates may fail to accurately represent true wildlife fecal loads. Our results highlight the differential utilization of riparian habitat by wildlife, owing to differences in landscape characteristics and land use, suggesting that equally distributing wildlife fecal loads across a watershed might result in poor model accuracy for predicting bacterial loads. For example, despite the presence of a large areas of suitable habitat in unprotected land, detections of impala and Cape buffalo (*Syncerus caffer*), were essentially absent outside the boundaries of the CNP. Cape buffalo are typically present at high density in the Chobe River study area during the dry season. Aerial surveys conducted by the Botswana Department of Wildlife and National Parks (DWNP) during the 2012 dry season recorded buffalo density along the Chobe River of over 450 large stock units (LSU)/km² (DWNP 2014). However, our results indicate that buffalo contributed surprisingly little to terrestrial fecal loads considering the large number of animals recorded using aerial survey, and do not appear to spend a significant amount time along the Chobe River. In fact, 71% of all buffalo dung identified along the transects came from males, likely resident bulls, which frequent the Chobe River floodplain throughout the year, and not from females in the large maternity herds present primarily during the dry season. Intensive dry season tracking of buffalo herds in the study area suggests some spend almost all daylight hours under cover of woodland and thick shrubland, and only move out to floodplain areas at twilight and during the middle of the night, while others frequently swim to Sedudu Island located mid-channel (Taolo 2003). This suggests caution should be used when extrapolating wildlife population data calculated from a single sampling effort, month, or season to characterize wildlife-source contributions to fecal bacteria loads within a watershed. The surprising lack of terrestrial fecal deposition from buffalo, also suggests that direct inputs of dung in the river course may represent a major and unquantified source of waterborne fecal bacteria in the Chobe River.

Conclusion

Distance-based dung surveys may be a way of improving accuracy and refining sensitivity of spatially-distributed watershed models used to simulate and predict fecal indicator bacteria concentrations in surface waters. Better representation of spatial variability and source characterizations of wildlife-source fecal loading within a watershed contributes to a more holistic understanding of bacterial fate and transport processes under different environmental

conditions. Sign from both impala and buffalo were almost never observed in the riparian zone outside of the Chobe National Park, despite there being large areas of suitable habitat. In contrast, elephants appear to be heavily utilizing unprotected land late in the dry season. These results have major implications for the commonly used modeling approach of equally distributing wildlife population data across all potential habitat for a species, and doing so may lead to high uncertainty and lower accuracy in predicting concentrations of waterborne fecal indicator bacteria in watersheds supporting large, free-ranging wildlife populations. In addition to aiding decisions of how wildlife fecal bacteria loadings are allocated across a landscape in the modeling environment, fecal transect surveys can shed light on animal utilization of riparian habitats, and their potential contribution to soil erosion and re-suspension of in-stream bacteria and sediments. Distance-based dung surveys may be timed to coincide with the arrival of migratory or transient wildlife species within a watershed in order to evaluate their potential contributions to bacteria source loads. In watersheds where wildlife heavily utilize agricultural land, dung surveys can help improve model sensitivity by considering contributions to bacterial transport under different tillage scenarios. The straightforward implementation and ease of repeatability of dung surveys also makes them particularly well-suited for building public participation in research through training of local stakeholders in survey techniques. A wealth of supplementary data such as wildlife population age structure, health, and reproductive status may also be concurrently collected. An important next step in improving watershed modeling in African systems is quantifying *E. coli* and fecal coliform present in dung of common African wildlife species, together with bacteria partition coefficients and loss rates occurring in a wide range of habitats and environmental conditions.

Literature cited

- Anderson, C. W., C. K. Nielsen, C. M. Hester, R. D. Hubbard, J. K. Stroud, and E. M. Schaubert. 2013. Comparison of indirect and direct methods of distance sampling for estimating density of white-tailed deer. *Wildlife Society Bulletin* **37**:146-154.
- Auer, M. T., and S. L. Niehaus. 1993. Modeling fecal coliform bacteria—I. Field and laboratory determination of loss kinetics. *Water Research* **27**:693-701.
- Badgley, B. D., F. I. Thomas, and V. J. Harwood. 2011. Quantifying environmental reservoirs of fecal indicator bacteria associated with sediment and submerged aquatic vegetation. *Environmental Microbiology* **13**:932-942.
- Baffaut, C., and A. Sadeghi. 2010. Bacteria modeling with SWAT for assessment and remediation studies: A review. *Transactions of the ASABE* **53**:1585-1594.
- Barnes, R. F. 2001. How reliable are dung counts for estimating elephant numbers? *African Journal of Ecology* **39**:1-9.
- Benham, B. L., C. Baffaut, R. W. Zeckoski, K. R. Mankin, Y. A. Pachepsky, A. M. Sadeghi, K. M. Brannan, M. L. Soupir, and M. J. Habersack. 2006. Modeling bacteria fate and transport in watersheds to support TMDLs. *Transactions of the ASABE* **49**:987-1002.
- Bordalo, A., R. Onrassami, and C. Dechsakulwatana. 2002. Survival of faecal indicator bacteria in tropical estuarine waters (Bangpakong River, Thailand). *Journal of Applied Microbiology* **93**:864-871.
- Calef, G. W. 1988. Maximum rate of increase in the African elephant. *African Journal of Ecology* **26**:323-327.
- Chapra, S. C. 2008. *Surface water-quality modeling*. Waveland press.
- de Brauwere, A., N. K. Ouattara, and P. Servais. 2014. Modeling fecal indicator bacteria concentrations in natural surface waters: a review. *Critical Reviews in Environmental Science and Technology* **44**:2380-2453.
- DWNP. 2014. *Aerial census of wildlife and some domestic animals in Botswana*. Department of Wildlife and National Parks. Monitoring Unit, Research Division. Gaborone.
- Ellis, A. M., and R. T. Bernard. 2005. Estimating the density of kudu (*Tragelaphus strepsiceros*) in subtropical thicket using line transect surveys of dung and DISTANCE software. *African Journal of Ecology* **43**:362-368.
- Ferguson, C., A. M. d. R. Husman, N. Altavilla, D. Deere, and N. Ashbolt. 2003. Fate and transport of surface water pathogens in watersheds.

- Fox, J. T., and K. A. Alexander. 2015. Spatiotemporal Variation and the Role of Wildlife in Seasonal Water Quality Declines in the Chobe River, Botswana. *PloS one* **10**:e0139936.
- Jachmann, H. 1991. Evaluation of four survey methods for estimating elephant densities. *African Journal of Ecology* **29**:188-195.
- Jachmann, H., and R. Bell. 1984. The use of elephant droppings in assessing numbers, occupancy and age structure: a refinement of the method. *African Journal of Ecology* **22**:127-141.
- Jamieson, R. C., D. M. Joy, H. Lee, R. Kostaschuk, and R. J. Gordon. 2005. Resuspension of Sediment-Associated in a Natural Stream. *Journal of Environmental Quality* **34**:581-589.
- Kress, M., and G. F. Gifford. 1984. Fecal coliform release from cattle fecal deposits. *Water Resources Bulletin* **20**:61-66.
- Neitsch, S. L., J. G. Arnold, J. R. Kiniry, and J. R. Williams. 2011. Soil and water assessment tool theoretical documentation version 2009. Texas Water Resources Institute.
- Newey, S., M. Bell, S. Enthoven, and S. Thirgood. 2003. Can distance sampling and dung plots be used to assess the density of mountain hares *Lepus timidus*? *Wildlife Biology* **9**:185-192.
- Parajuli, P. B., K. R. Mankin, and P. L. Barnes. 2009. Source specific fecal bacteria modeling using soil and water assessment tool model. *Bioresource Technology* **100**:953-963.
- Perroll, K., and K. Sandström. 1995. Correlating Landscape Characteristics and Infiltration. A Study of Surface Sealing and Subsoil Conditions in Semi-Arid Botswana and Tanzania. *Geografiska Annaler. Series A. Physical Geography*:119-133.
- Redfern, J. V., R. Grant, H. Biggs, and W. M. Getz. 2003. Surface-water constraints on herbivore foraging in the Kruger National Park, South Africa. *Ecology* **84**:2092-2107.
- Springer, E. P., G. F. Gifford, M. P. Windham, R. Thelin, and M. Kress. 1983. Fecal coliform release studies and development of a preliminary nonpoint source transport model for indicator bacteria.
- Srinivasan, R., X. Zhang, and J. Arnold. 2010. SWAT ungauged: hydrological budget and crop yield predictions in the Upper Mississippi River Basin. *Transactions of the ASABE* **53**:1533-1546.
- Suter II, G. W., L. W. Barnhouse, and R. V. O'Neill. 1987. Treatment of risk in environmental impact assessment. *Environmental Management* **11**:295-303.
- Thomas, L., S. T. Buckland, E. A. Rexstad, J. L. Laake, S. Strindberg, S. L. Hedley, J. R. Bishop, T. A. Marques, and K. P. Burnham. 2010. Distance software: design and analysis of distance sampling surveys for estimating population size. *Journal of Applied Ecology* **47**:5-14.
- Tooth, S. 2000. Process, form and change in dryland rivers: a review of recent research. *Earth-Science Reviews* **51**:67-107.

Turner, M. G. 1989. Landscape ecology: the effect of pattern on process. *Annual Review of Ecology and Systematics*:171-197.

Vandewalle, M. 2003. Historic and recent trends in the size and distribution of northern Botswana's elephant population. Pages 7-16 *in* Effects of fire, elephants and other herbivores on the Chobe riverfront ecosystem. Proceedings of a Conference organised by the Botswana-Norway institutional Cooperation and Capacity Building Project (BONIC). Gaborone: Government Printer.

Tables

Table 4-1. Distance sampling estimates of wildlife fecal densities (dung piles/ha) by month for unprotected (UP) and protected (CNP) land use, along with the percent coefficient variation (%CV), associated degrees of freedom (df) and 95% confidence intervals (%CV). Fecal density estimates listed as “Other” include all species for which <50 dung piles were recorded or %CV was 50% or higher. Dashes (-) indicate that dung piles were recorded, but that detections were too few to model within acceptable confidence limits. Species with zero density estimates indicate that no dung piles were recorded within that particular land use.

Month	Species	UP	%CV	df	95% CI	CNP	%CV	df	95% CI
January	Other	21.6	41.0	34	9.7, 48.1	88.4	21.0	45	58.2, 134.3
February	Elephant	2.2	49.3	34	0.8, 5.7	18.5	33.3	32	9.5, 35.8
	Other	11.7	45.9	33	4.8, 28.4	38.3	35.0	30	19.2, 76.2
April	Elephant	25.4	42.3	30	11.1, 58.1	75.4	19.4	27	50.9, 111.7
	Other	18.4	31.4	33	9.9, 35.6	180.9	27.4	29	104.3, 313.6
July	Elephant	10.3	28.6	34	5.8, 18.3	94.7	23.6	31	58.9, 152.4
	Impala	-	-	-	-	125.0	28.9	29	70.2, 223.7
	Other	47.7	39.3	33	22.1, 103.0	89.6	26.6	35	52.7, 152.3
August	Buffalo	0.0	-	-	-	22.0	36.7	31	10.7, 45.4
	Cow	37.1	29.8	40	20.6, 66.9	0.0	-	-	-
	Elephant	70.6	24.3	31	43.3, 115.1	92.4	23.2	26	57.6, 148.1
	Impala	-	-	-	-	168.0	22.1	30	107.3, 261.9
	Other	36.7	47.9	31	14.1, 90.2	138.4	25.3	30	83.2, 230.2
September	Cow	51.2	25.3	40	31.0, 84.7	0.0	-	-	-
	Elephant	113.3	19.1	31	77.0, 166.7	185.1	16.4	26	132.5, 258.4
	Impala	-	-	-	-	160.0	24.5	33	98, 261
	Warthog	-	-	-	-	31.0	42.3	37	13, 70
	Other	30.6	48.8	30.0	11.9, 78.5	64.4	31.8	27.0	34.1, 121.8

Table 4-2. Summary of t-test results comparing seasonal fecal loadings and land use.

	t-value	df	p-value	Mean difference	95% CI
Dry CNP - Wet CNP	7.084	74	6.844E-10	237.8	170.9, 304.7
Dry UP - Wet UP	5.686	89	1.631E-07	72.8	47.4, 98.3
Dry CNP - Dry UP	8.796	102	3.787E-14	280.6	217.4, 343.9
Wet CNP - Wet UP	5.719	88	1.434E-07	115.6	76.5, 155.8

Table 4-3. Summary of OLS regression results comparing seasonal mean fecal loadings and percent ground cover.

Variable	Dry Season				Wet Season			
	Coefficient	Std. error	t-value	p value	Coefficient	Std. error	t-value	p value
Mean fecal density	5.60E-06	2.59E-06	2.158	0.0421	4.74E-06	2.00E-06	2.376	0.0266
Degree bank slope	7.72E-03	1.47E-02	0.524	0.6055	3.19E-02	1.13E-02	2.813	0.0101
%grass cover	-3.78E-05	4.32E-03	-0.009	0.9931	8.87E-03	3.32E-03	2.67	0.014
%shrub cover	-1.45E-02	1.14E-02	-1.273	0.2163	-6.88E-03	8.78E-03	-0.784	0.4413

Table 4-4. Summary of Partial Least Squares regression results comparing seasonal mean fecal loadings and percent ground cover.

	Dry Season		Wet Season	
	adjCV	% variance explained	adjCV	% variance explained
Mean fecal density	0.4178	18.52	0.3955	9.88
Degree bank slope	0.4403	22.61	0.3589	30.74
% grass cover	0.4396	24.76	0.3275	47.16
%shrub cover	0.4611	24.91	0.3348	47.34

Figures

Figure 4-1. Map of the study site showing fecal transect locations and dominant land use along the Chobe River. The blue arrow indicates flow direction.

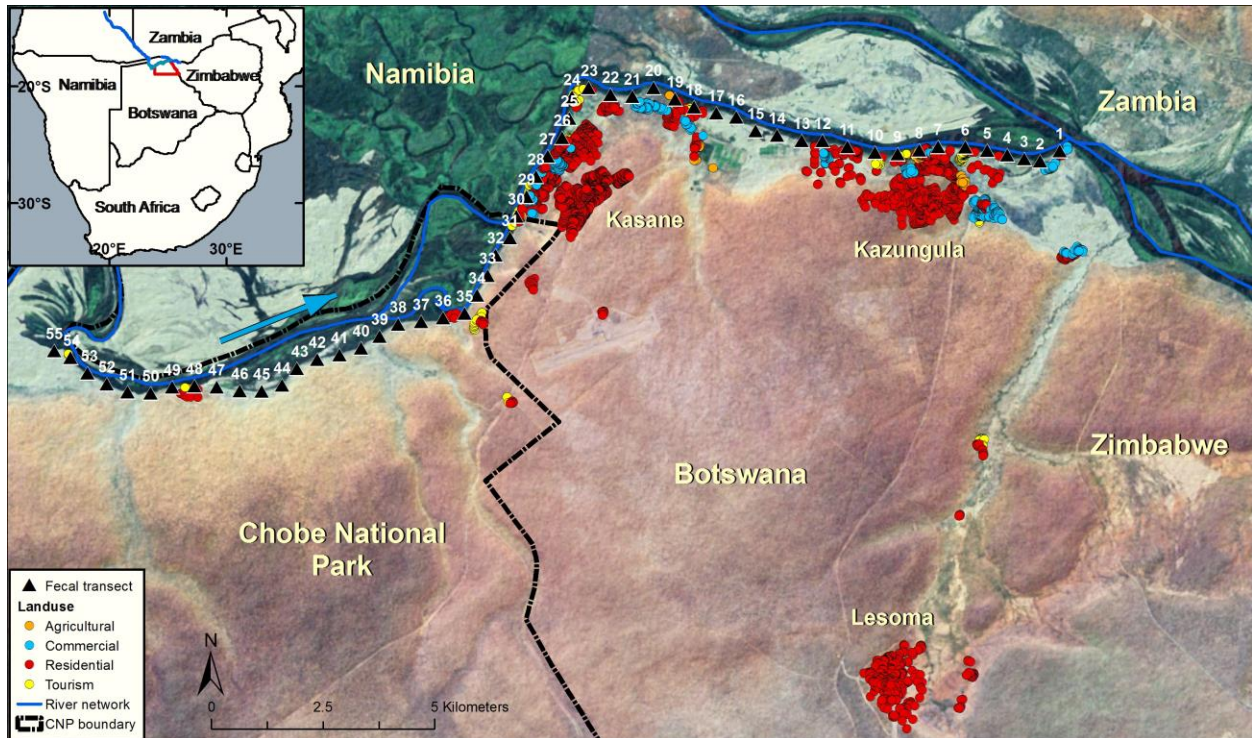


Figure 4-2. Bar graph showing relative monthly contributions to fecal counts for species for which <50 dung piles recorded or %CV of fecal density estimate were >50%. Numbers correspond to calendar months with wet season on top and dry season below.

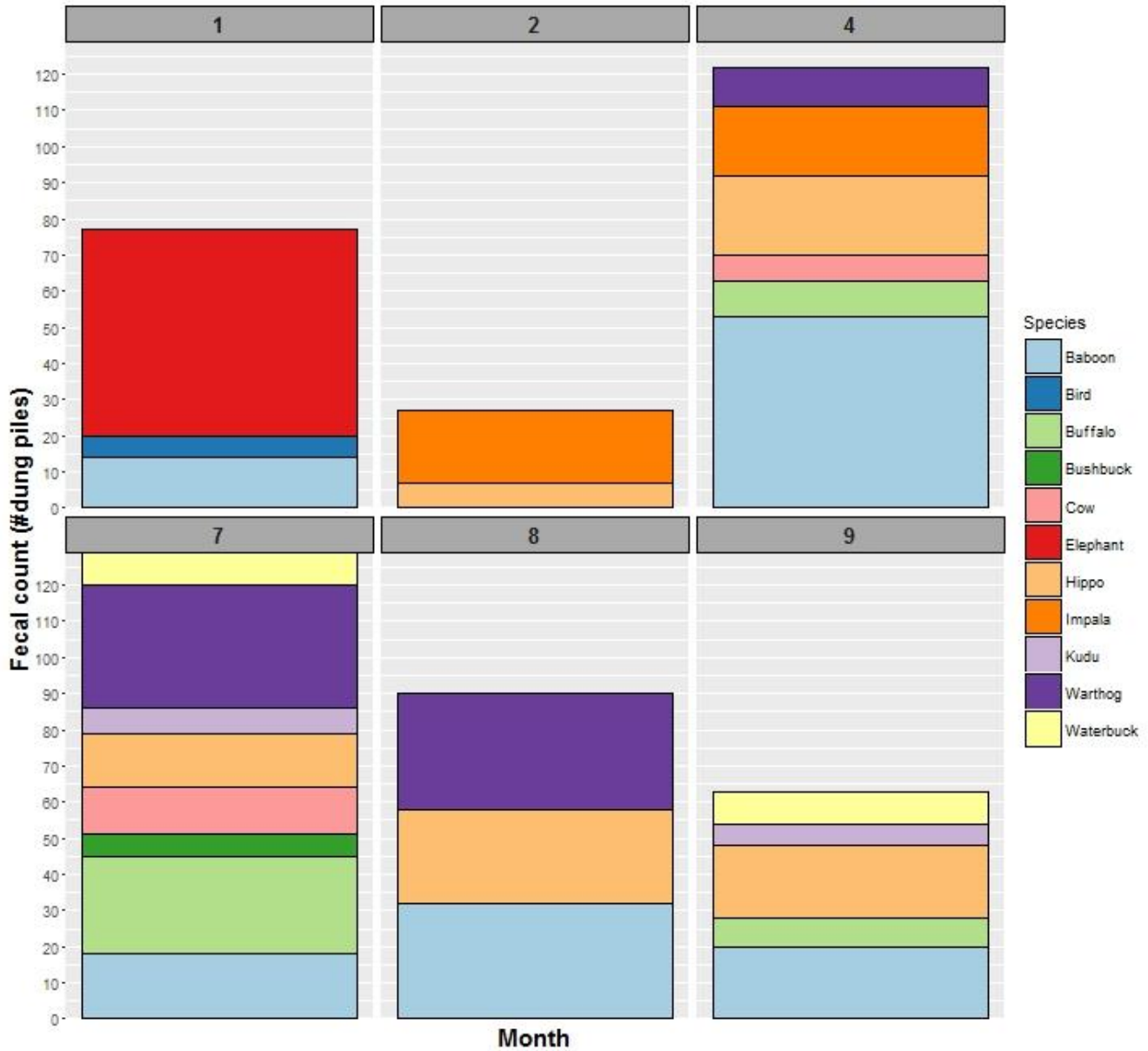


Figure 4-3. Wildlife fecal density estimates (dung piles/ha) for unprotected (UP) and protected (CNP) land are shown, together with associated 95% confidence intervals. Species for which too few dung piles were recorded or fecal density estimate %CV was >50% were lumped and modelled as a single source designated as “other”. Dry season fecal density estimates were significantly higher than those in wet season in both the CNP and in UP land. Dry season fecal loading was also significantly higher in protected compared to UP land in both seasons, No impala or buffalo sign was recorded in the riparian zone outside of the protected area, and no domestic cattle were observed inside the boundaries of the Chobe National Park.

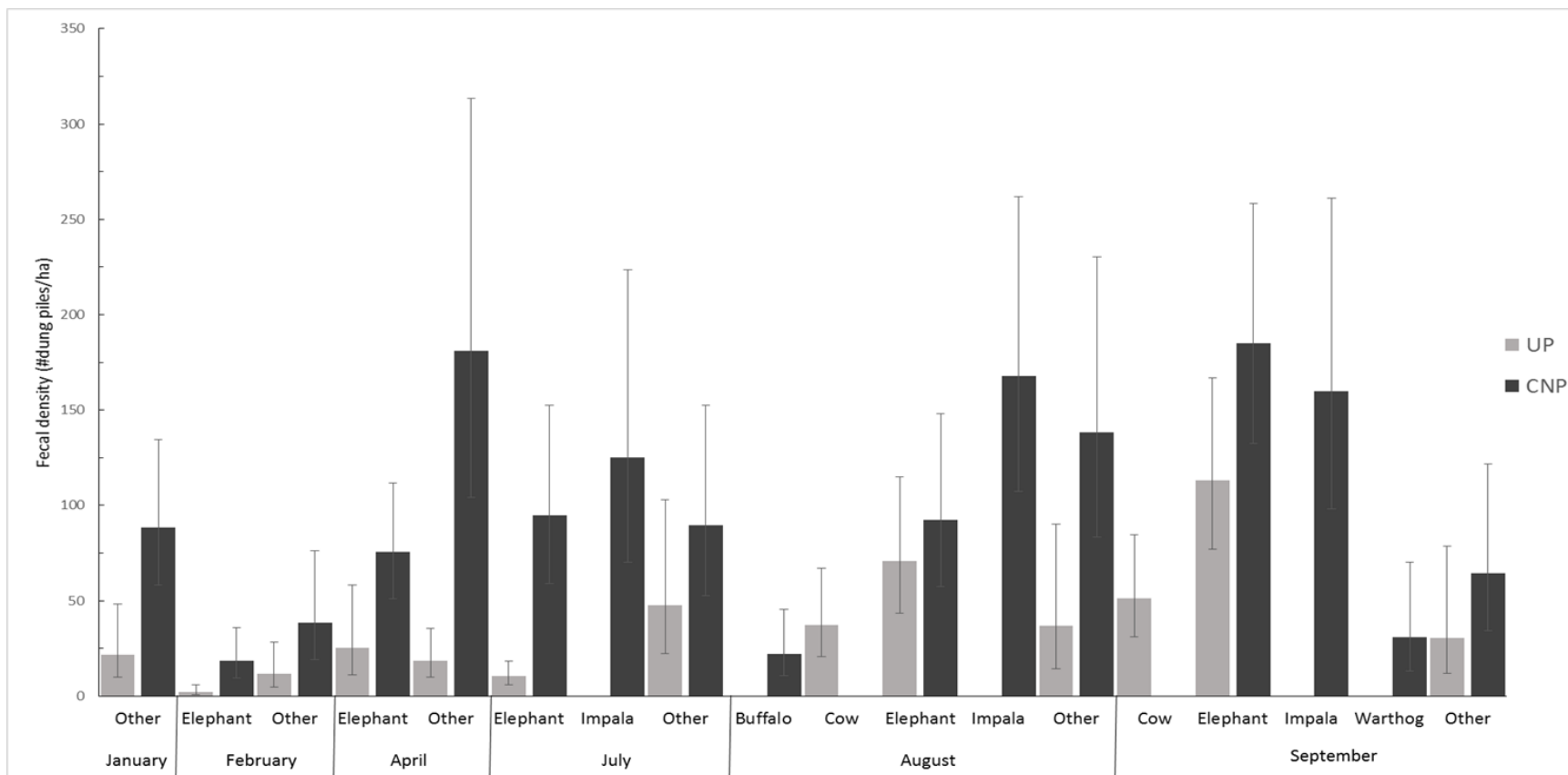


Figure 4-4. Fecal density estimates (#dung piles/ha.) for transects in unprotected and protected land. Numbers correspond to calendar months with wet season on top and dry season below. Wildlife tended to cluster in similar locations in both wet and dry seasons, albeit at much higher densities during the dry season. Wildlife fecal loadings were consistently lowest at transect points in and near the town of Kasane and highest between transects 35-39 in the CNP. Elephant and impala were by far the largest contributors to terrestrial fecal loads in the Chobe National Park, with impala fecal densities exceeding those of elephant throughout the dry season. Sign from both impala and buffalo were almost never observed in the riparian zone outside of the Chobe National Park, despite there being large areas of suitable habitat. In contrast, elephants appear to be heavily utilizing unprotected land late in the dry season

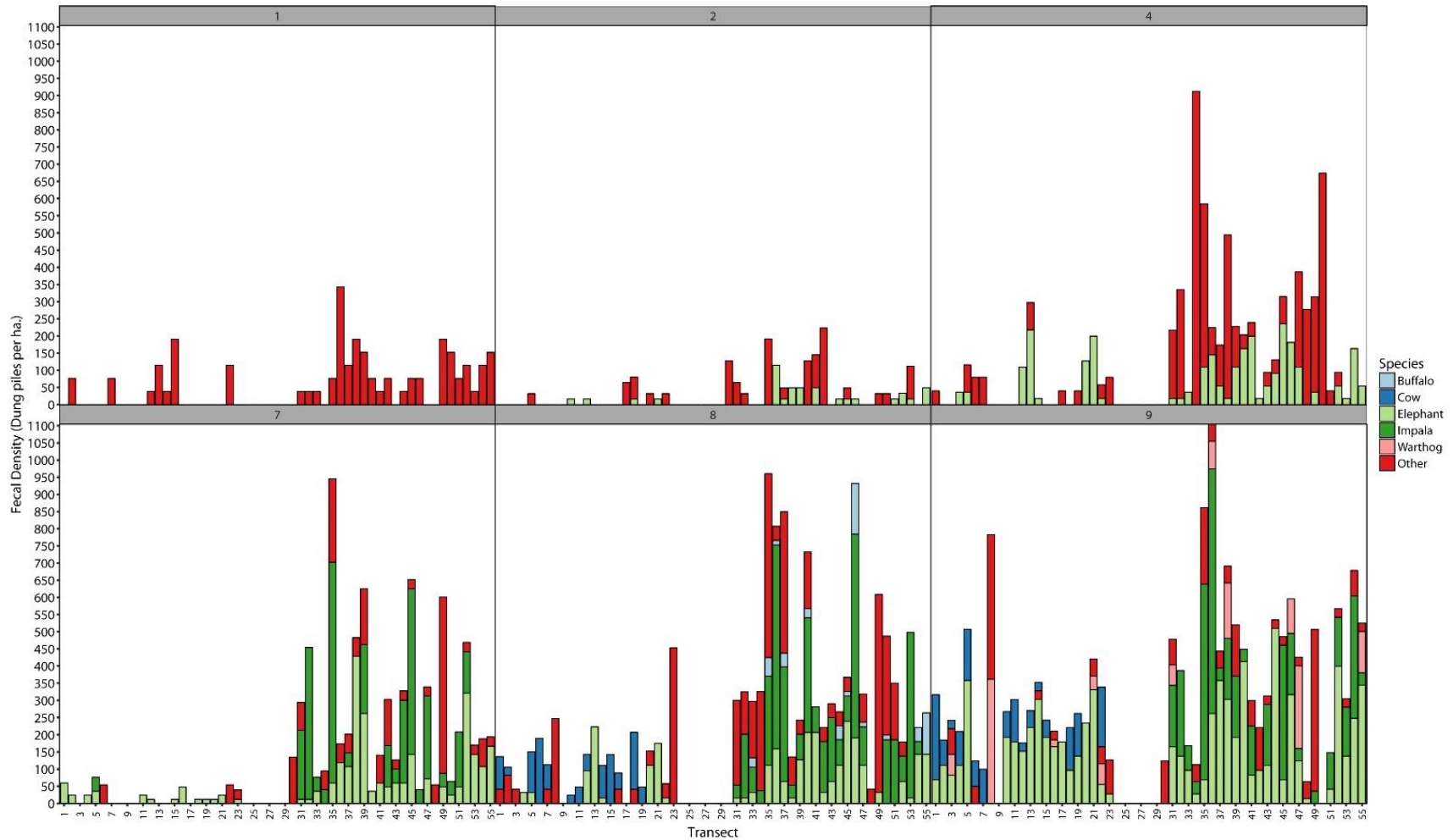
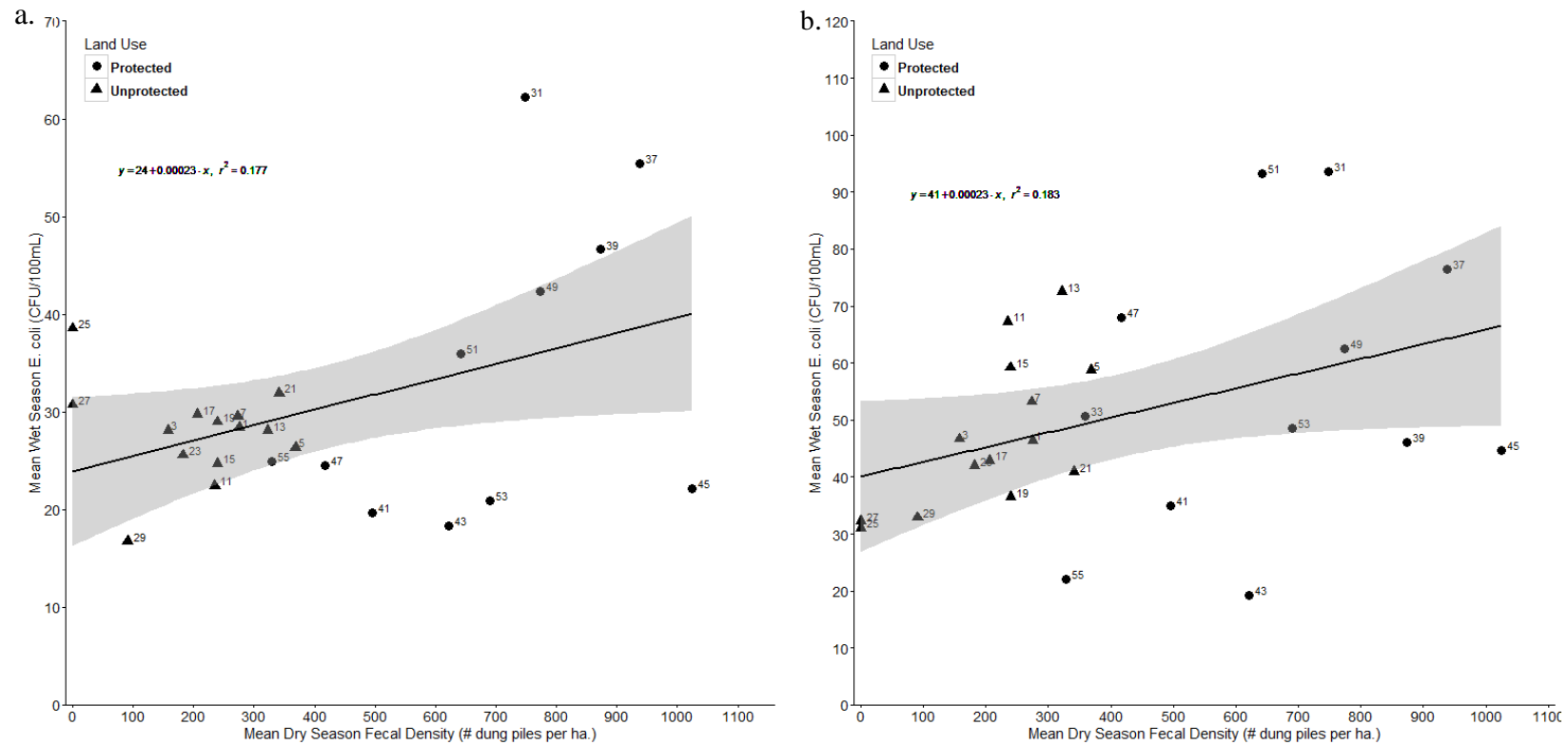
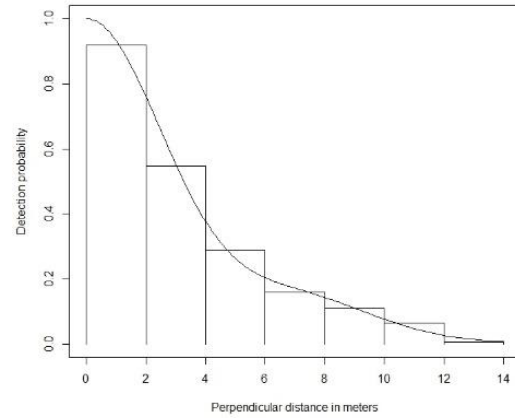
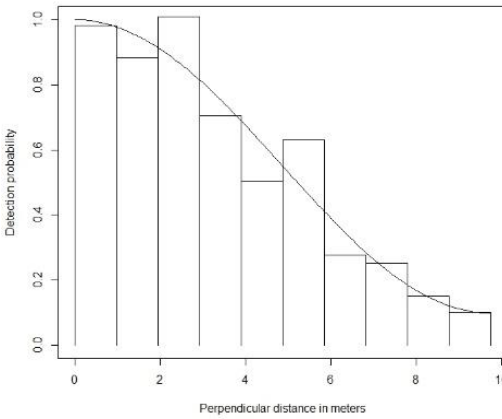
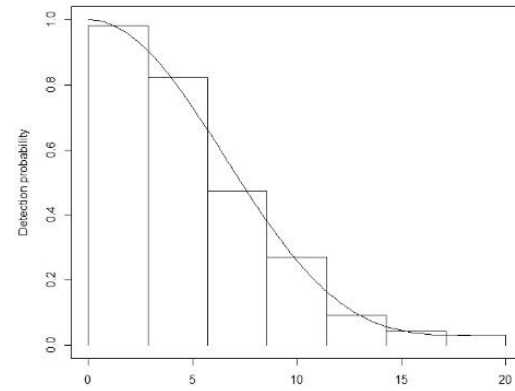
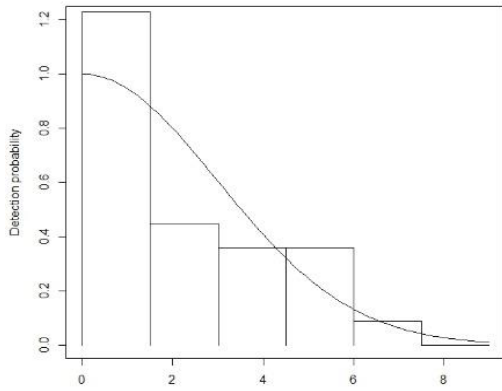
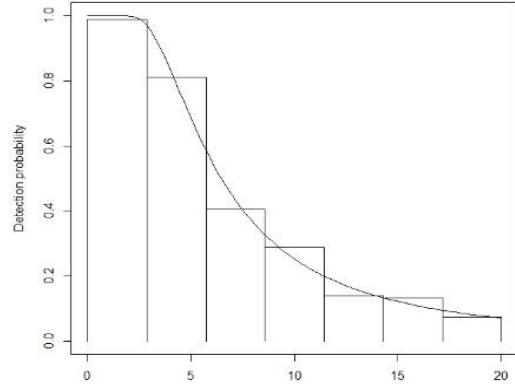
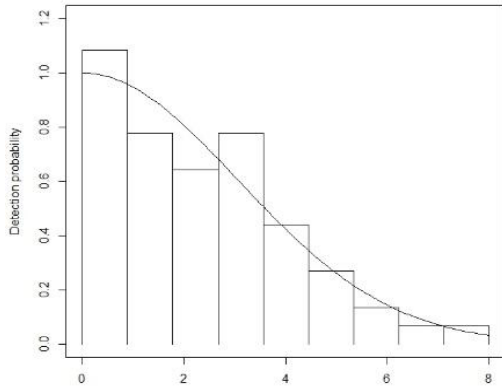


Figure 4-5. Scatterplots showing the relationship between (a) mean dry season fecal loading (#dung piles/ha) and mean dry season *E. coli* concentration (CFU/100ml), and (b) mean dry season fecal loading and mean wet season *E. coli* concentration in the first three months of the wet season. (December-February)



Appendices

Appendix N. Histograms of perpendicular distances and fitted detection functions for wet season (a) January, (b) February, and dry season (c) April, (d) July, (e) August, and (f) September.



CHAPTER 5: Synthesis

In this dissertation I addressed three distinct but highly interconnected aspects of spatiotemporal patterns of change in a semi-arid savanna ecosystem located in northeastern Botswana. In Chapter 2, I described seasonal water quality declines in the Chobe River, where concentrations of the fecal bacterium *Escherichia coli* significantly associated with high suspended solids in the wet season levels of riparian fecal loading by elephant and other wildlife during the dry season. Locations of elevated *E. coli* were also significantly associated with protected land use and the presence of well-developed floodplain accessible to wildlife. In contrast to water quality patterns observed at locations in Mixed urban and Town land use, where elevated fecal bacteria and suspended solid concentrations coincided with periods of heavy rainfall and the arrival of seasonal flood waters, water quality dynamics inside the Chobe National Park were notably decoupled from precipitation and flood-pulse events. This suggests that wildlife populations, and elephants in particular, can significantly modify river water quality patterns both through direct input. Loss of habitat and limitation of wildlife access to perennial rivers and floodplains in water-restricted regions may increase the impact of species on surface water resources.

These findings have important implications to land use planning in southern Africa's dryland river ecosystems, particularly given future climate change scenarios for southern Africa which predict a general drying trend across the region (Milly et al. 2005). With 94% of Botswana's surface water resources shared among neighboring countries (Mutembwa and Initiative 1998), improved understand of water quality dynamics is essential for sustainable conservation of perennial surface water sources. In southern Africa, limited surface water resources are under increasing pressure to accommodate competing needs of both humans and wildlife. Future land use and development planning in the Chobe District and other dryland regions of southern Africa should consider potential impacts of landscape alteration on wildlife movements and access to perennial sources of surface water. Specific consideration of availability and access to surface water and floodplain habitat should be included in the design and management of protected areas in dryland regions like Chobe which support large, free-ranging wildlife populations. Maintaining sufficient access for water-dependent wildlife in

dryland regions is not only important for sustainable conservation planning, but also for preserving vital clean water resources and improving human health.

Wildlife play an essential role in maintaining the long-term integrity of river corridors in southern Africa, adding nutrients and increasing patch heterogeneity in riparian landscapes (Naiman and Rogers 1997a). However, in watersheds where wildlife concentrate at high density in riparian corridors, their influence may extend beyond the terrestrial-aquatic interface to impact seasonal water quality dynamics. Developing accurate predictions of how complex natural processes and land use and management scenarios in large watersheds influence bacterial surface water quality remains a significant challenge. Building upon research presented in Chapter 2, in Chapter 4 of my dissertation, I presented a standardized Distance sampling method for quantifying wildlife-source contributions to fecal bacterial loading of surface waters. Use of this Distance-based method proved to be a simple, cost-effective, and statistically-robust way to estimate wildlife fecal densities, and has several advantages compared to other methods for estimating wildlife distributions for use in watershed models (Barnes 2001). The ability to describe actual riparian fecal loading represents a major improvement beyond simply assuming equal distribution of fecal loading by wildlife across a watershed or river basin for modelling purposes. In addition to aiding decisions of how wildlife fecal bacteria loadings are allocated across a landscape in the modeling environment, my results help shed light on how animals utilize riparian habitats, and their potential contribution to soil erosion and re-suspension of in-stream bacteria and sediments. Dung surveys may be timed to coincide with the arrival of migratory or transient wildlife species within a watershed in order to evaluate their potential contributions to bacteria source loads. In watersheds where wildlife heavily utilize agricultural land, dung surveys can also help improve watershed model sensitivity by considering contributions to bacterial transport under different tillage scenarios. The straightforward implementation and ease of repeatability of dung surveys also makes them particularly well-suited for building public participation in research through training of local stakeholders in Distance sampling techniques.

In Chapter 3, I assessed spatiotemporal patterns and intensity of land cover changes occurring across the 21,000 km² Chobe District and its protected areas from 1990-2013 in the

context of rainfall, recent fire history, and elephant browsing. I showed that LC changes across the Chobe District were not strictly linear in nature, a characteristic which has also been noted for other dryland regions (Diouf and Lambin 2001). Transition-level intensity analysis indicated active bi-directional exchange between woodland and shrubland was a highly influential process and that clusters of significant fire hot spots across the Chobe District spatially coinciding with locations undergoing active LC transitions. Changes in LC across the District also appear to be highly responsive to climatic fluctuations, with a long term trend of decreasing woodland cover and expansion of shrubland and grassland. Fire frequencies were highly variable from year to year, with more active fires recorded in years with higher rainfall, likely associated with higher wet season plant biomass and resulting increase in dry season fuel loads. Fire frequency also varied greatly among the different protected areas, ranging from 1.5 fires*year⁻¹/km² in the Kasane Forest Reserve to >6 fires*year⁻¹/km² in Kazuma Forest Reserve and Kasane Forest Reserve Extension. Mean fire intensity tended to be higher in the protected areas than in the buffer area surrounding human settlements. The highest area-adjusted fire frequency (8.4 fires*year⁻¹/km²) was observed in the riparian corridor within the Chobe Enclave, with a large significant fire hot spot located in the extensive reed beds on the Namibian side of the river. Another significant cluster of fire hot spots was observed in the southeastern portion of the District in the area between the Kazuma and Maikaelelo Forest Reserves, both of which experienced high woodland losses over the study period. The location and timing of fires, most of which occurred late in the dry season before the arrival of large convective storms associated with lightning production, suggests the majority of ignitions are anthropogenic in origin. Analysis of active fire location in relation to classified land cover showed the majority of ignitions in 2003 were located in wet/irrigation vegetation, but in 2013 woodland burned more frequently than any other LC class.

A continental-scale analysis of tree cover in African savannas by Bucini and Hanan (2007) suggests the magnitude of disturbance effects largely depend upon mean annual precipitation (MAP) regimes across rainfall zones. In semi-arid and mesic savannas (MAP 400-1600mm) like those found in northern Botswana, MAP exerts a stronger control over maximum tree cover along with disturbances that act as strong modifiers. In more mesic savannas (MAP <1600mm), precipitation no longer strongly limits tree cover, and disturbance impacts become more important in maintaining the system, while in arid savannas (MAP <400mm) the opposite

is true (Bucini and Hanan 2007). Long term (>50 year) fire exclusion experiments in Kruger National Park and other locations in South Africa have shown that grasslands with annual rainfall >650mm tend to be colonized by fire-sensitive woodland species in the absence of fire, but no comparable invasion of woody species occurred at sites with lower rainfall (Bond et al. 2003). Time series analysis of rainfall patterns in the Chobe District from 1922-2014 showed long-term average annual precipitation recorded at the Kasane Meteorological Station was 632mm ±181mm, ranging between 301-1205mm. This suggests that tree-grass dynamics in the savanna of the Chobe District may alternate between greater responsiveness to climate-dependency in unusually dry periods and more fire-dependent during years of above average rainfall. Such short term oscillations can have important long term implications for Chobe savanna plant community structure and composition given the strong couplings and feedbacks between climate, fire, herbivory, and anthropogenic disturbance (Bond et al. 2003, Archibald et al. 2005, Staver and Levin 2012). Increasing fire frequency as a result of climate-induced changes across the southern African region (Milly et al. 2005, Pricope and Binford 2012) may have profound effects on the distribution of woodlands in savanna systems. My analysis contributes to understanding of long-term land cover changes in this complex and dynamic savanna ecosystem, and in particular, how fire affects woodland cover stability. The results of this and other research using remote-sensing to monitor disturbance and land cover in southern Africa are essential to enabling societies across the region to locally manage ecosystem resources to increase their resilience to future climate change.

There is a wealth of ecosystem services supported by perennial dryland river systems in southern Africa, and preserving the headwaters of the Chobe, Zambezi, and Okavango rivers is vital to maintaining a naturally-functioning ecosystem. Construction of dams and large-scale water diversions can dramatically alter floodplain connectivity and lateral exchange of matter and organisms across river floodplains -the essence of the flood pulse concept proposed by Junk et al. (1989). In Egypt for example, building the Aswan Low and High Dams resulted in Schistosomiasis infection rates in human population rising from around 21 to 75% (Steinmann et al. 2006). And in Kenya, waterborne diseases which were once relatively uncommon they now impact nearly 100% of children in areas around Lake Victoria where large-scale perennial irrigation projects have been implemented (Steinmann et al. 2006).

Given the highly seasonal nature of water quality and availability in the Chobe Region, as well as the dynamic and non-linear nature of land cover changes associated with rainfall and fire frequency and intensity, future changes in climate and land use will have significant implications for wildlife, fisheries, and human health and livelihoods. This research contributes to improving our understanding of the coupling points, thresholds, and feedbacks in dynamic dryland savanna ecosystems.

Literature Cited

- Archibald, S., W. Bond, W. Stock, and D. Fairbanks. 2005. Shaping the landscape: fire-grazer interactions in an African savanna. *Ecological Applications* **15**:96-109.
- Bond, W., G. Midgley, F. Woodward, M. Hoffman, and R. Cowling. 2003. What controls South African vegetation—climate or fire? *South African Journal of Botany* **69**:79-91.
- Bucini, G., and N. P. Hanan. 2007. A continental-scale analysis of tree cover in African savannas. *Global Ecology and Biogeography* **16**:593-605.
- Junk, W. J., P. B. Bayley, and R. E. Sparks. 1989. The flood pulse concept in river-floodplain systems. *Canadian special publication of fisheries and aquatic sciences* **106**:110-127.
- Milly, P. C., K. A. Dunne, and A. V. Vecchia. 2005. Global pattern of trends in streamflow and water availability in a changing climate. *Nature* **438**:347-350.
- Mutembwa, A., and G. S. F. Initiative. 1998. Water and the potential for resource conflicts in southern Africa. *Global Security Fellows Initiative*.
- Naiman, R. J., and K. H. Rogers. 1997. Large animals and system-level characteristics in river corridors. *Bioscience*:521-529.
- Pricope, N. G., and M. W. Binford. 2012. A spatio-temporal analysis of fire recurrence and extent for semi-arid savanna ecosystems in southern Africa using moderate-resolution satellite imagery. *Journal of Environmental Management* **100**:72-85.
- Staver, A. C., and S. A. Levin. 2012. Integrating theoretical climate and fire effects on savanna and forest systems. *The American Naturalist* **180**:211-224.
- Steinmann, P., J. Keiser, R. Bos, M. Tanner, and J. Utzinger. 2006. Schistosomiasis and water resources development: systematic review, meta-analysis, and estimates of people at risk. *The Lancet infectious diseases* **6**:411-425.